AFAPL-TR-64-138

AD610256

EXPERIMENTAL NOISE INVESTIGATION OF MODEL NOZZLES

David F. Pernet

IIT Research Institute

TECHNICAL REPORT AFAPL-TR-64-138

December 1964

COPY 2 OF 3
HARD COPY $. 4.00
MICROFICHE $. 1.00

149P

Air Force Aero Propulsion Laboratory
Research and Technology Division
Air Force Systems Command
Wright-Patterson Air Force Base, Ohio

DDC
RECEIVED
JAN 28 1965
DDC-IRA C

ARCHIVE COPY

NOTICES

When Government drawings, specifications, or other data are used for any purpose other than in connection with a definitely related Government procurement operation, the United States Government thereby incurs no responsibility nor any obligation whatsoever; and the fact that the Government may have formulated, furnished, or in any way supplied the said drawings, specifications, or other data, is not to be regarded by implication or otherwise as in any manner licensing the holder or any other person or corporation, or conveying any rights or permission to manufacture, use, or sell any patented invention that may in any way be related thereto.

Copies of this report should not be returned to the Research and Technology Division unless return is required by security considerations, contractual obligations, or notice on a specific document.

FOREWORD

This report was prepared by IIT Research Institute, Chicago, Illinois on Air Force Contract AF 33(615)-1164, "Experimental and Theoretical Noise Investigation of Model Nozzles." The work was administered under the direction of the Air Force Aero Propulsion Laboratory. This work was performed under Project No. 3066 and Task No. 306601. Mr. E. E. Buchanan was task engineer of the laboratory.

The work was begun in November 1963, and ended in December 1964. The project leader was D. F. Pernet. Other contributors were W. C. Sperry who directed the program at its commencement; C. S. Caccavari who performed the majority of the data acquisition and reduction for both hot and cold jet nozzle flows; G. Hruska who assisted in data acquisition; and V. J. Raelson who performed a literature search. B. N. Glicksberg, M. J. Fisher, and C. Solbrig designed, constructed, and operated the hot jet and thrust facilities.

ABSTRACT

Far field sound pressure levels were measured in an anechoic room for noise generated by cold air flow through a wide variety of small nozzle configurations. These nozzles included converging, converging-diverging, annular plug, annular center core flow, and ejector types. The results are examined in terms of mass flow and acoustic power performance. Thrust determinations were made for selected nozzles showing good acoustic performance, permitting an ultimate evaluation of their acoustic performance in terms of their thrust performance. Optimized nozzles from each of four nozzle configurations are recommended for a full-scale evaluation. These are a plug, a center core flow, a converging-diverging, and a converging-diverging plug nozzle. The noise generated by hot air flow through a converging nozzle was determined, enabling only partial corroboration of the scaling technique developed in a previous study. One of the recommended nozzle types, the plug nozzle, was investigated under hot flow conditions and its acoustic performance was found to remain superior to that of a converging nozzle.

Publication of this technical documentary report does not constitute Air Force approval of the report's findings or conclusions. It is published only for the exchange and stimulation of ideas.

TABLE OF CONTENTS

TABLES

ILLUSTRATIONS

ILLUSTRATIONS (Continued)

ILLUSTRATIONS (Continued)

ILLUSTRATIONS (Continued)

ILLUSTRATIONS (Continued)

SYMBOLS AND UNITS

The English system of units will be used and those assigned to the symbols are directly applicable to theoretical formulation and graphical coordinates unless specifically stated otherwise.

Symbol	Units	Definition
A	ft^2	Exit area of nozzle
A_a	ft^2	Annulus area of nozzle
A_b	ft^2	Area of solid bar
A_c	ft^2	Center core area of nozzle
A_m	ft^2	Minimum area of nozzle
C_1	---	Normalization factor
C_4	---	Normalization factor
c	fps	Velocity of sound at nozzle exit
c_o	fps	Velocity of sound for ambient conditions
D	ft	Diameter of nozzle exit
F	lb	Thrust
f	cps	frequency
K	---	Constant for eighth power relations (assumed equal to 4.5×10^{-5})
k	---	Sound survey azimuth station number
L	ft	Nozzle length
M	---	Mach number
M_o	---	Mach number in terms of fully expanded flow pressure ratio, Eq. (45)
m	slugs/sec	Mass flow
n	---	Total number of sound survey stations
P	watts	Acoustic power

SYMBOLS AND UNITS (Continued)

Symbol	Units	Definition
PWL	decibels re 10^{-13} watts	Sound power level
p	psfa	Pressure at nozzle exit
p_k	dynes/cm^2	Sound pressure at azimuth station k
p_o	lb/ft^2	Ambient pressure
p_s	psfa	Stagnation or total pressure
R	ft^2/sec x °R)	Ideal gas constant
SPL	decibels re 0.0002 dynes/cm^2	Sound pressure level
s_k	ft^2	Incremental surface area at azimuth station k
T	°R	Temperature at nozzle exit
T_o	°R	Ambient temperature
T_s	°R	Stagnation or total temperature
U	fps	Average nozzle exit velocity
V	ft^3	Volume of air storage system
α	degrees	Incremental azimuth angle
γ	---	Specific heat ratio
θ	degrees	Azimuth direction angle
ρ	slugs/ft^3	Density at nozzle exit
$\rho_o c_o$	rayles	Characteristic impedance of air

SECTION I

INTRODUCTION AND SUMMARY

The research reported in the following sections is an extension of the work reported in references 1, 2, 3, and 4 with major emphasis on that of reference 4. During the period of this latter work, a large number of model cold air jet nozzles were examined in terms of both their acoustic and their flow performance. These nozzles included converging, converging-diverging, and annular types with and without center core flow. Engineering expressions for flow and acoustic performance were developed for both size and temperature, which showed good agreement between small cold jet nozzles, large hot jet nozzles, and jet engines.

Some of the nozzles examined during that study showed considerable potential in regard to their acoustic performance, and it was the major aim of this program to optimize these nozzles, as well as to examine further types of nozzles and optimize any of these exhibiting similar acoustic potential. In addition to fulfilling the above objectives in this program, we have redeveloped the flow expressions for nozzles and attempted to consolidate the previously developed normalizing techniques by carrying out a selected hot jet nozzle program and searching for large hot jet and jet engine data. Furthermore, consideration has been given to other problems, such as the roughness effect in nozzles, and the screech effect.

The approach to the task of optimizing a nozzle of any particular nozzle configuration, for example an annular plug nozzle, may be made in either of two ways. A theoretical approach may be developed by which the noise produced by a nozzle may be described in terms of characteristics of the nozzle and the flow, such as the ratio of the plug dimension to the basic nozzle, or the flow velocity. Examination of any such theory should then lead to an optimum nozzle design. The alternative approach is an empirical one in which each characteristic of the nozzle or flow is modified in turn in a logical and ordered manner and the effects on the acoustic performance of the nozzle observed. The advantages of the former theoretical approach to the problem of nozzle optimization are obvious. However, to date, the theoretical approach to the jet noise problem has produced small return for the considerable effort involved. In the study reported in reference 4, a theory was forwarded which attempted to explain the improved acoustic performance of annular plug nozzles compared to converging nozzles. Further consideration of this theory

---

Manuscript released by author 31 December 1964 for publication as an RTD Technical Report.

in the current program has shown that erroneous assumptions were made in its development and that it is, therefore, no longer tenable. Consequently, this current study has adopted the empirical approach as one which shows more promise of achieving the objectives of the program. However, there exist practical limitations to this approach. The nozzles which were examined in the study reported in reference 4 were frequently composite nozzles being constructed from interchangeable basic units, enabling large numbers of nozzle configurations to be produced using only a small number of these basic nozzle units. There is a limit to the number of composite nozzles which can be assembled in such a manner. If, for example, one were attempting to discover the effect of the ratio of the diameter of the plug to the diameter of the basic nozzle on the acoustic performance of an annular plug nozzle, one might require a large number of plugs, each having a different radius, for any given basic nozzle. Similarly, extending this reasoning to include the other parameters of nozzles which might be anticipated to affect acoustic performance, one sees that the number of basic nozzle units required and the time involved in performing the experimental study precludes the adoption of such an extensive empirical study in this program. Consequently, the empirical approach adopted in this study, while being far from the most desirable, since it is based on very limited studies aided by educated guesswork, is the most practical approach to the problem available to us.

This approach has enabled a limited study to be made of each of a number of different types of nozzle. Together with the results of nozzles investigated in the work reported in reference 4, an acoustic evaluation of nozzles in terms of mass flow performance, and to a limited extent, thrust performance, has been made. This has led to our recommending a full-scale study of four types of model jet nozzles which show good acoustic potential.

SECTION II

EXPERIMENTAL FACILITY

Three separate facilities have been utilized in this program. They are:

a) a jet noise facility utilizing an anechoic room for 'cold' measurements,

b) a jet noise facility located outdoors for 'hot' measurements, and

c) a thrust facility.

The cold jet noise facility is shown in Figs. 1(a) through (d). The facility is of the blowdown type where compressed air was dried, filtered, and stored in tanks having a total volume of 80 cubic feet at a maximum pressure of 125 psig. The stored air was released by a manually controlled, 3-inch, quick-opening ball valve where it then successively passed through a 3-inch pressure reducing valve, a 4-inch flexible tube through the wall of the anechoic room, a calming tank, and a nozzle. The pressure-reducing valve is capable of precisely controlling the pressure in the calming tank from 2 to 60 psig. The 16-inch diameter by 39-inch long calming tank contains six fine mesh woven wire screens designed to minimize the turbulence generated by air flow through piping and valves. Temperature and pressure sensors, located in the calming tank between the screens and nozzle, were remotely monitored at the control station located outside the anechoic room. Because of the large ratio of calming tank diameter to nozzle diameter, stagnation conditions were maintained in the tank with an error less than 0.1%.

Mass flow through all nozzles was measured by timing the pressure decrease in the storage tanks. Over-all sound pressure levels were measured at seven stations located in a horizontal plane and on a circular arc having a radius of 88-inches measured from the nozzle exit as shown in Fig. 1(d). The stations have an angular separation of 15 degrees and are located at the 15 through 105 degree angles where 0 degrees is considered to be the downstream jet axis. One microphone was used; consequently, seven air flow runs were required for one survey, moving the microphone from station to station between runs. The microphone was a Brüel and Kjaer, type 4136. This microphone replaces that used in the study reported in reference 4, and enables acoustic measurements to be made to significantly higher frequencies. The microphone used in the study of reference 4 had a 16 kc/s response, while the Brüel and Kjaer microphone response is flat to 40 kc/s in the particular manner in which it is mounted. Over-all acoustic pressure levels were monitored using the linear setting on a

Brüel and Kjaer 1/3 octave band analyzer, type 2112. Repeatability of pressure, temperature, and sound was excellent. The acoustic environment was essentially free-field as the air jet exhausted into and the sound pressure measurements were made in an anechoic room having a usable volume of about 1600 cubic feet with a lower cut-off frequency of about 130 c/s.

The outdoor jet noise facility shown in Fig. 1(e), with which hot jet noise measurements were made, is located on the roof of a four-story building. The calming tank is situated close to the edge of the roof, and acoustical absorbent material covers the roof in the vicinity of the tank. No buildings or other obstructions are located in the immediate vicinity of the facility, so that an assumption of free-field conditions is a reasonable one. This is borne out by cold jet measurements made with the facility.

A Solar-Mars gas turbine combustor, burning No. 2 grade fuel oil, is attached to the inlet end of the calming tank to heat the incoming air to the desired temperature. The compressed air facility was of sufficient capacity, 1000 scfm at 100 psi, to enable continuous running of the system under almost all the required operating conditions. No screens were located in the calming tank, which was constructed from a 6-foot length of 6-inch diameter pipe, because of the large amount of soot produced during the initial ignition period. Pressure and temperature sensors located in the calming tank enabled the gas conditions to be monitored. Mass flow rates were not determined experimentally, but were calculated from knowledge of the gas pressure and temperature. Over-all sound pressure levels were measured at the same seven station positions as those used in the anechoic facility, using a boom to position the microphone over the edge of the roof.

Tape recordings of the noise of the jet for a few selected operating conditions were made using an Ampex AR200. Direct recording at 15 ins/sec was used and the response of the recorder was $\pm$ 3 db from 300 c/s through 60 kc/s. One-third octave band analysis was performed of signals on tape loops replayed through an Ampex FR1100 using a Brüel and Kjaer 1/3 octave band analyzer, type 2112, and narrow band analysis (3 cycles bandwidth) was performed using a Hewlett-Packard wave analyzer, type 302A.

The thrust facility shown in Fig. 1(f) consists of a calming tank, identical to that used in the cold jet facility, suspended from flexible cantilever plates and connected to an air supply by means of a flexible pipe. The air is supplied from a 1000 scfm at 100 psi compressor, allowing continuous running. The thrust system is calibrated by means of weights suspended from a cord which passes over a pulley and which is attached to the calming tank.

The nozzles investigated in this program include converging, converging-diverging, annular plug, center core flow, ejector, and rough nozzles. However, all the composite nozzles investigated were assembled from elementary units consisting of basic nozzles, bars, and terminations. The numbering system of those nozzles examined in reference 4 has been revised in order to establish a system capable of logical growth. Although composite nozzles have a cumbersome number designation, they are both logical and descriptive. Tables I and II list the nozzles, bars, and terminations used during this program. Composite nozzle numbers consist of a series of numbers separated by colons. The first number, 1, 2, 3, or 4, indicates whether the composite nozzle is an annular plug, center core flow, ejector, or rough nozzle, respectively. The rest of the numbers represent the information given in columns two through five respectively of Tables III through VI. Hence, composite nozzle designation numbers define the nozzle completely.

When reference is made in this report to those nozzles examined in reference 4, the nozzle number adopted in that report is given together with the new number, using current nomenclature, in parentheses.

SECTION III

PERFORMANCE REPRESENTATION AND MEASUREMENT TECHNIQUE

To facilitate comparison between the results of this program and those reported in reference 4, so that over-all conclusions and recommendations can be made based on both studies, we have continued to determine and represent nozzle performance in the manner reported in reference 4. However, we have modified, and added to, the representation of nozzle performance where we have felt this to be necessary. One modification consists of a reconsideration of the area which we adopt to be representative of any nozzle. In all nozzle configurations, the characteristic area has been chosen to be the minimal flow cross-sectional area (A_m). This replaces the scheme adopted in reference 4, in which for center core flow nozzles the characteristic area adopted was the minimal flow area (A_m), but in all other configurations the exit area of nozzles was used (A). The reasoning upon which this is based is described in Section IV.

The representation of acoustic performance of nozzles relative to their mass flow rate might be criticized on the grounds that it is neither a meaningful nor a realistic method of comparing the acoustic performance of nozzles. Our contention has been that the nozzle performance representation is in terms of parameters which our system enabled us to measure with a high degree of accuracy and not in terms of theoretical or calculated parameters. Thus, nozzle performance relates the over-all acoustic power generated by a nozzle of a given cross section to the mass flow rate through that nozzle and not in terms of velocity or thrust or Lighthill parameter. We have been able to extend our measuring program to include the measurement of thrust in a limited number of cases so that our final recommendations are based on the acoustic performance in terms of both mass flow rate and thrust.

Therefore, the quantities of interest for this program are pressure ratio (p_s/p_o), mass flow (m), thrust (F), acoustic power level (PWL), sound pressure level (SPL) at various azimuthal stations, frequency (f), and stagnation temperature (T_s). From measurement of the above quantities, it is the objective of the program to:

a) determine the noise-generating capabilities of various nozzle configurations in addition to those examined in reference 4;

b) optimize those nozzles which show potential of producing a more desirable acoustic performance than a conventional converging nozzle, bearing in mind the

practicalities and limitations of scaling up these nozzles to practical operational nozzles;

c) recommend the full-scale evaluation of those nozzles whose acoustic performance is found to be good; and

d) corroborate those normalizing parameters developed in reference 4 which permit scaling for both size and temperature.

To aid in achieving these objectives, nozzle performance is represented by the following types of graphs:

1. Mass flow versus pressure ratio

$$\frac{m}{A_m} \text{ versus } \frac{p_s}{p_o}$$

2. Power level versus mass flow

$$PWL - 10 \log A_m \text{ versus } m/A_m$$

3. Thrust versus pressure ratio

$$F/A_m \text{ versus } p_s/p_o$$

4. Power level versus thrust

$$PWL - 10 \log A_m \text{ versus } F/A_m$$

In addition, some limited data is represented on graphs plotting directionality, power spectral distribution, and normalized performance of hot jet nozzles.

MASS FLOW MEASUREMENTS

Mass flow through all nozzles was determined by measuring air storage pressures and temperatures and the time rate of change of each for a condition of constant stagnation pressure and temperature. For a blowdown system, the mass flow of the evacuating fluid can be expressed as

$$m = - V \frac{d\rho}{dt} \tag{1}$$

where V is the volume of the storage system, ρ is the density of the stored fluid, t is time, and the negative sign indicates fluid loss. For an ideal gas,

$$\rho = \frac{p}{RT} \tag{2}$$

where p and T are the pressure and temperature, respectively, of the stored fluid, and R is the ideal gas constant. Then

$$m = - \frac{V}{R} \frac{d}{dt} \left| \frac{p}{T} \right| \tag{3}$$

and

$$\frac{d}{dt} \left| \frac{p}{T} \right| = - \frac{mR}{V} = C \tag{4}$$

which is a constant for any controlled blowdown run. Then

$$\frac{p}{T} = Ct + C_1 \tag{5}$$

When $t = 0$, then $p = p_2$ and $T = T_2$, where p_2 and T_2 are the pressure and temperature, respectively, in the storage system at the beginning of the constant mass flow run. Therefore,

$$C_1 = \frac{p_2}{T_2} \tag{6}$$

and

$$\frac{p}{T} = Ct + \frac{p_2}{T_2} \tag{7}$$

When $t = \Delta t$, then $p = p_1$ and $T = T_1$, where p_1 and T_1 are the pressure and temperature, respectively, in the storage system at the end of the constant mass flow run. Therefore,

$$C = \frac{1}{\Delta t}\left(\frac{p_1}{T_1} - \frac{p_2}{T_2}\right) = -\frac{mR}{V} \tag{8}$$

and

$$m = 5.83 \times 10^{-4}\,\frac{V}{\Delta t}\left(\frac{p_2}{T_2} - \frac{p_1}{T_1}\right) \tag{9}$$

where

$$R = 1716\ ft^2/(sec^2 \times {}^\circ R) \tag{10}$$

for air. Hence, the mass flow for any controlled flow condition is readily obtained from measurements of pressures and temperatures of the stored air and the length of time of the controlled run, and knowledge of the volume of the storage system.

NOISE MEASUREMENTS

For an axially symmetric but directional source, the sound pressure p is a function of the azimuth angle θ. The procedure for determining the acoustic power is to measure p at a sufficient number of stations to ensure small measurement error and use a numerical integration process. Thus

$$P = \frac{1}{\rho_o c_o} \sum_{k=1}^{n} p_k^2 s_k \tag{11}$$

where P is the acoustic power and p_k and s_k are the sound pressure and incremental surface area, respectively, at station k. The total number of equally spaced survey stations around a hemisphere at the equator including those at the poles is given by

$$n = \frac{\pi}{\alpha} + 1 \tag{12}$$

where α is the constant increment angle. For $\rho_o c_o$ in rayles (dyne sec/cm^3), p in dynes per square centimeter, and s in square feet,

$$P = \frac{930 \times 10^{-7}}{\rho_o c_o} \sum_{k=1}^{n} p_k^2 s_k \tag{13}$$

For sound pressure level referred to 2×10^{-4} dynes per square centimeter and power level referred to 10^{-13} watts,

$$PWL = 10 \log \left(\frac{37.2}{\rho_o c_o} \sum_{k}^{n} s_k \text{ antilog } \frac{SPL_k}{10} \right) \tag{14}$$

The incremental surface areas are given by

$$s_1 = s_n = 2\pi r^2 \left(1 - \cos \frac{\alpha}{2} \right) \tag{15}$$

$$s_k = 4\pi r^2 \sin \frac{\alpha}{2} \sin \theta_k \tag{16}$$

where r is the radius from the nozzle exit to each measurement station and s_1 and s_n represent the polar areas.

For this program, the following conditions were chosen:

$$\begin{aligned} T_o &= 70°F \\ p_o &= 14.7 \text{ psi} \\ \rho_o c_o &= 40.6 \text{ rayles} \\ r &= 88 \text{ inches} = 7.33 \text{ feet} \\ \alpha &= 15° \end{aligned} \tag{17}$$

and stations 2 through 8 were considered to be the only significant contributors to sound. Hence,

$$PWL = 10 \log \sum_{k=2}^{8} s_k \text{ antilog } \frac{SPL_k}{10} \tag{18}$$

where

$$s_k = 88.2 \sin \theta_k \tag{19}$$

SECTION IV

THEORETICAL PREDICTIONS

MASS FLOW AND THRUST

In continuation of the philosophy expressed in reference 4, we represent performance data in graphical form where both ordinate and abscissa consist of measured quantities and are not in terms of any parameters which are theoretical or which we have not experimentally determined. However, theoretical performance curves are superimposed on graphs for comparison purposes. These theoretical performance curves are based upon isentropic ideal gas flow assumptions utilizing the following basic equations:

Equation of State

$$p = C\rho^{\gamma} \tag{20}$$

Ideal Gas Relations

$$p = R\rho T \tag{21}$$

$$c^2 = \gamma RT \tag{22}$$

Euler Equation of Motion for Steady Flow

$$\frac{\partial U}{\partial x} + \frac{1}{\rho} \cdot \frac{\partial p}{\partial x} = 0 \tag{23}$$

The development from these basic equations of the flow performance of nozzles is routine. The following relationships are reproduced in the form in which they appear in reference 4.

$$\frac{m}{A} = \left(\frac{\gamma}{RT_s}\right)^{1/2} p_o\left(\frac{p_s}{p_o}\right) M\left(\frac{\gamma - 1}{2} M^2 + 1\right)^{-\frac{\gamma + 1}{2(\gamma - 1)}} \tag{24}$$

$$\frac{F}{A} = \gamma p_o \left(\frac{p_s}{p_o}\right) M^2 \left[\frac{\gamma - 1}{2} M^2 + 1\right]^{-\frac{\gamma}{\gamma + 1}} \tag{25}$$

where

$$M = \frac{U}{c} = \left(\frac{2}{\gamma - 1}\right)^{1/2} \left[\left(\frac{p_s}{p_o}\right)^{\frac{\gamma - 1}{\gamma}} - 1\right]^{1/2} \tag{26}$$

The above relations are general in the sense that they depend upon stagnation temperature and nozzle exit pressure. The equations for mass flow and thrust are then degenerated to the case where stagnation temperature and exit pressure are assumed equivalent to ambient conditions. The designation "fully expanded flow" is given to this assumption. That is, for

$$\left.\begin{aligned} T_s &= T_o = 530°R \\ p &= p_o = 2117 \text{ psfa (fully expanded)} \\ R &= 1716 \text{ ft}^2/(\text{sec} \times °R) \\ \gamma &= 1.4 \end{aligned}\right] \tag{27}$$

mass flow and thrust are given by

$$\frac{m}{A} = 2.63 \left(\frac{p_s}{p_o}\right) M_o \left(\frac{M_o^2 + 5}{5}\right)^{-3} \tag{28}$$

$$\frac{F}{A} = 2970 \left(\frac{p_s}{p_o}\right) M_o^2 \left(\frac{M_o^2 + 5}{5}\right)^{-7/2} \tag{29}$$

where

$$M_o = 5^{1/2} \left(\left(\frac{p_s}{p_o}\right)^{2/7} - 1\right)^{1/2} \tag{30}$$

Fully expanded flow assumptions may be realistic below critical pressure ratios, but should not be expected to hold for nozzles operated at pressure ratios exceeding this value, except for converging-diverging nozzles operated at design pressure ratios. Assume, for a converging nozzle, that the assumption, fully expanded flow, is valid below Mach unity, which is further assumed to be the upper limit of velocity. Then we have

$$\frac{m}{A} = 2.63 \frac{p_s}{p_o} M_o \left(\frac{M_o^2 + 5}{5} \right)^{-3} \qquad 0 < M_o \leq 1 \tag{31}$$

$$\frac{m}{A} = 1.523 \frac{p_s}{p_o} \qquad M_o \geq 1 \tag{32}$$

The theoretical curve proves to be in excellent agreement with measured jet data for converging nozzles as reported in reference 4.

Using the same reasoning as was used for mass flow, the equations for thrust are

$$\frac{F}{A} = 2970 \frac{p_s}{p_o} M_o^2 \left(\frac{M_o^2 + 5}{5} \right)^{-7/2} \qquad 0 < M \leq 1 \tag{33}$$

$$\frac{F}{A} = 1570 \frac{p_s}{p_o} \qquad M \geq 1 \tag{34}$$

This latter equation, reported in reference 4, is incorrect, since no allowance is made for the pressure thrust effect. A converging nozzle operated at pressure ratios exceeding 1.89 has a velocity thrust term, as expressed above, but also has an additional pressure thrust term due to the difference between the exit and ambient pressure.

The exit pressure of a converging nozzle operated above the critical pressure ratio is

$$p = \left(\frac{2}{\gamma + 1}\right)^{\frac{\gamma}{\gamma - 1}} p_o \left(\frac{p_s}{p_o}\right)$$

$$= .5283\, p_o \left(\frac{p_s}{p_o}\right)$$

$$= 1118.4 \left(\frac{p_s}{p_o}\right) \qquad M \geq 1 \qquad (35)$$

So

$$p - p_o = \frac{p_s}{p_o}\left(1118.4 - \left(\frac{p_o}{p_s}\right) \cdot p_o\right) \qquad M \geq 1 \qquad (36)$$

Therefore, the additional thrust term for a converging nozzle produces a total thrust of

$$\frac{F}{A} = 1570 \frac{p_s}{p_o} + (p - p_o)$$

$$= \left(1570 + 1118.4 - 2117 \frac{p_o}{p_s}\right) \frac{p_s}{p_o}$$

$$= \left(2688.4 - 2117 \frac{p_o}{p_s}\right) \frac{p_s}{p_o} \qquad M \geq 1 \qquad (37)$$

It is of value at this stage to discuss how these flow performance equations are interpreted for converging-diverging nozzles. The work of reference 4 treated the converging-diverging nozzle with the exit area regarded as the characteristic area. However, if we are comparing the flow performance of the converging and the converging-diverging nozzle, it may be more meaningful to adopt a minimal cross-sectional flow area. Certainly, in cases where nozzles are operated at pressure ratios exceeding the critical pressure ratio, the mass flow of a nozzle, operated at a given pressure ratio, is governed solely by the minimal flow area, since it is at this section of the nozzle that choking occurs and the flow velocity becomes Mach unity. The purpose of the divergent section of a converging-diverging nozzle is to allow complete pressure recovery, allowing the exit pressure of

the flow to attain ambient value and so obtain maximum thrust, when the nozzle is operated at the design pressure ratio. Consequently, equations 31 and 32 might justifiably be rewritten as

$$\frac{m}{A_m} = 2.63 \frac{p_s}{p_o} M_o \left(\frac{M_o^2 + 5}{5} \right)^{-3} \qquad 0 < M \leqslant 1 \tag{38}$$

$$\frac{m}{A_m} = 1.523 \frac{p_s}{p_o} \qquad M_o > 1 \tag{39}$$

These equations will then be valid for both converging and converging-diverging nozzles as is borne out by experiment as shown, for example, in Figs. 3(a) and (c). Figures 3(b), (d), (e), and (f) show that these equations are equally applicable to annular plug and center core flow nozzles.

It may be noted that the area ratio for a converging-diverging nozzle operating at a design pressure ratio of p_s/p_o is

$$\frac{A}{A_m} = \frac{\left(\frac{2}{\gamma + 1} \right)^{\frac{1}{\gamma - 1}} \left(\frac{p_s}{p_o} \right)^{\frac{1}{\gamma}}}{\left[\frac{\gamma + 1}{\gamma - 1} \left(1 - \left(\frac{p_s}{p_o} \right)^{\frac{1 - \gamma}{\gamma}} \right) \right]^{1/2}}$$

$$\frac{A}{A_m} = \frac{0.5786}{M_o \left(\frac{M_o^2 + 5}{5} \right)^{-3}} \tag{40}$$

This explains why a converging-diverging nozzle operated only at the design pressure ratio was noted, in reference 4, to have a measured mass flow equal to that given by equation 31. In reference 4, the characteristic converging-diverging nozzle area was taken to be A, the exit area.

Consequently, equation 31 may be rewritten for a converging-diverging nozzle using expression 40

$$\frac{m}{A} = 2.63 \left(\frac{p_s}{p_o} \right) M_o \left(\frac{M_o^2 + 5}{5} \right)^{-3}$$

$$= 2.63 \frac{p_s}{p_o} \cdot \frac{A_m}{A} (0.5786)$$

$$= 1.523 \frac{p_s}{p_o} \frac{A_m}{A} \qquad (41)$$

Equation 41 may be expressed as

$$\frac{m}{A_m} = 1.523 \frac{p_s}{p_o}$$

which is the form of equation 39 and is further evidence of the correctness of the modified mass flow relationships as applied to both converging and converging-diverging nozzles. Similarly, equation 33 for thrust is shown later in this report to hold only at the design pressure ratio for a converging-diverging nozzle. Thus, if we transform equation 33 to one in terms of the minimal flow area, using equation 40, it becomes

$$\frac{F}{A_m} = \frac{F}{A} \cdot \frac{A}{A_m}$$

$$= 3843 \frac{p_s}{p_o} \left(1 - \frac{p_s}{p_o}^{-2/7} \right)^{1/2} \qquad (42)$$

This represents the true thrust expression for converging-diverging nozzles at design pressure and is approximately numerically equal to equation 37 in the range of interest, i.e., up to pressure ratios of 5. The numerical value increases above that for the converging nozzle as the pressure ratio increases. For example, at a pressure ratio of 10, the two expressions have numerical values for F/A_m of 26,690 and 24,767. Consequently,

we infer that the converging-diverging nozzle has significant advantage over the converging nozzle only for large values of design pressure ratio. At lower design pressure ratios, the two types of nozzle have almost identical thrust performance.

In summary, then, we are adopting the following flow equations as being equally applicable to converging and converging-diverging nozzles:

$$\frac{\dot{m}}{A_m} = 2.63 \frac{p_s}{p_o} M_o \left(\frac{M_o^2 + 5}{5} \right)^{-3} \qquad 0 < M \leqslant 1 \qquad (43)$$

$$\frac{\dot{m}}{A_m} = 1.523 \frac{p_s}{p_o} \qquad M_o \geqslant 1 \qquad (44)$$

where

$$M_o = 5^{1/2} \left(\frac{p_s}{p_o}^{2/7} - 1 \right)^{1/2} \qquad (45)$$

and A_m represents the minimal flow cross section of a nozzle. Also,

$$\frac{F}{A_m} = 2970 \frac{p_s}{p_o} M_o^2 \left(\frac{M_o^2 + 5}{5} \right)^{-7/2} \qquad 0 < M \leqslant 1 \qquad (46)$$

$$\frac{F}{A_m} = \left(2688 - 2117 \frac{p_o}{p_s} \right) \frac{p_s}{p_o} \qquad M \geqslant 1 \qquad (47)$$

This latter equation is applicable to the converging nozzle, while the expression for the converging-diverging nozzle at design is

$$\frac{F}{A_m} = 3843 \frac{p_s}{p_o} \left(1 - \frac{p_s}{p_o}^{-2/7} \right)^{1/2} \qquad M \geqslant 1 \qquad (48)$$

However, both these expressions are numerically equal to within 2% up to a pressure ratio of 5. These equations for mass flow and thrust for both converging and converging-diverging nozzles are shown in Figs. 2(a) and (b).

ACOUSTIC POWER

Acoustic power representation of nozzle performance is in terms of measured parameters, the acoustic power level, and mass flow. Theoretical curves will be superimposed for comparison only. The theoretical relation which was adopted for both the previous and the current study is

$$\frac{P}{A} = K \frac{\rho_o U^8}{c_o^5} \tag{49}$$

When isentropic flow relations previously developed are used, then

$$\frac{P}{A} = 204 \left(\frac{p_s}{p_o} \right)^{-8/7} M_o^8 \tag{50}$$

when

$$\left.\begin{aligned} K &= 4.5 \times 10^{-5} \\ T_s &= T_o = 530°R \\ p &= p_o = 2117 \text{ psfa (fully expanded)} \\ R &= 1716 \text{ ft}^3/(\text{sec} \times °R) \\ \gamma &= 1.4 \end{aligned}\right] \tag{51}$$

This expression is superimposed on all acoustic performance graphs as a broken curve.

STROUHAL AND MODIFIED STROUHAL NUMBER

The study reported in reference 4 showed that in order to successfully normalize the spectral distribution of the noise generated by a jet the conventional Strouhal number had to be modified.

The dimensionless Strouhal number is defined as

$$S = \frac{f \cdot D}{U} \tag{52}$$

where f is the frequency, D is a characteristic dimension, such as exit diameter, and U is the average exit velocity.

For fully expanded flow this may be re-expressed using flow equations as

$$S = \frac{p_o}{RT_o} \frac{fD}{\left(\frac{m}{A}\frac{T_s}{T_o}\right)} \left(\frac{p_s}{p_o}\right)^{\frac{\gamma - 1}{\gamma}} \tag{53}$$

The modified Strouhal number used in reference 4 was

$$S_m = \frac{fD}{\left(\frac{m}{A}\frac{T_s}{T_o}\right)^{1/2}} \left(\frac{p_s}{p_o}\right)^{\frac{\gamma - 1}{\gamma}} \tag{54}$$

SECTION V

MEASURED RESULTS

MASS FLOW

The mass flow performance of every nozzle that was examined acoustically in this program was determined in the manner reported in Section III. The flow performance of all nozzles examined was found to agree with theoretical predictions to better than 2% except in a few cases of very long nozzles or nozzles having small annular flow areas where the flow rate was less than predicted, but these differences were always less than 10%. In general, these differences were small, and consequently, flow performances shown in Figs. 3(a) through (f) are only for a few selected nozzles of each nozzle configuration. However, it must be stressed that although the flow performances of only a few nozzles are shown, the mass flow performance of every nozzle was determined as a function of pressure ratio and was used in the evaluation of the acoustic power performance of nozzles. Thus, acoustic performance of nozzles is thereby measured in terms of the experimentally determined flow rate and not the calculated flow rate for any given pressure ratio. Figure 3(a) shows the flow performance of four geometrically similar converging nozzles (N01, N02, N03, and N04). Figure 3(b) shows the flow performance of a typical extended converging nozzle (N50:NT31). Figure 3(c), showing the flow performance of a converging-diverging nozzle (N63), supports our contention that the characteristic area of a converging-diverging nozzle should be the minimal or throat area. Figures 3(d) and (f) show the flow performance of plug nozzles utilizing a converging and a converging-diverging nozzle respectively. Figure 3(e) shows the flow performance of a typical annular nozzle with center core flow (2:04:51:31 + 0).

ACOUSTIC POWER OF COLD JET FLOW NOZZLES

The acoustic power performance of all nozzles operated using the cold jet facility is shown in Figs. 4, 5, 6, 7, 8, 9, and 10, the nozzles being categorized as basic and extended converging nozzles, annular plug nozzles, annular center core flow nozzles, ejector nozzles, converging-diverging nozzles, converging-diverging plug nozzles and "rough" nozzles.

Basic and Extended Converging Nozzles

Because of the adoption of a microphone having a higher frequency response than that of the microphone used in the study reported in reference 4 (40 kc/s and 16 kc/s respectively), the acoustic performance of the geometrically matched set of converging nozzles was remeasured in order to determine whether any significant amount of acoustic energy generated by these nozzles escaped detection by the microphone used in the previous study. Figures 4(a) and (b) show the results for nozzles N01 and N02. Square symbols represent measurements made in the previous program, and circle symbols pertain to measurements made for this program. The results show that the lower frequency response microphone used in the previous study was adequate for acoustic measurements of basic converging nozzles.

Reconsideration of the curve adopted as the average for the acoustic performance of basic nozzles in the previous program has led to the adoption of a new average curve which does not give weight to the results obtained with nozzle N00 because of the poor flow performance of this small nozzle and associated doubtful acoustic performance compared to that of the larger nozzles, N01, N02, and N03 (see Fig. 3(a), reference 4).

Figure 4(c) shows the acoustic performance of a converging nozzle, N04, constructed for this program, the largest that can be operated satisfactorily at a sufficiently high pressure ratio with our flow system. Figure 4(d) shows the curve of acoustic performance which has been adopted as representing the average of the acoustic performance of basic converging nozzles (N01, N02, N03, and N04) together with the broken curve for acoustic power given by equation 50. These two curves will be superimposed upon all other acoustic power curves for comparison purposes. Figures 4(e) through (i) show the performance of basic converging nozzles with long extensions which were designed for use in center core flow nozzles. The basic nozzles, N50 and N51, are identical except that N50 is one inch longer than N51. The termination NT30 is a straight termination but NT31 is convergent, so that the choking of nozzles utilizing this latter termination occurs at the exit plane of this termination. The acoustic performance of the shortest of these extended converging nozzles (N50 and N51:NT30, shown in Figs. 4(e) and (g)) compares closely to that standard converging nozzle curve; but a longer nozzle (N50:NT31) is seen in Fig. 4(h) to show a slight departure from the curve at high flow rates.

Annular Plug Nozzles

The annular plug nozzle, designated 347 (1:03:30:30 + 2) in the previous program, was reinvestigated in this program, and Fig. 5(a) shows its performance compared to that measured during the previous program. This redetermination shows that, over the entire range of operation, a considerable amount of energy was escaping detection (approximately 4 db over the majority of the range). This annular plug nozzle is now re-evaluated to be a maximum of only 10 db superior in performance to a converging nozzle. Study of the performance of annular plug nozzles examined during the previous program shows that those nozzles exhibiting superior acoustic performance had a large value of the ratio of plug diameter to basic nozzle diameter. Subsequently, a smaller total mass flow rate relative to the over-all physical size of the nozzle is produced. Consequently, a nozzle whose ratio of plug diameter to outer basic nozzle diameter is small, commensurate with good acoustic performance, is desirable. Estimates of the limiting value of this ratio were used in designing nozzle 1:04:40:40 + 0, whose acoustic performance is shown in Fig. 5(b). Any further decrease in the ratio would lead to reduced acoustic improvement over converging nozzles. The effect of extending the plug out of the basic nozzle is shown in Figs. 5(c) and (d). Only slight differences in acoustic performance between these nozzles may be noted. Figures 5(b), (e), (f), (g), and (h) show how the contouring of the plug termination affects the acoustic performance of the nozzle. The contoured terminations had straight, convex, concave, convex-concave, or exponential profiles. Little difference in acoustic performance is apparent between these various plug nozzles, except that in case of the concave and exponential plug nozzle terminations, deterioration is apparent (Figs. 5(f) and (h)). The exponential termination could be expected to produce deterioration in the acoustic performance of a plug nozzle because of the abrupt ending to this plug termination. The deterioration in the case of the concave termination plug nozzle is less easy to explain, but it is interesting to note that acoustic performance deterioration is concurrent with decrease in over-all profile cross section. The results of these studies indicate that no significant loss in acoustic performance occurs for change of plug termination profile except for the case of the concave profile section, where considerable deterioration in acoustic performance occurred at very high flow rates ($m/A > 5$). These studies of the plug nozzle, together with those performed in the previous study, are sufficient to enable an evaluation of the potential of plug nozzles.

Annular Center Core Flow Nozzles

Of those center core flow nozzles examined in the previous study, nozzle 274 (2:02:44:20 + 0) was considered to have a good acoustic performance. Figure 6(a) shows our current re-evaluation of this nozzle using the high frequency microphone. This shows that at flow rates above the choked flow condition (m/A> 2.88), the results of the two studies are identical. However, it may be noticed that below this point, in the subsonic flow regime, the nozzle's acoustic performance is now found to be poor compared to a converging nozzle. We may attribute this to aeolian tone generation as was noted in other center core flow nozzles examined in the previous study (reference 4, p. 27). It was anticipated in reference 4 that this particular nozzle would exhibit this poor acoustic performance in the subsonic flow range when measured with a higher frequency microphone than that used in that study. Figures 6(b) and (c) show the performance of two center core flow nozzles, 2:04:51:30 + 0 and 2:04:44:20 + 0 respectively, with smaller values of the ratio of the inner nozzle diameter to the basic converging nozzle diameter (equivalent to the parameter which appeared important for evaluating the performance of the annular plug nozzles). The acoustic performance at flow conditions above choking does deteriorate as this ratio decreases in a manner similar to that for annular plug nozzles. Figure 6(d) shows the performance of the best of the center core flow nozzles with an extension of the inner nozzle further downstream of the basic nozzle, forming nozzle 2:02:44:20 + 1.625. It is seen there is little or no change in acoustic performance with this extension by comparison with Fig. 6(a), except in the subsonic flow range where the acoustic performance improves, presumably due to a decrease in the aeolian tone contribution. Figure 6(e) shows the performance of a center core flow nozzle with an extension of the inner nozzle further downstream out of the basic nozzle. With the previously examined extended nozzle, 2:02:44:20 + 1.625, the nozzle's acoustic performance was identical to that of the unextended nozzle in the choked flow region, but with this latter extended nozzle, 2:04:50:30 + 1.0, a slight improvement is noted (Fig. 6(b)) over the unextended nozzle, 2:04:50:30 + 0. An increased improvement is noticed when a third center core flow nozzle is operated in this extended manner as illustrated by comparing the performance of nozzle 2:04:44:20 + 1.0, shown in Fig. 6(f), with that of the unextended nozzle, 2:04:44:20 + 0, shown in Fig. 6(c).

The performance of center core flow nozzles, when the inner nozzle component is withdrawn into the interior of the basic nozzle, is shown in Figs. 6(g) and (h). In these nozzles, 2:04:51:30 - 1.0 and 2:04:44:20 - 1.0, the tapered outer surface of the terminations caused the outer annular flow passage to behave as a converging-diverging nozzle, exhibiting poor acoustic performance at low flow rates due to separation effects.

The terminations of those annular flow nozzles reported so far have an exit area equal to that of the inner nozzle to which they are attached. A termination was constructed having a tapered profile so that its exit area is less than the area of the inner nozzle component to which it is attached. Figure 6(i) shows the performance of a center core flow nozzle, 2:04:51:31 + 0, in which this latter termination is used. Figures 6(j) and (k) show the performance with the inner nozzle termination occupying different positions both within and downstream of the outer converging nozzle.

The results of these studies on center core flow nozzles together with those reported in reference 4 are used to form the basis of recommendations for this type of nozzle.

Ejector Nozzles

Figures 7(a) through (d) show the performance of four ejector nozzles which were examined for acoustic performance. In these very limited studies there was little or no suggestion of any potential in these devices although they have been shown by others to produce acoustic improvement. It may be remarked that the exceptionally high acoustic levels, even at very low subsonic conditions, were due to discrete frequencies emitted by these devices.

Converging-Diverging Nozzles

Figure 8(a) shows the performance of a converging-diverging nozzle, 122 (N62), examined during the previous study, but the data has been replotted so that the minimal flow area replaces the exit area as the characteristic nozzle area. Comparison of the plotted data illustrates the significance as to which area is adopted as characteristic of the nozzle. The unfavorable acoustic performance of the nozzle below choking condition is probably due to overexpansion and its associated separation effect. Figures 8(b) and (c) show the performance of two converging-diverging nozzles, N63 and N64. The previous study showed that acoustic performance improvement accompanied decrease in angle of the divergent section of the nozzle, especially at flow rates just below choking conditions where separation effects in the nozzle produced higher acoustic levels than in a converging nozzle. The nozzle N64, whose performance is shown in Fig. 8(c), consists of a standard converging-diverging nozzle with a final straight section added to the divergent section. The nozzle of Fig. 8(b) is one of equal over-all length, but the divergent section is continuous and of uniform profile, and consequently has a smaller divergent angle. It is this nozzle whose acoustic

performance is most favorable of all the converging-diverging nozzles tested. Little or no separation effect is apparent in regions below choking and the performance at or close to design approaches the dashed curve given by equation 50.

Plugged Converging-Diverging Nozzles

Figure 9(a) shows the performance of nozzle 621 (1:62:10:10 + 0) taken from reference 4, but replotted in terms of the minimal area. The acoustic performance of this nozzle is shown to be favorable at design conditions and exhibits little or no separation effects.

Figure 9(b) shows the performance of a plugged converging-diverging nozzle with a considerably smaller value of the ratio of plug to nozzle diameter, 1:63:10:10 + 0.781. The acoustic performance is seen to be very good over a considerably wide operating range.

It may be noted that a plugged converging nozzle, having an equivalent value of the ratio of plug to nozzle diameter, for example, nozzle 371, whose performance is shown in Fig. 8(h) of reference 4, has a poor acoustic performance in comparison to this plugged converging-diverging nozzle.

'Rough' Nozzles

A converging nozzle was modified to study the effects of roughness on the performance of a nozzle. The roughness was produced using screws which were threaded into the nozzle from the outside and could protrude a measurable distance inside. Figure 10(a) shows the effects of roughness obtained by using eight screws mounted in two rows of four screws equally distributed around the inner circumference of the nozzle. This shows that while deterioration in acoustic performance occurs in the subsonic flow region, some improvement is noted in the overchoked region. Unfortunately, it was not possible to extend this study of roughness effects beyond a few brief spot measurements. These brief tests showed that decrease in the protrusion of the screws resulted in better performance subsonically though still not as good as a 'smooth' converging nozzle, accompanied by deterioration in regions above choking, the performance being slightly better than the 'smooth' converging nozzle. Figures 10(b) and (c) show the spectral analysis of a 'smooth' compared to this 'rough' convergent nozzle as obtained by a narrow band (3 cycle) analysis at the 30° and 90° stations only, at mass flow rate of 5.5 approximately. It is observed that the roughness introduced

into the nozzle eliminates the screech component at both stations and modifies the spectral distribution considerably in the lower frequency range at the 90° station, and in the higher frequency range at the 30° station. We did not investigate the effects of roughness on other types of nozzle. But since the major effect of roughness in the convergent nozzle is to remove the discrete frequency screech components, no further improvement when roughness is added to nozzles possessing good acoustic performance will necessarily occur. For example, spectral analysis of plug nozzles (reference 4) shows no discrete frequency content so it may be anticipated that roughness will not improve plug nozzle performance.

THRUST OF COLD JET FLOW NOZZLES

In order that those nozzles whose performance was judged favorable, when evaluated in terms of their mass flow rate, could be further evaluated in terms of their thrust performance, probably a more realistic method of nozzle evaluation, thrust measurements on selected nozzles were made. These are shown in Figs. 11(a) through (j). The broken curves on these figures represent average performances and are used in Section VII in evaluating nozzle performance.

Figure 11(a) shows the thrust performance of a converging nozzle N02. This shows that over the whole operating range its thrust values are approximately 10% less than given by the theoretical curve. Figure 11(b) shows the thrust performance of a converging-diverging nozzle N61, plotted in terms of both exit and throat area. The justification for the throat, or minimal, area is quite apparent. The thrust values are less than those predicted for a converging-diverging nozzle operated at design, but as the pressure ratio increases, the performance approaches that predicted for a converging nozzle and equals it at a pressure ratio of 4.0. Figure 11(c) shows the thrust performance of another converging-diverging nozzle N63. This nozzle, which was found to be acoustically superior to the previous nozzle N61, has a poorer thrust performance.

Figures 11(d) and (e) show the thrust performance of plug nozzles 347 (1:03:30:30 + 2) and 1:04:40:40 + 0. Both these nozzles have thrust values considerably lower than predicted and also lower than that of the converging nozzle N02. Figures 11(f) through (i) show thrust performances of four annular center core flow nozzles having good acoustic performances. Nozzles 2:02:44:20 + 0 and 2:02:44:20 + 1.625 are seen in Figs. 11(f) and (g) to exhibit very poor thrust performances. Nozzles 2:04:51:31 + 0 and 2:04:50:31 + 1.0 show better thrust performance in Figs. 11(h) and (i), but these are still less than the predicted values.

Figure 11(j) shows the thrust performance of a converging-diverging plug nozzle 1:63:10:10 + 0.781 having a good acoustic performance.

The results of these studies show that the best thrust performances are obtained with a converging-diverging nozzle, whose performance is better than that of a converging nozzle. Annular plug and center core flow nozzles show considerable thrust reduction over predicted values. These thrust measurements, together with acoustic power studies of nozzles, are utilized in Section VII to evaluate the acoustic performance of nozzles as a function of their thrust.

POWER SPECTRAL DENSITY

Figure 12(a) shows the results of a 1/3 octave band analysis of converging nozzle N01, as measured using the high frequency microphone of this current program. The analysis was carried out below, at and above choking conditions. The screech effects are apparent under the latter operating conditions. Figure 12(b) shows the attempt to normalize this data according to the technique developed in reference 4, and Figs. 12(c) and (d) show similar attempts at normalizing equivalent data acquired for nozzles N02 and N04. The screech content was removed before normalization was attempted. These figures show that the technique is only partially successful. The data for below and just at the choked condition normalizes well, but overchoked data does not. Normalizing, using the unmodified Strouhal number as a parameter, would not overcome the problem because the velocity which would have to be adopted for overchoked conditions would be the local velocity of sound and for successful normalization this would imply that the peak frequency of the spectrum of overchoked data should be a constant. Inspection of Fig. 12(a) shows that the peak frequency, disregarding the screech peaks, of the highest mass flow data is approximately twice the peak frequency of the data obtained at the onset of choking conditions. Because of the success of the normalizing techniques developed for hot nozzle flow data in reference 4, we believe that a possible explanation for inability to normalize cold data is that mechanisms are present in cold overchoked flow nozzles that are not present in hot jet flows and which introduce additional noise and prevent successful normalization. It is interesting to note in Figs. 15(a) through (d) in reference 4 that good normalization occurred only with hot jet data, while erratic results occurred using cold jet data.

SECTION VI

MEASURED RESULTS FOR HOT NOZZLES

In the course of the program attempts were made to acquire data from the results of other investigators suitable for applying the normalizing technique developed in reference 4. Despite the wealth of published data, little is sufficiently complete for our purposes. Consequently, we performed our own hot model jet nozzle experiments with a view to (a) acquiring data suitable for attempting to verify normalizing techniques, and (b) comparing performance of a converging nozzle to that of other nozzle configurations.

In order to substantiate the normalizing technique for temperature which was developed in the study reported in reference 4, and which was based on data taken from the work of Lee, Tatge, and Wells (refs. 5 and 6), hot model jet nozzle studies were performed using the outdoor facility. As it was not possible to measure the mass flow through the nozzles in this system, this was computed from knowledge of the pressure ratio and temperature ratio. A converging one-inch diameter stainless steel nozzle was used in this study. This nozzle was identical to a one-inch nozzle N02 used in the cold study whose mass flow performance was indistinguishable from its theoretical performance. Consequently, the pressure and temperature ratio was assumed sufficient to enable the mass flow to be calculated to within a reasonable degree of accuracy. Figure 13(a) shows the acoustic performance of this nozzle operated with cold flow obtained using this outdoor facility, and the results are shown to be in good agreement except at very high mass flow rates with those taken in the anechoic facility.

Figure 13(a) also shows the performance of the converging nozzle when operated at elevated temperatures of 600° and 1000°F. Figure 13(b) shows the attempt at normalizing this data using the parameters developed in reference 4. The results are only moderately successful. In all cases, for successful normalization, the over-all noise, before normalization was attempted, should have been less. It was noted that noise, in addition to that from the jet, was being emitted from the walls of either the combustor or calming tank. However, it was not possible to determine its magnitude.

Tape recordings were taken at all stations for all those runs in which the nozzle was operating above choking conditions.

Figures 13(c) and (d) show 1/3 octave band analysis of the acoustic output of this converging nozzle at the 30° and 90° stations for various stagnation pressure and temperature ratios. It is interesting to note that at the lower stagnation pressure,

the screech effect is most pronounced at a stagnation temperature of 600°F and is negligible at 90°F and 1000°F. But, at the higher pressure ratio, the screech effect is pronounced at all stagnation temperatures.

One annular plug nozzle was operated at elevated temperatures and Fig. 13(e) shows the performance of this plug nozzle 1:04:40: 40 + 0 compared to a converging nozzle.

Figure 13(f) shows 1/3 octave band analysis of the acoustic performance of this nozzle at the 30° and 90° stations for temperatures of 90° and 1000°F.

SECTION VII

NOZZLE PERFORMANCE COMPARISONS

The types of nozzle which have been examined in both this current and the preceeding program are the basic converging, the annular plug, the center core flow, the converging-diverging, the converging-diverging plug, the ejector, and the rough convergent nozzle.

Of these nozzles, those showing good acoustic performance relative to that of a convergent nozzle are:

1. the annular plug nozzle,
2. the center core flow nozzle,
3. the converging-diverging nozzle, and
4. the converging-diverging plug nozzle.

ACOUSTIC PERFORMANCE OF NOZZLES

Mass Flow Comparison

The Annular Plug Nozzle

The annular plug nozzle has been operated with the base of the cone in the interior of the converging nozzle, in the exit plane of the nozzle, and in the extended position. In the first case, the plug nozzle acts as a converging-diverging nozzle and in the few studies we have made of these nozzles, their acoustic performance has been poor and has included noise resulting from separation effects which is peculiar to converging-diverging nozzles. Acoustic performance improvement in plug nozzles has been noted when the base of the cone of the plug is either in the exit plane of the nozzle or extended downstream of this point. The majority of plug nozzle studies in both the previous and current programs have been devoted to nozzles whose cone base is in the exit plane of the nozzle. Figure 14(a) shows the acoustic improvement for a number of plug nozzles. This improvement has a tendency to reach a maximum for a mass flow rate of 5, and the improvement accompanies increase in the ratio of the plug to nozzle diameter. Nozzle 1:04:40:40 + 0 appears to represent a critical nozzle in which good acoustic performance is still being obtained and yet the plug to nozzle diameter ratio is sufficiently small (0.707) to produce a reasonably large total flow rate for

the over-all size of the nozzle. It should be remarked that this nozzle is the only one of those shown in Fig. 14(a) whose performance was determined with the high frequency microphone. If the performance of those nozzles having good acoustic performance and possessing a small annular gap between the plug and the nozzle, e.g., 375, 327, their performance may have been a few decibels poorer. Nozzle 347, whose annular gap has the same value as that of nozzle 327, and whose performance, redetermined during this study as nozzle 2:03:30:30 + 2.0, was 4 db poorer, would lend evidence to this. Consequently, had the performances of nozzles 327 and 375 been redetermined, they may have rated performance close to that of 1:04:40:40 + 0. Plug nozzles having only moderate performance, e.g., 471, showed further improvement when the plug was extended, e.g., 491. But those plug nozzles whose acoustic performance was most superior, e.g., 375 or 1:04:40:40 + 0, showed little or no further improvement with extension of the plug, e.g., 347 or 1:04:40:40 + 2. Nozzle performance of the better plug nozzle was little affected by the various profiles adopted for the plug terminations. Consequently, a plug nozzle such as 1:04:40:40 + 0 would appear to represent a plug nozzle having as large a total mass flow rate for size of nozzle as is possible, commensurate with good acoustic performance. This nozzle, whose performance was also evaluated under high temperature flow conditions, continued to exhibit good acoustic performance.

The Center Core Flow Nozzle

Comparison of the results of this and the previous study show that, as with the plug nozzles, acoustic improvement occurs only in nozzles where a portion of the inner plug or inner tube extends beyond the exit plane of the nozzle. Figure 14(b) shows comparison between a small number of nozzles, whose inner nozzles and their terminations are geometrically similar, with the base of the termination in the exit plane of the nozzle. Nozzle 274 shows the best acoustic performance. Extension of the termination beyond the nozzle exit does not produce any significant benefit in acoustic performance, but some slight improvement was noted in those nozzles having poorer initial acoustic performance. Poor subsonic performance of many of the center core flow nozzles was reported in reference 4 as being due to aeolian tones effects. This does not mean that center core flow nozzles cannot be considered as possible full-scale nozzles, but it does mean that consideration would have to be given to eliminating this effect or ensuring that the frequency of the generated tones did not cause inconvenience. For example, center core flow nozzles in which the inner nozzle protrudes a considerable distance downstream of the basic nozzle, e.g., nozzle 2:02:44:20 + 1.625, do not exhibit a very significant aeolian tone effect. This may possibly be explained by the difference in flow velocities between

the flow through the inner nozzle and that flow surrounding the inner nozzle, whichis caused by the outer flow retardation by the stagnant atmosphere surrounding the jet. If this hypothesis is correct, a deliberately produced velocity differential could be produced in a full-scale nozzle to suppress the aeolian tone production. Alternatively, the nozzle termination thickness and the flow rates could be adjusted so that the frequency of generated tones were beyond audible ranges.

The Converging-Diverging Nozzle

These nozzles, unlike the annular plug and the center core flow nozzles, have a limited application in that their acoustic improvement occurs only when they are operated at or close to design conditions when evaluated in terms of their mass flow performance. Comparison between nozzles 121 (N61) and N63 and between 120 (N60) and 122 (N62) shows that nozzles with long divergent sections show slightly better acoustic performances. However, the peak improvement that has been observed is between 7-8 db when compared on the mass flow basis which is less than that observed with annular plug or center core flow nozzles.

The Converging-Diverging Plug Nozzle

Only three converging-diverging plug nozzles have been examined in reference 4 or in the current program. Of these, however, nozzles 621 (1:22:10:10 + 0) and 1:63:10:10 + .781 show good acoustic performance. Nozzle 1:63:10:10 + .781 particularly shows excellent performance over the whole operational range of interest. This nozzle has a plug to nozzle diameter ratio, which if reproduced in a standard plug nozzle utilizing a convergent nozzle, would cause this nozzle's acoustic performance to be poor. Consequently, a converging-diverging plug nozzle having good acoustic performance can also be designed to possess a higher over-all flow compared to the over-all size of nozzle used than for a converging plug nozzle.

Thrust Comparison

The nozzle evaluation which has been attempted so far in this section has consisted of a comparison of the over-all acoustic power produced by nozzles for a given mass flow rate. However, the following evaluations of nozzle performance are made from thrust measurements determined for an over-all number of

nozzles whose acoustic performance was shown to be good when evaluated in this manner. Combining both the data of acoustic performance against mass flow and thus against pressure ratio, and that of thrust against pressure ratio, the noise output of nozzles against their thrust was determined.

Figure 15 shows the acoustic performance of several of the acoustically good nozzles, representing all nozzle types against their measured thrust. The solid curve is that obtained for converging nozzle N02. It is apparent that there is little to choose between the annular plug nozzle, the center core flow nozzle, and the plugged converging-diverging nozzle. These nozzles produce almost identical acoustic performance with thrust over the whole operating range of interest. The converging-diverging nozzle has only a moderately good acoustical performance producing its best performance at or close to its design operating conditions. Under these conditions its performance is equal to that of either plug or center-core flow nozzles.

If we consider the performance of nozzles over the flow regions (a) subsonic, where the pressure ratio is less than 1.89, and (b) supersonic, or more strictly, the region in which the flow is choked for all nozzles where the pressure ratio is greater than 1.89, we may draw the following conclusions.

In the subsonic region, the nozzles all have performances equal to that of the converging nozzle, except the following. The annular center core flow nozzle 2:02:44:20 + 0 has a poor acoustic performance due to the aeolian tone generation, and produces up to 8 db more sound power output than a converging nozzle of equal thrust output. The converging-diverging nozzle N63 and the converging-diverging plug nozzle 1:63:10:10 + 781 show an improvement over a converging nozzle. The value of the improvement is limited by experimental error but appears to be between 1 and 6 db over the subsonic flow range.

In the transitional region between subsonic and overchoked flow regions, all nozzles have performances comparable to the converging nozzle.

In the overchoked flow region ($p_s/p_o > 1.89$), the plugged converging, plugged converging-diverging, and the center core flow nozzles all produced approximately equal improvement over the converging nozzle, exhibiting up to a 10 db reduction in over-all sound power. The converging-diverging nozzle N63 is seen to have a performance equal to these nozzles only at or close to its operating conditions ($p_s/p_o = 3.67$).

RECOMMENDED NOZZLES

In deciding upon the optimized nozzle in each of the four nozzle groups showing good acoustic performance, it is necessary to be aware of the problems involved in operating scaled-up versions of these nozzles. For example, the nozzles' physical size should be such as to allow a sufficiently large total gas flow to occur. Plug nozzles may possibly suffer in this respect since the annular flow passage produces a total flow rate which can be achieved with a converging or a center core flow nozzle of far smaller dimensions. The over-all size and shape of the nozzle will also affect the drag produced by a nozzle operated under service conditions. Again, the plug nozzle may suffer in this respect because of the increase in nozzle size compared to a converging nozzle required for an equal flow rate. Drag increase will also be caused if the plug or center nozzle of plug or center core flow nozzles, respectively, is made to protrude a considerable distance downstream of the exit plane of the outer nozzle.

Consequently, of those nozzles we have examined, we will recommend those which produce an improved acoustic performance over a converging nozzle and which meet the requirements of a nozzle which might be scaled up to a practical service nozzle, and ignore nozzles whose acoustic performance is only slightly better (e.g., 1 db improvement) if this is achieved at the expense of non-practicability. For example, plug nozzle 1:04:40:40 + 0, whose performance is shown in Figure 5(b) would be recommended in preference to nozzle 1:04:40:40 + 9 as shown in Figure 5(d).

The following list contains the individual nozzles showing best acoustic potential in each group:

a) center core flow nozzle 2:02:44:20 + 1.625 or 2:04:50:31 + 1.0 (produces less aeolian tone effects)

b) basic plug nozzle 1:04:40:40 + 0

c) converging-diverging plug nozzle 1:63:10:10 + 0.781

d) converging-diverging nozzle N63

In attempting to recommend those individual nozzles which we feel show potential and should be operated under full-scale service conditions certain limitations must be borne in mind. The first is that it has been impossible to attempt nozzle optimization in as an exhaustive manner as is desirable. Consequently, the specifications for the design of any recommended nozzles are not necessarily those of the optimum nozzles, but those of what we consider to be optimum as the result of this limited study. Secondly, because certain nozzles exhibit a better acoustic

performance than a convergent nozzle when operated cold, this does not imply that they will necessarily do so when operated hot. Since there is no complete understanding of the various mechanisms which occur in the production of the over-all noise of a jet, it is not possible to state categorically that acoustically good cold jet nozzles will be acoustically good hot jet nozzles.

SECTION VIII

CONCLUSIONS AND RECOMMENDATIONS

As a result of this research concerning flow and acoustic performance of high velocity jet streams, the following conclusions and recommendations are made.

CONCLUSIONS

1) Four types of cold jet flow nozzles have been found to show good acoustic performance commensurate with good thrust performance compared to the performance of a converging nozzle. These nozzles are:

   a) an annular center core flow nozzle,

   b) an annular plug nozzle,

   c) a converging-diverging plug nozzle, and

   d) a converging-diverging nozzle.

2) Of these nozzles, only converging-diverging plug nozzles and converging-diverging nozzles have superior performance to the converging nozzle in the subsonic flow region. In the immediate transonic flow region, no nozzle is superior to the converging nozzle. In the overchoked flow region, the basic plug nozzle, the center core flow nozzle, and the converging-diverging plug nozzle produce almost identical performance, giving a maximum of approximately 10 db reduction in sound power compared to the sound power output of a converging nozzle operating at an equal thrust level. The converging-diverging nozzle produces this maximum of 10 db acoustic power reduction only when operating at or close to design flow conditions.

3) Of the four types of nozzles showing good acoustic performance, the following list contains the individual nozzles showing the best performance in each group:

   a) center core flow nozzle 2:02:44:20 + 1.625 or 2:04:50:31 + 1.0,

   b) basic plug nozzle 1:04:40:40 + 0,

c) converging-diverging plug nozzle 1:63:10:10 + .781, and

d) converging-diverging nozzle N63.

4) The basic plug nozzle 1:04:40:40 + 0 still showed good acoustic performance compared to a basic converging nozzle when both were operated at elevated temperatures.

5) Attempts to normalize both the over-all power of hot model jets or the power spectral distribution of cold model jets according to the technique developed in reference 4 were only partially successful.

6) A limited study of the effect of roughness in a convergent nozzle shows that a small improvement in acoustic performance occurs at high mass flow rates chiefly through the suppression of the discrete frequency screech effect, but that this is accompanied by an increase in the sound power level of the nozzle in the subsonic flow region.

RECOMMENDATIONS

1) The optimized nozzle of each of the four nozzle types exhibiting a good acoustic potential should be scaled up and attached to a small jet engine to establish that a noise reduction is still obtained compared to a converging nozzle when these nozzles are operated under realistic service conditions.

2) If the results of the study recommended above are successful, further effort should be devoted to establishing whether each of the recommended nozzles are the truly optimized nozzles of their respective nozzle types.

3) Further consideration should be given to the problem of scaling the performance of a small cold model jet to that of a large hot jet and ultimately to a jet engine exhaust.

4) The success of the above recommendation ultimately rests upon more fundamental studies of the mechanism of noise production of both hot and cold, subsonic and overchoked jet flows.

REFERENCES

1. Sperry, W.C. (Editor), Fundamental Study of Jet Noise Generation and Suppression, WADD Technical Report 61-21, Volume I, Wright Air Development Division, Wright-Patterson Air Force Base, Ohio, December 1960.

2. Emmitt, Margaret, Fundamental Study of Jet Noise Generation and Suppression, Volume II — Bibliography, Wright-Patterson Air Force Base, Ohio, December 1960.

3. Sperry, W.C., Kamo, R., and Peter, A., Experimental and Theoretical Studies of Jet Noise Phenomena, Technical Documentary Report ASD-TDR-62-303, Aeronautical Systems Division, Wright-Patterson Air Force Base, Ohio, February 1962.

4. Sperry, W.C., Peter, A., and Kamo, R., Fundamental Study of Jet Noise Generation and Suppression, Technical Documentary Report ASD-TDR-63-326, Aeronautical Systems Division, Wright-Patterson Air Force Base, Ohio, March 1963.

5. Lee, R., et al, Research Investigation of the Generation and Suppression of Jet Noise, General Electric Co., U.S.N. Bureau of Weapons, Contract NOas 59-6160c, January 1961.

6. Tatge, R.B., Wells, R.J., "Model Jet Noise Study at Alplaus Facility," General Electric Co., Report No. 61 GL 25, January 1961.

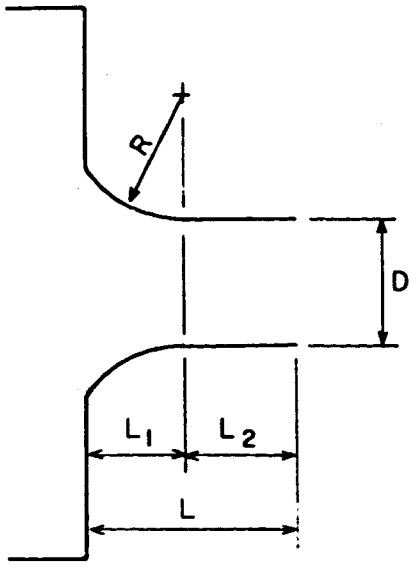

Nozzle No.	D in.	R in.	L_1 in.	L_2 in.	L in.	A_2 in^2	L_1/L	L_2/L	L/D
N00	0.533	0.533	0.422	0.484	0.906	0.223	0.466	0.534	1.700
N01	0.750	0.750	0.600	0.681	1.281	0.442	0.468	0.531	1.708
N02	1.000	1.000	0.792	0.908	1.700	0.785	0.466	0.534	1.700
N03	1.375	1.375	1.094	1.250	2.344	1.485	0.468	0.534	1.705
N04	1.414	1.414	1.120	1.278	2.398	1.570	0.468	0.534	1.694

Table I. Details of Basic Nozzles
(a) Geometrically Matched Converging Nozzles with Short Extensions

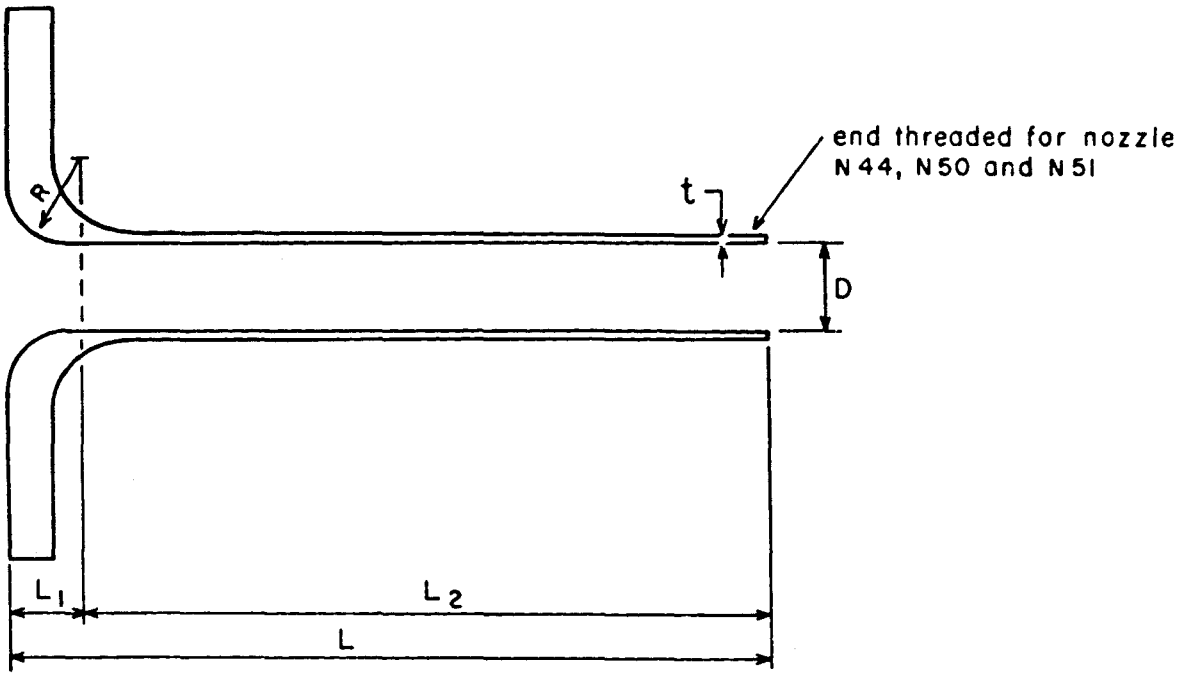

Nozzle No.	D in.	R in.	L_1 in.	L_2 in.	L in.	A in.^{2}	L_1/L	L_2/L	L/D	t in.
N40	0.533	0.533	0.422	1.922	2.344	0.223	0.180	0.820	4.40	0.050
N41	0.533	0.533	0.422	2.922	3.344	0.223	0.126	0.875	6.27	0.050
N42	0.533	0.533	0.422	3.922	4.344	0.223	0.0973	0.904	8.15	0.050
N43	0.533	0.533	0.422	4.922	5.344	0.223	0.0790	0.920	10.02	0.050
N44	0.533	0.533	0.422	3.922	4.344	0.223	0.0973	0.904	8.15	0.126
N50	0.750	0.750	0.600	3.744	4.344	0.442	0.138	0.862	5.79	0.125
N51	0.750	0.750	0.600	2.792	3.392	0.442	0.177	0.823	4.52	0.125

Table I. Details of Basic Nozzles
(b) Converging Nozzles with Long Extensions

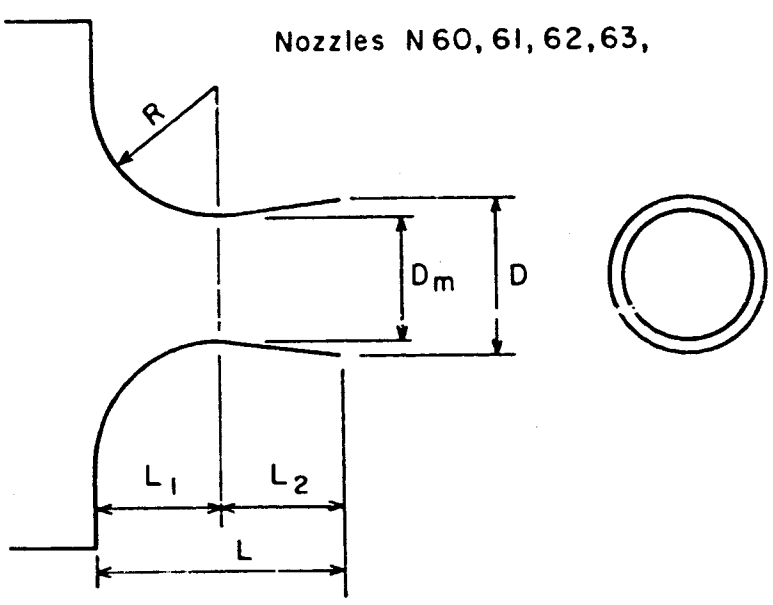

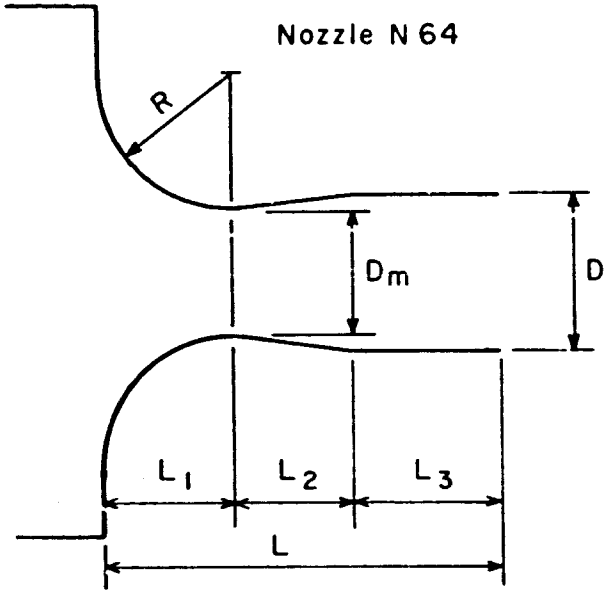

Nozzle No.	D in.	R in.	L_1 in.	L_2 in.	L_3 in.	L in.	Exit A_2 in.^{2}	L/D	Throat D_m in.	Throat A_m in.^{2}	A/A_m
N60	0.75	0.75	0.600	0.681	-----	1.281	0.442	1.708	0.691	0.375	1.178
N61	1.00	1.00	0.792	0.908	-----	1.700	0.785	1.700	0.922	0.667	1.178
N62	0.75	0.75	0.600	2.073	-----	2.673	0.442	3.564	0.691	0.375	1.178
N63	1.00	1.00	0.792	2.765	-----	3.557	0.785	3.557	0.922	0.667	1.178
N64	1.00	1.00	0.792	0.908	1.857	3.557	0.785	3.557	0.922	0.667	1.178

Table I. Details of Basic Nozzles
(c) Converging-Diverging Nozzles

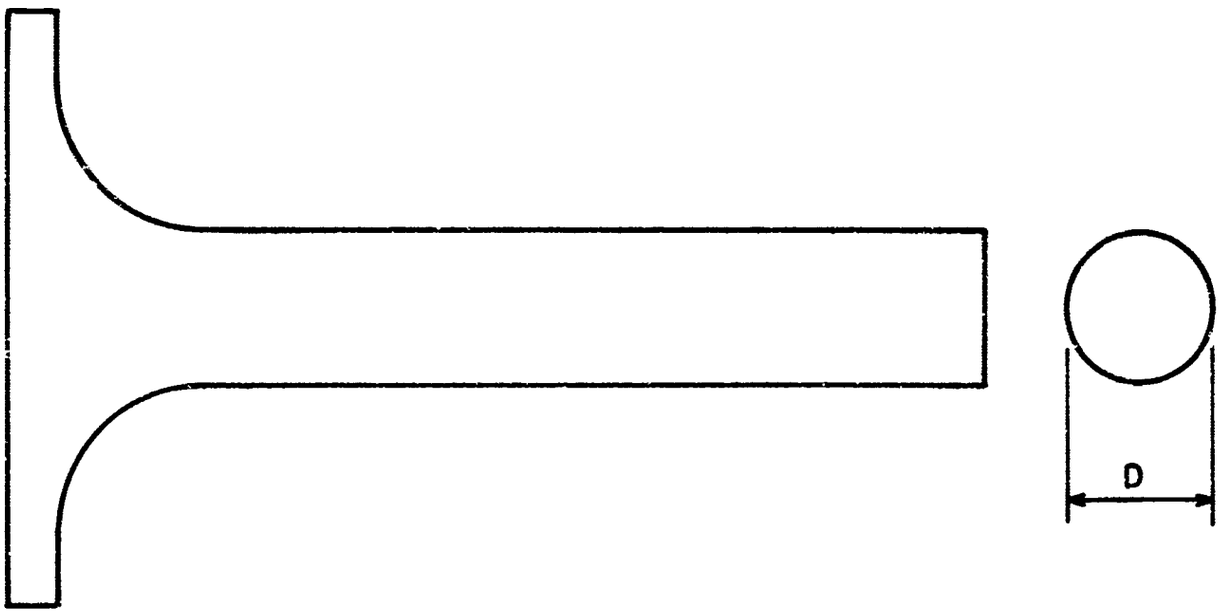

Bar No.	D in.	A in.^{2}
B10	0.316	0.0794
B20	0.786	0.4850
B30	1.080	0.9159
B40	1.000	0.785

Table II. Details of Nozzle Appurtenances
(a) Solid Bars

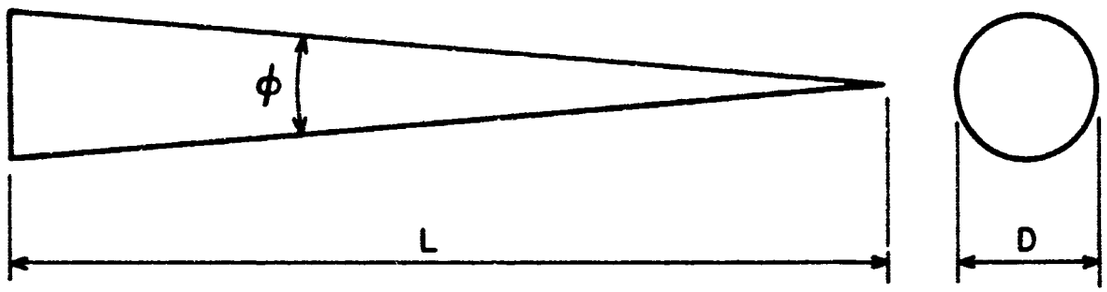

Bar Termination No.	D in.	L in.	ϕ deg.
BT00	No Termination		
BT10	0.318	1.817	10.0
BT11	0.318	0.902	20.0
BT12	0.318	0.594	30.0
BT20	0.786	4.82	9.33
BT30	1.080	6.18	9.33
BT40	1.000	6.105	9.33
BT50	1.000	6.105	See Table II(c)
BT51	1.000	6.105	See Table II(c)
BT52	1.000	6.105	See Table II(c)
BT70	1.000	3.535	See Table II(c)

Table II. Details of Nozzle Appurtenances
(b) Bar Terminations

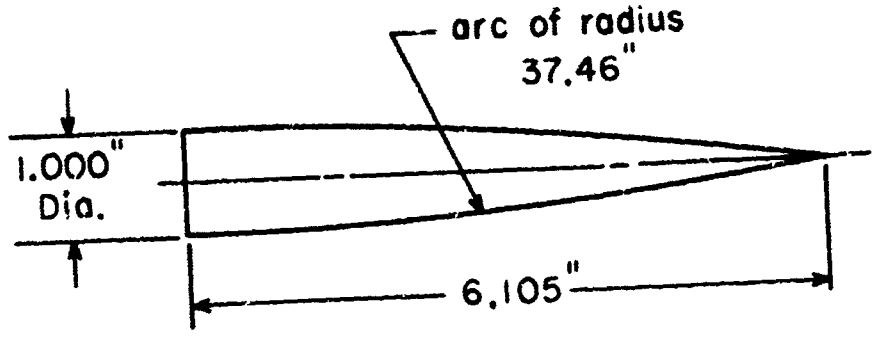

(a) BT 50

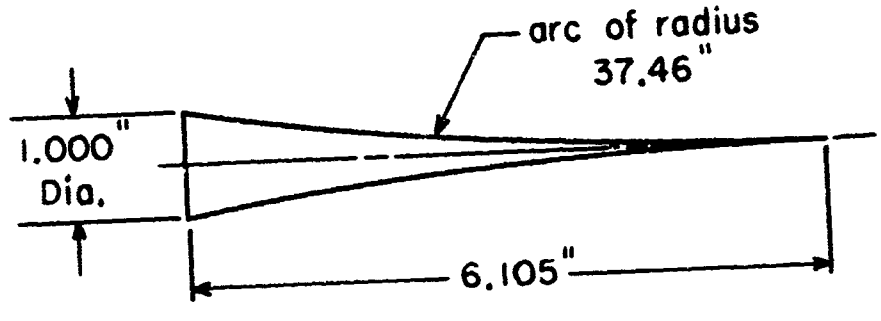

(b) BT 51

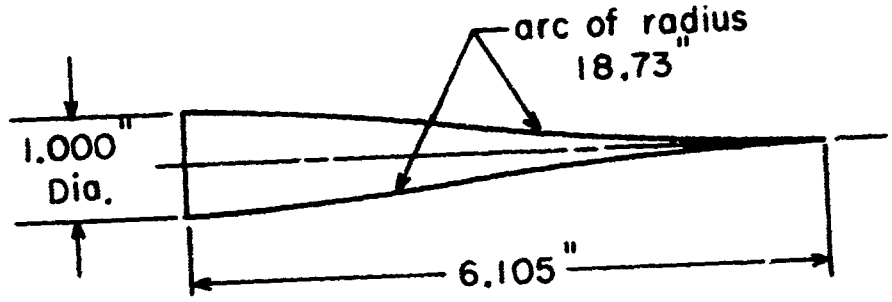

(c) BT 52

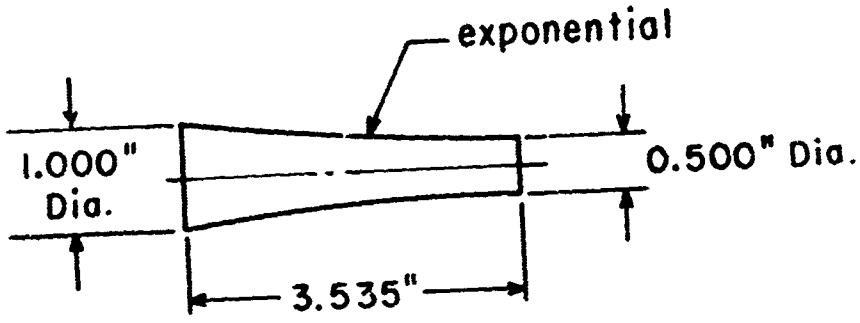

(d) BT 70

Table II. Details of Nozzle Appurtenances
(c) Details of Bar Terminations

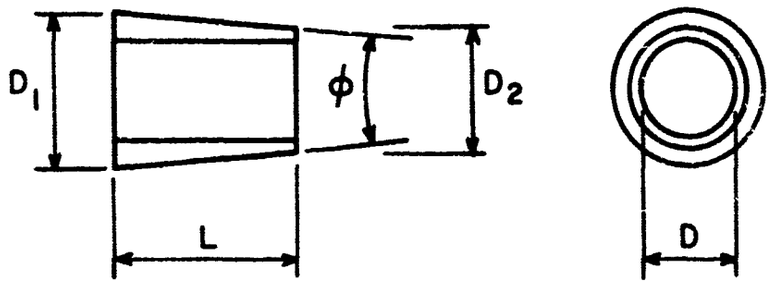

Terminating No.	D in.	L in.	ϕ deg.	D_1 in.	D_2 in.
NT00		No Termination			
NT20	0.533	1.000	9.33	0.786	0.623
NT21	0.533	1.000	----	0.786	0.786
NT30	0.750	1.375	9.33	1.000	0.840
NT31	0.533	2.307	9.33	1.000	0.623

Table II. Details of Nozzle Appurtenances
(d) Nozzle Terminations

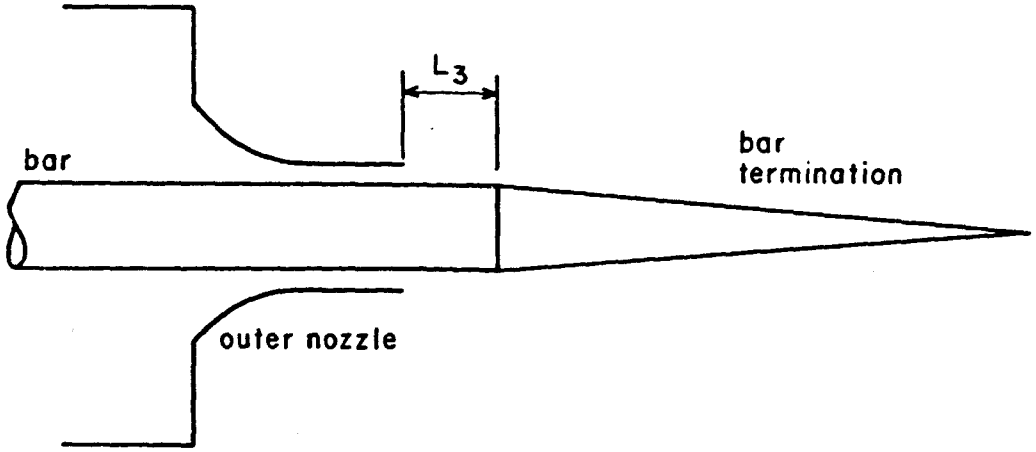

Composite Nozzle No.	Outer Nozzle	Bar	Bar Termin.	L_3 in.	A in.^{2}	A_m in.^{2}	A_b in.^{2}	A/A_m	A/A_b
1:04:40:40 + 0	N04	B40	BT40	0	0.785	0.785	0.785	1.000	1.000
1:04:40:40 + 2	N04	B40	BT40	2.0	0.785	0.785	0.785	1.000	1.000
1:04:40:40 + 9	N04	B40	BT40	9.0	0.785	0.785	0.785	1.000	1.000
1:04:40:50 + 0	N04	B40	BT50	0	0.785	0.785	0.785	1.000	1.000
1:04:40:51 + 0	N04	B40	BT51	0	0.785	0.785	0.785	1.000	1.000
1:04:40:52 + 0	N04	B40	BT52	0	0.785	0.785	0.785	1.000	1.000
1:04:40:70 + 0	N04	B40	BT70	0	0.785	0.785	0.785	1.000	1.000
347 (1:03:30:30 + 2)	N03	B30	BT30	2.0	0.569	0.569	0.9159	1.000	0.621

Table III. Details of Converging Plug Nozzles

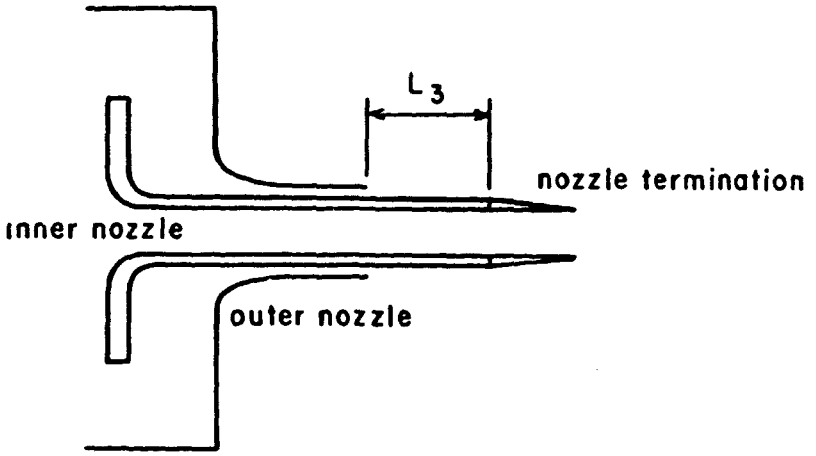

Composite Nozzle No.	Outer Nozzle	Inner Nozzle	Inner Nozzle Termin.	L_3 in.	A in.^{2}	A_{m2} in.^{2}	A_{a2} in.^{2}	A_{c2} in.^{2}	A/A_m	A/A_c	A/A_a	A_a/A_c
274 (2:02:44:20+0)	N02	N44	NT20	0	0.523	0.523	0.300	0.223	1.000	2.350	1.743	1.345
2:02:44:20+1.625	N02	N44	NT20	1.625	0.523	0.523	0.300	0.223	1.000	2.350	1.743	1.345
2:04:51:30 + 0	N04	N51	NT30	0	1.227	1.227	0.785	0.442	1.000	2.776	1.563	1.776
2:04:44:20 + 0	N04	N44	NT20	0	1.309	1.309	1.086	0.223	1.000	5.870	1.205	4.870
2:04:50:30 + 1.0	N04	N50	NT30	+1.0	1.227	1.227	0.785	0.442	1.000	2.776	1.563	1.776
2:04:44:20 + 1.0	N04	N44	NT20	+1.0	1.309	1.309	1.086	0.223	1.000	5.870	1.205	4.870
2:04:51:30 - 1.0	N04	N51	NT30	-1.0	1.456	1.227	0.785	0.442	1.187	3.294	1.855	1.776
2:04:44:20 - 1.0	N04	N44	NT20	-1.0	1.488	1.309	1.086	0.223	1.137	6.673	1.370	4.870
2:04:51:31 + 0	N04	N51	NT31	0	1.008	1.008	0.785	0.223	1.000	4.520	1.284	3.520
2:04:50:31 + 1.0	N04	N50	NT31	+1.0	1.008	1.008	0.785	0.223	1.000	4.520	1.284	3.520
2:04:51:31 - 1.0	N04	N51	NT31	-1.0	1.008	1.008	0.785	0.223	1.000	4.520	1.284	3.520

Table IV. Details of Center Core Flow Nozzles

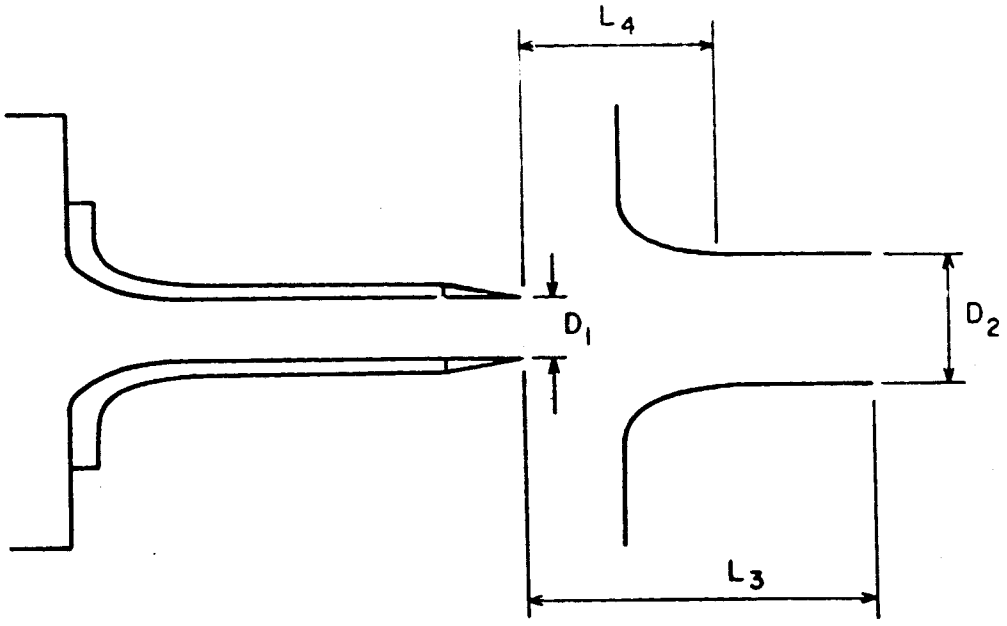

Composite Nozzle No.	Basic Nozzle	Basic Nozzle Termination	Ejector Nozzle	L_3 in.	L_4 in.	D_1 in.	D_2 in.
3:51:30:04 + 0.750	N51	NT30	N04	0.750	-0.528	0.750	1.414
3:51:30:04 + 1.750	N51	NT30	N04	1.750	0.472	0.750	1.414
3:51:30:04 + 3.375	N51	NT30	N04	3.375	2.097	0.750	1.414
3:51:30:02 + 2.750	N51	NT30	N02	2.750	1.842	0.750	1.000

Table V. Details of Ejector Nozzles

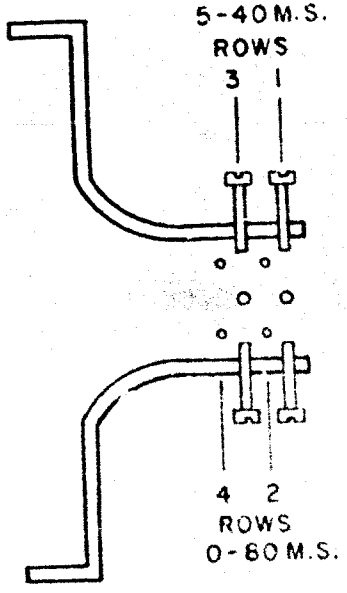

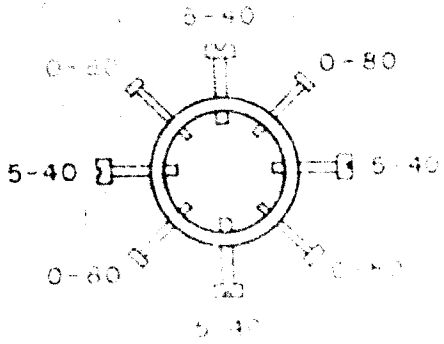

MACHINE [illegible]

Composite Nozzle No.	Basic Nozzle No.	[illegible]
[illegible]	NOZ	

TABLE VI. [illegible]

Best Available Copy

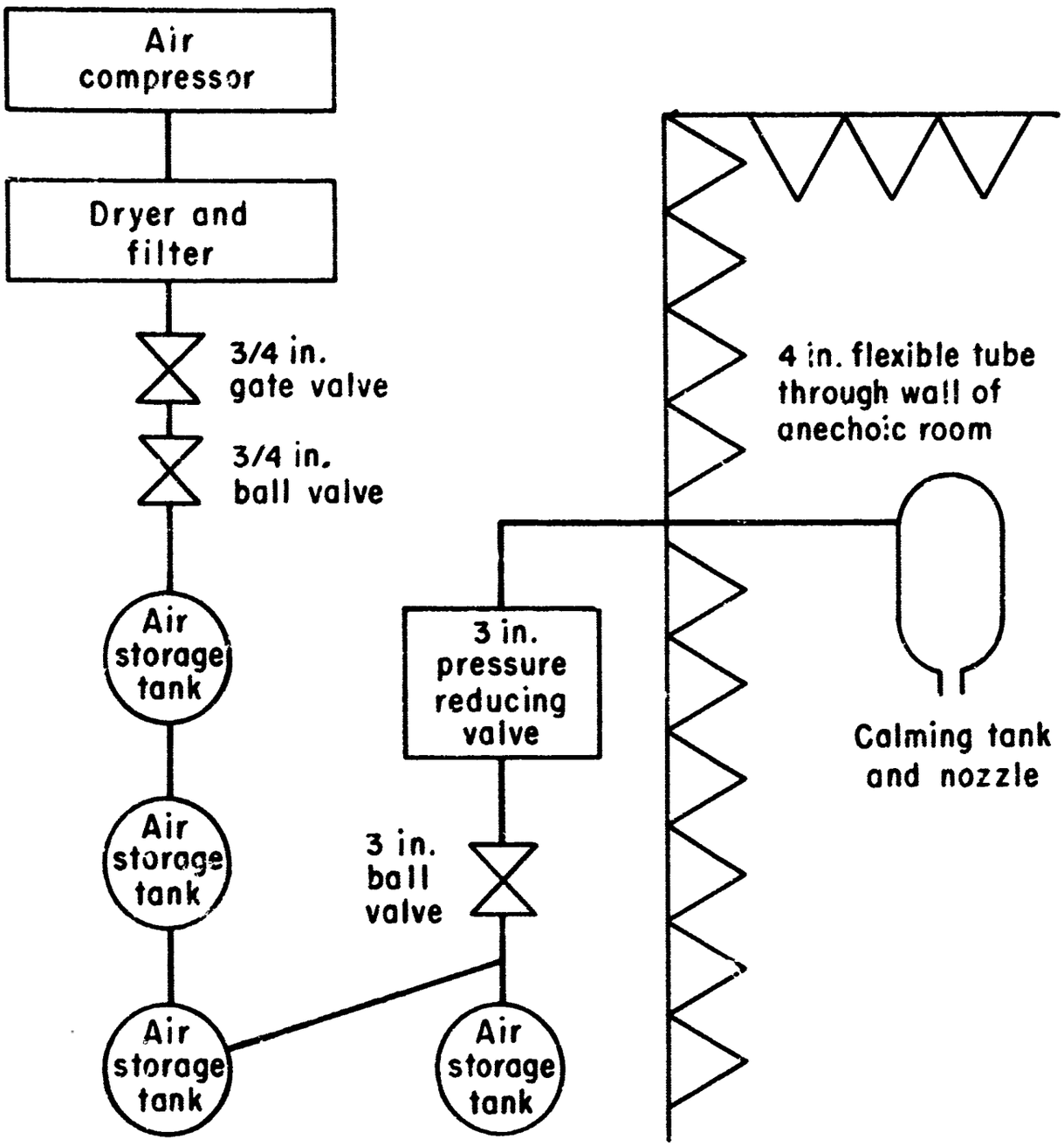

Figure 1. Jet Noise Facility
(a) Air Supply Equipment

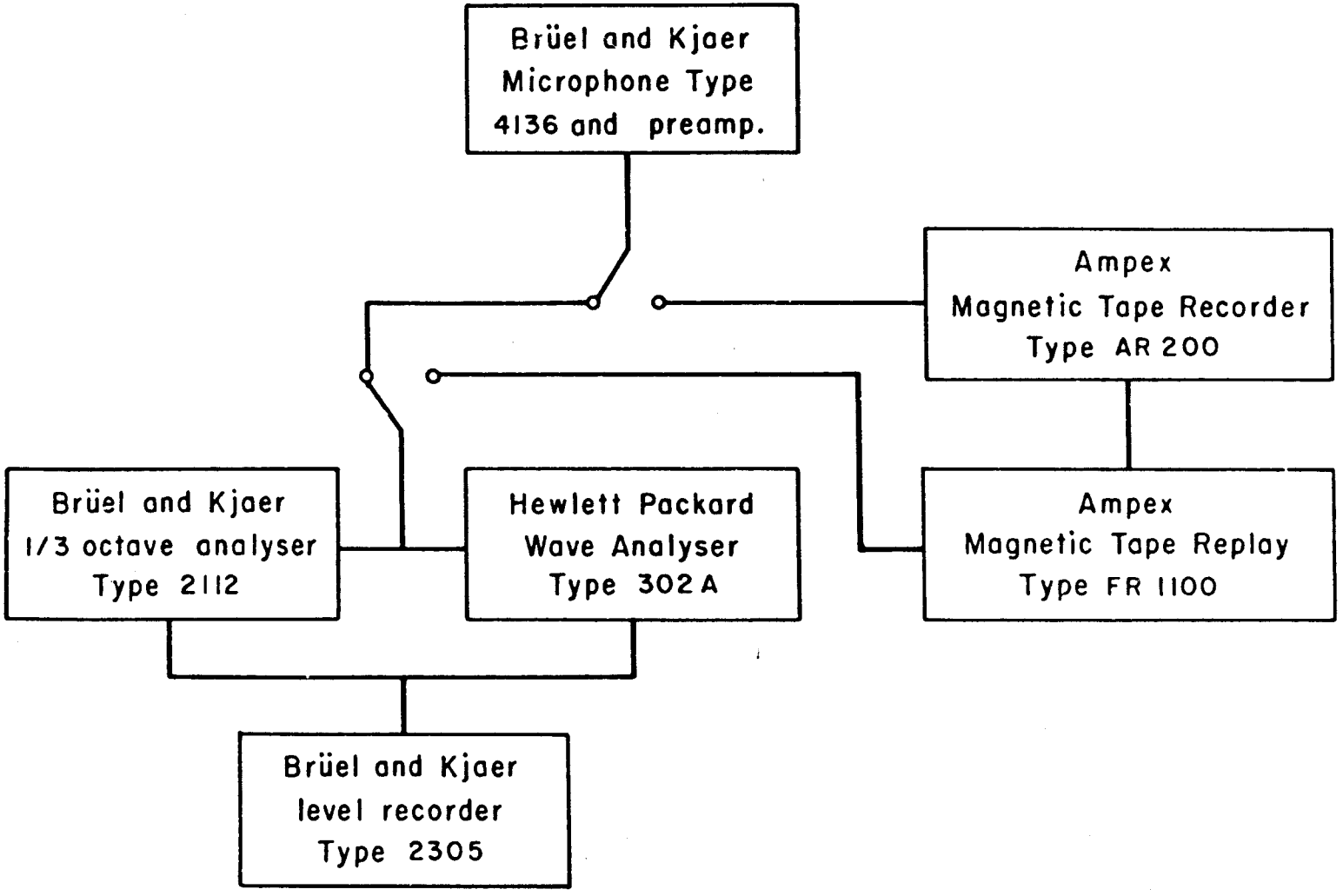

Figure 1. Jet Noise Facility
(b) Noise Measuring Equipment

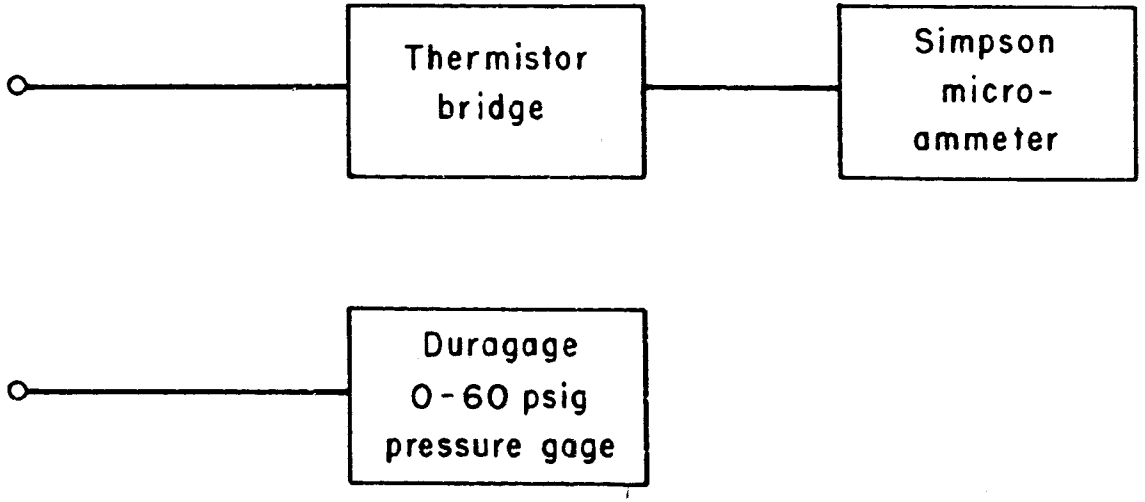

Figure 1. Jet Noise Facility
(c) Pressure and Temperature Measuring Equipment

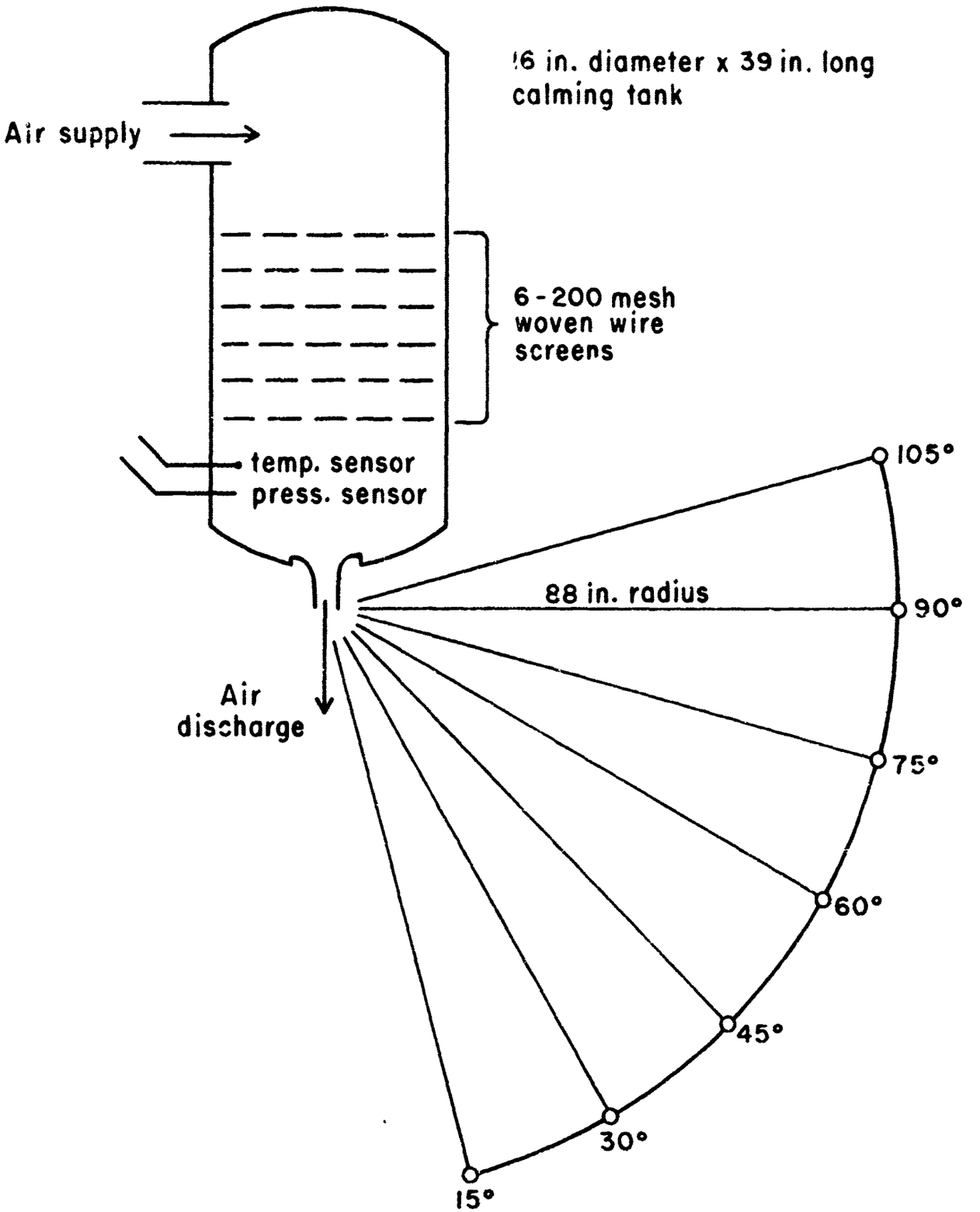

Figure 1. Jet Noise Facility
(d) Calming Tank Details and Noise Survey Stations

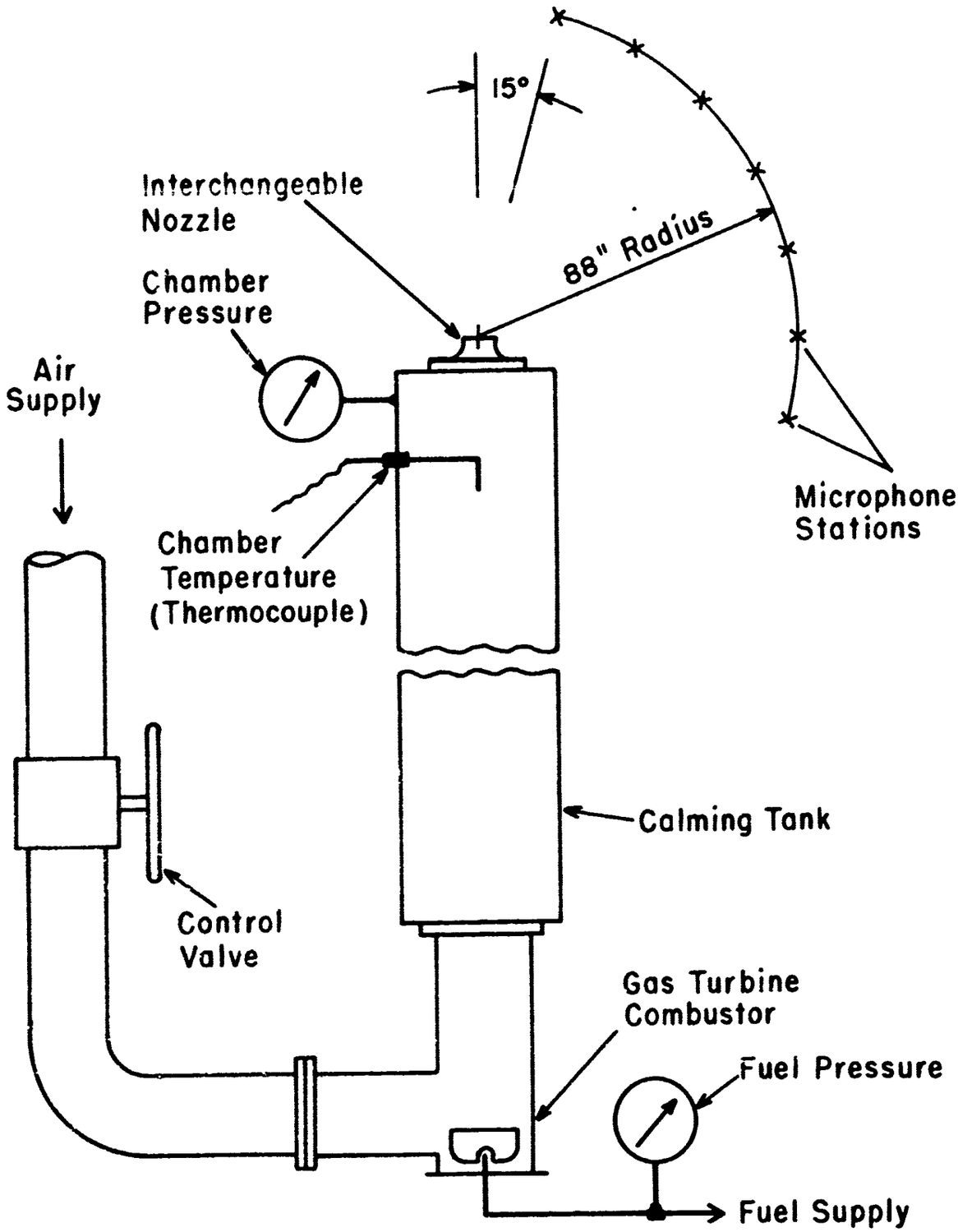

Figure 1. Jet Noise Facility
(e) Hot Jet Facility

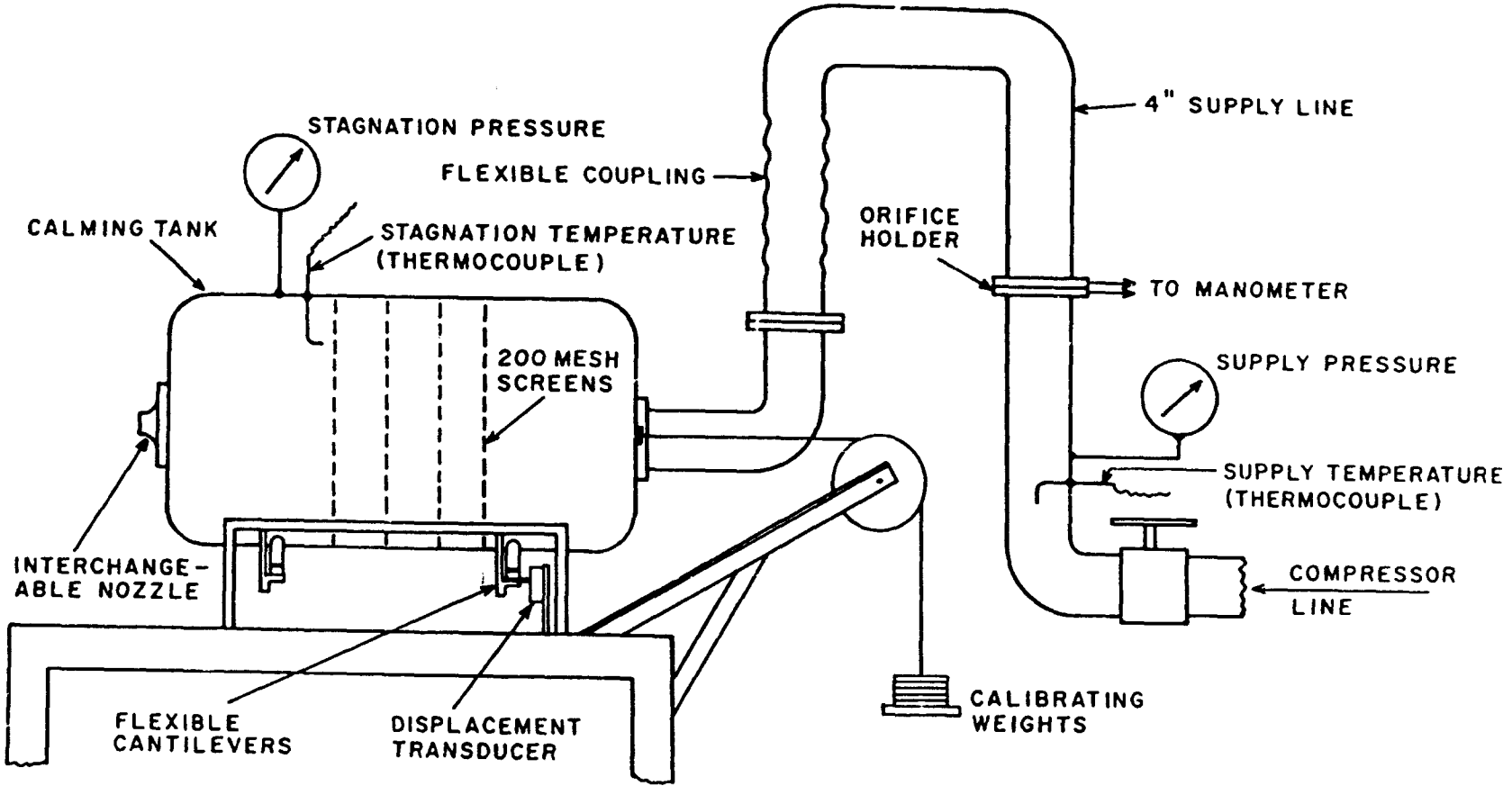

Figure 1 Jet Noise Facility
(f) Thrust Stand

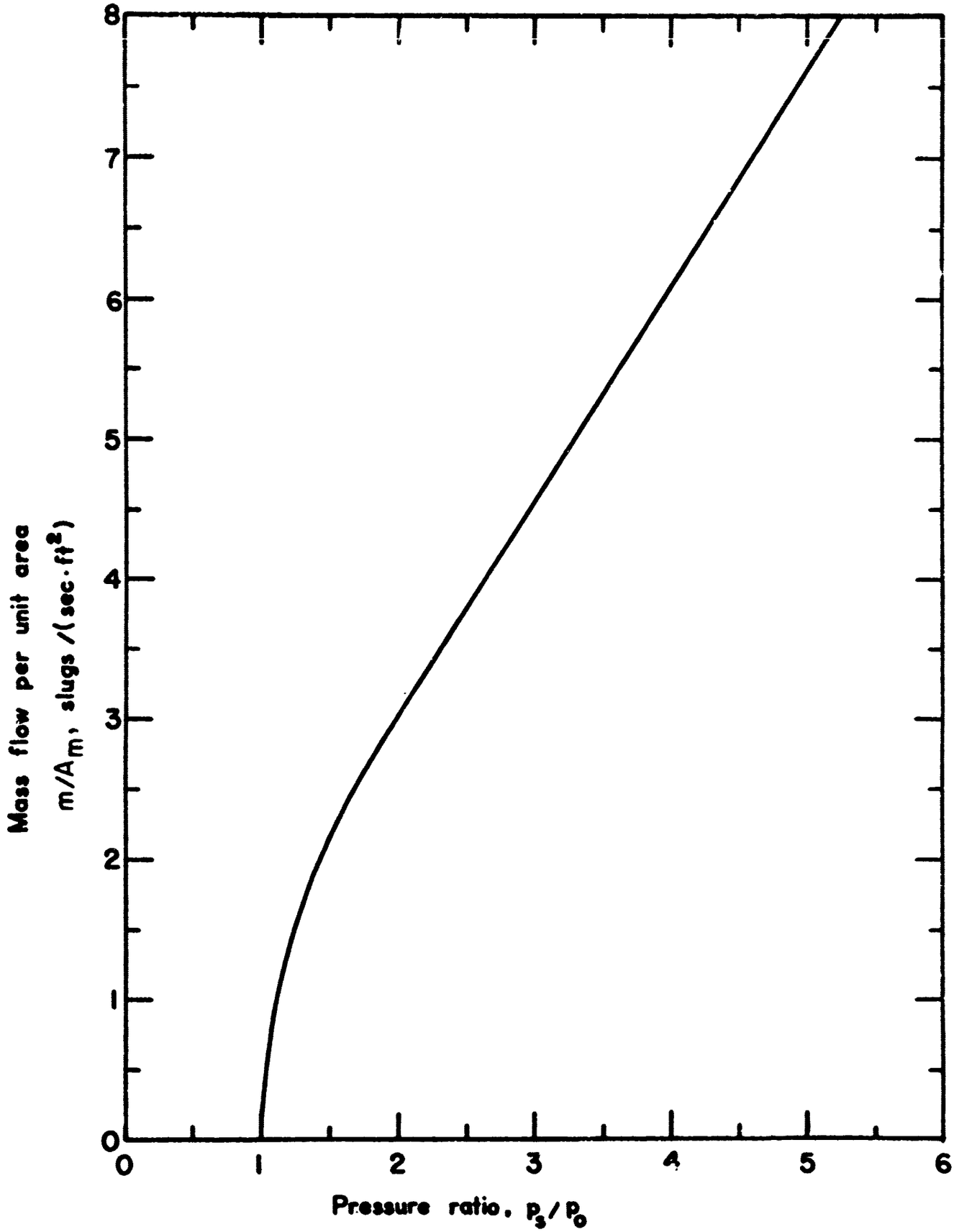

Figure 2. Theoretical Performance
(a) Mass Flow vs Pressure Ratio

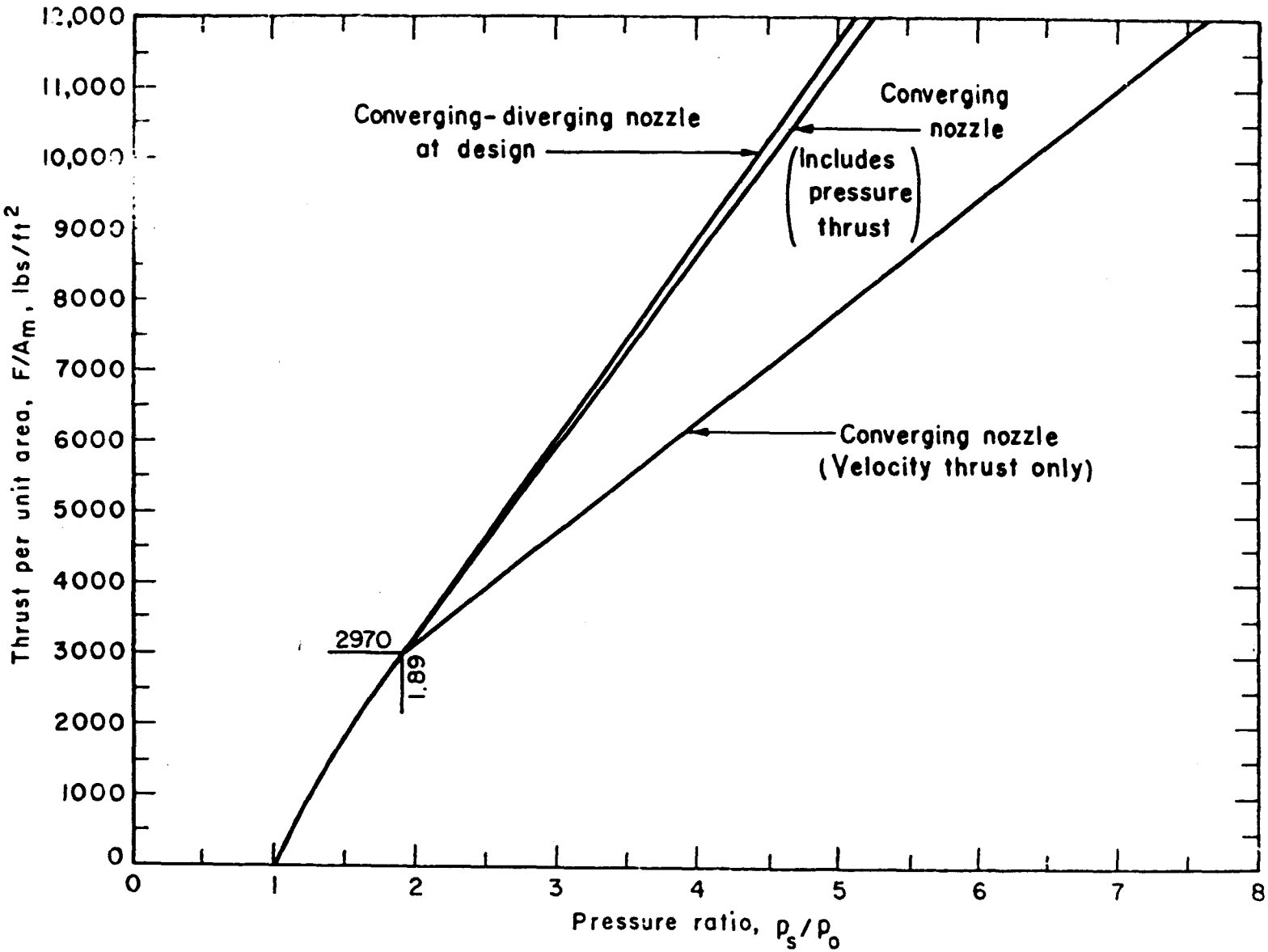

Figure 2. Theoretical Performance
(b) Thrust vs Pressure Ratio

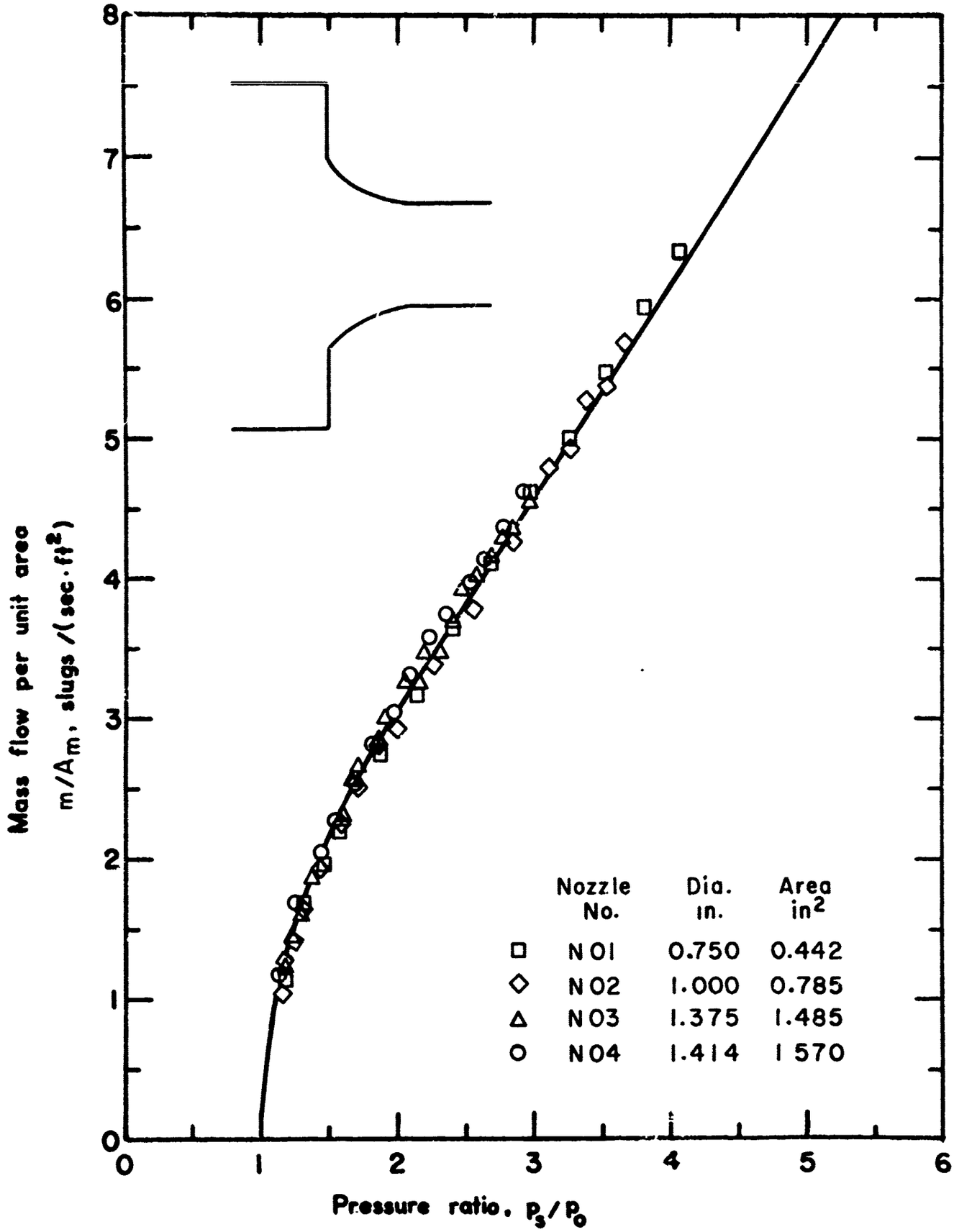

Figure 3. Flow Performance of Nozzles
(a) Converging Nozzles Nos. N01, N02, N03, and N04

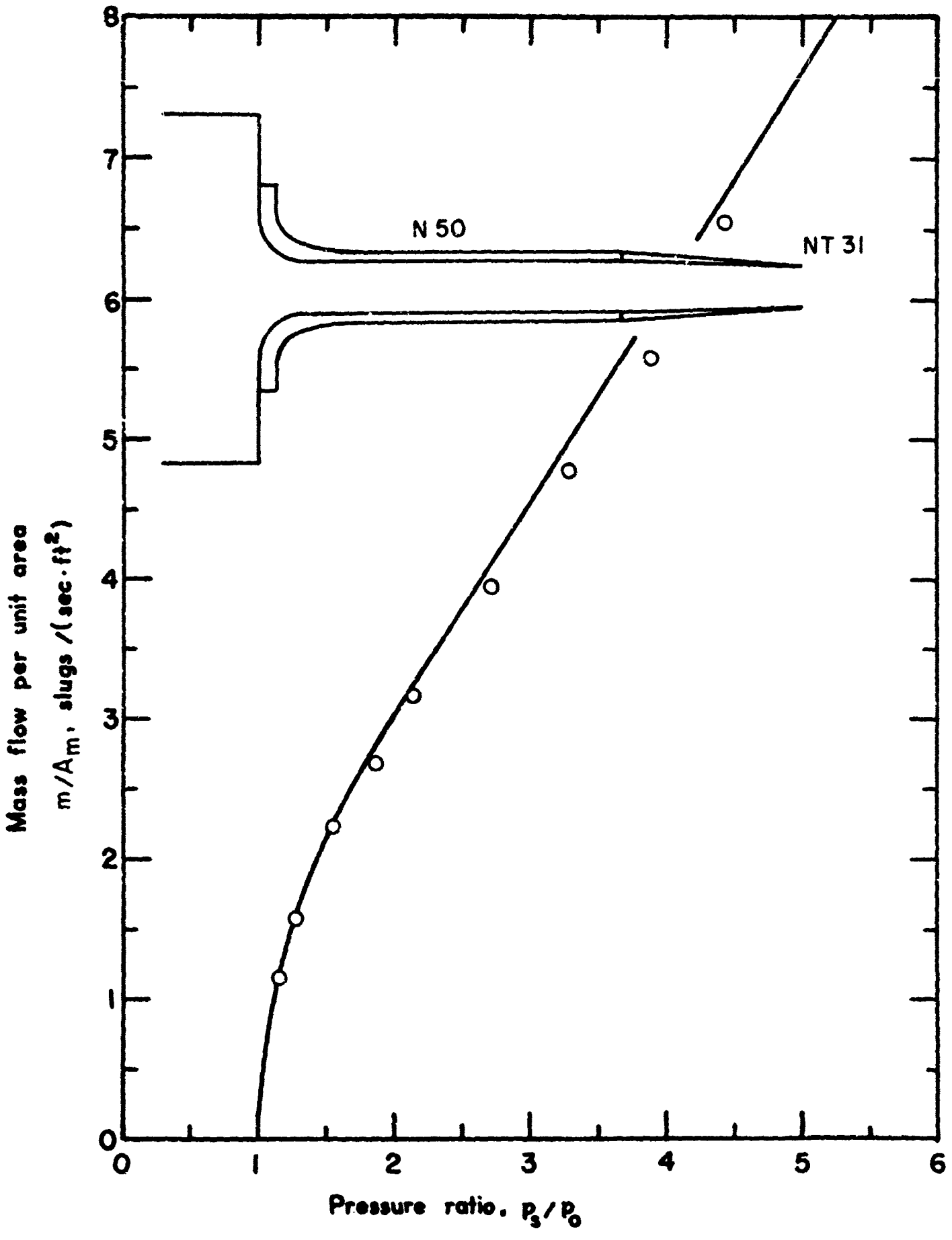

Figure 3. Flow Performance of Nozzles
(b) Extended Converging Nozzle, No. N50:NT31

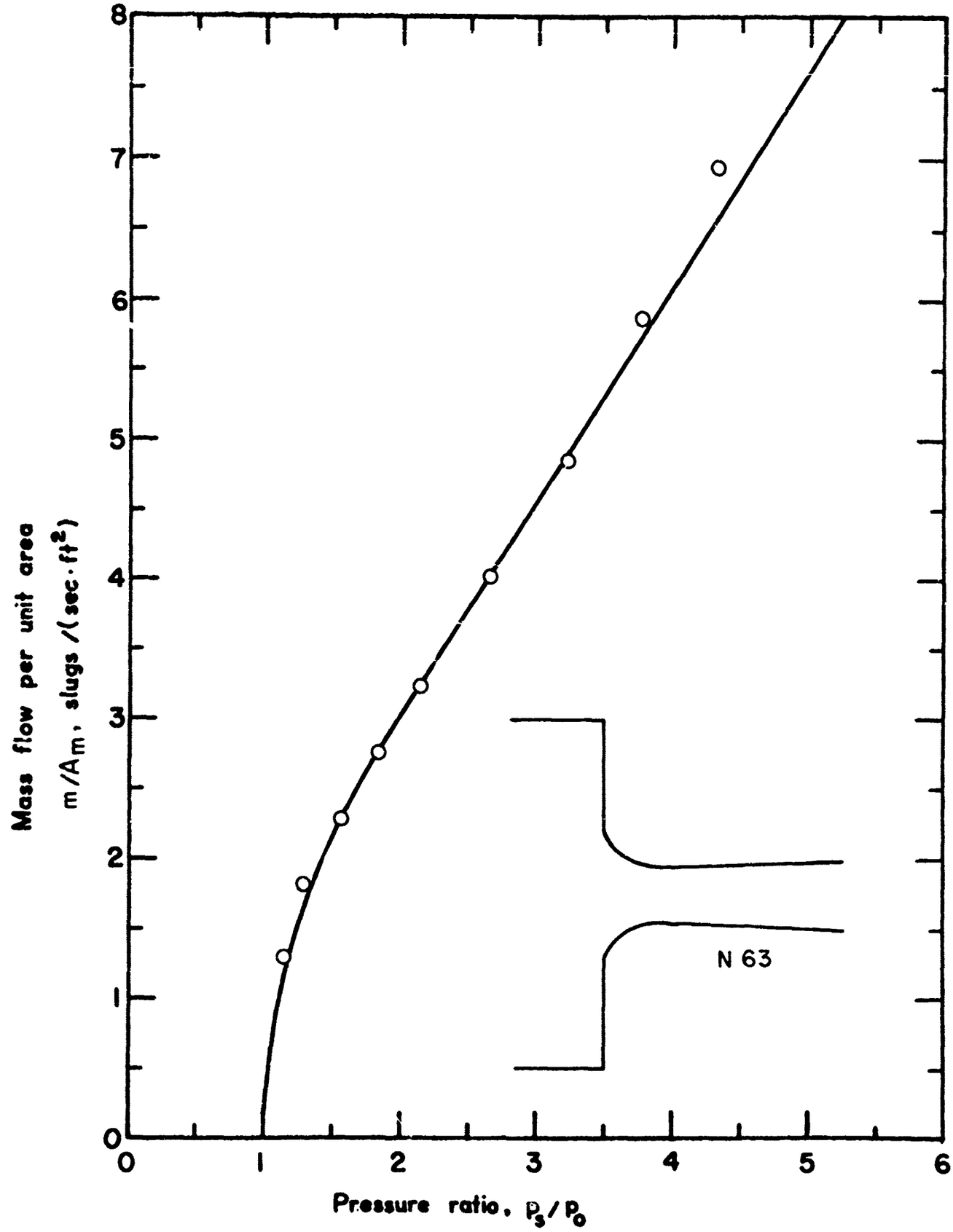

Figure 3. Flow Performance of Nozzles
(c) Converging-Diverging Nozzle, No. N63

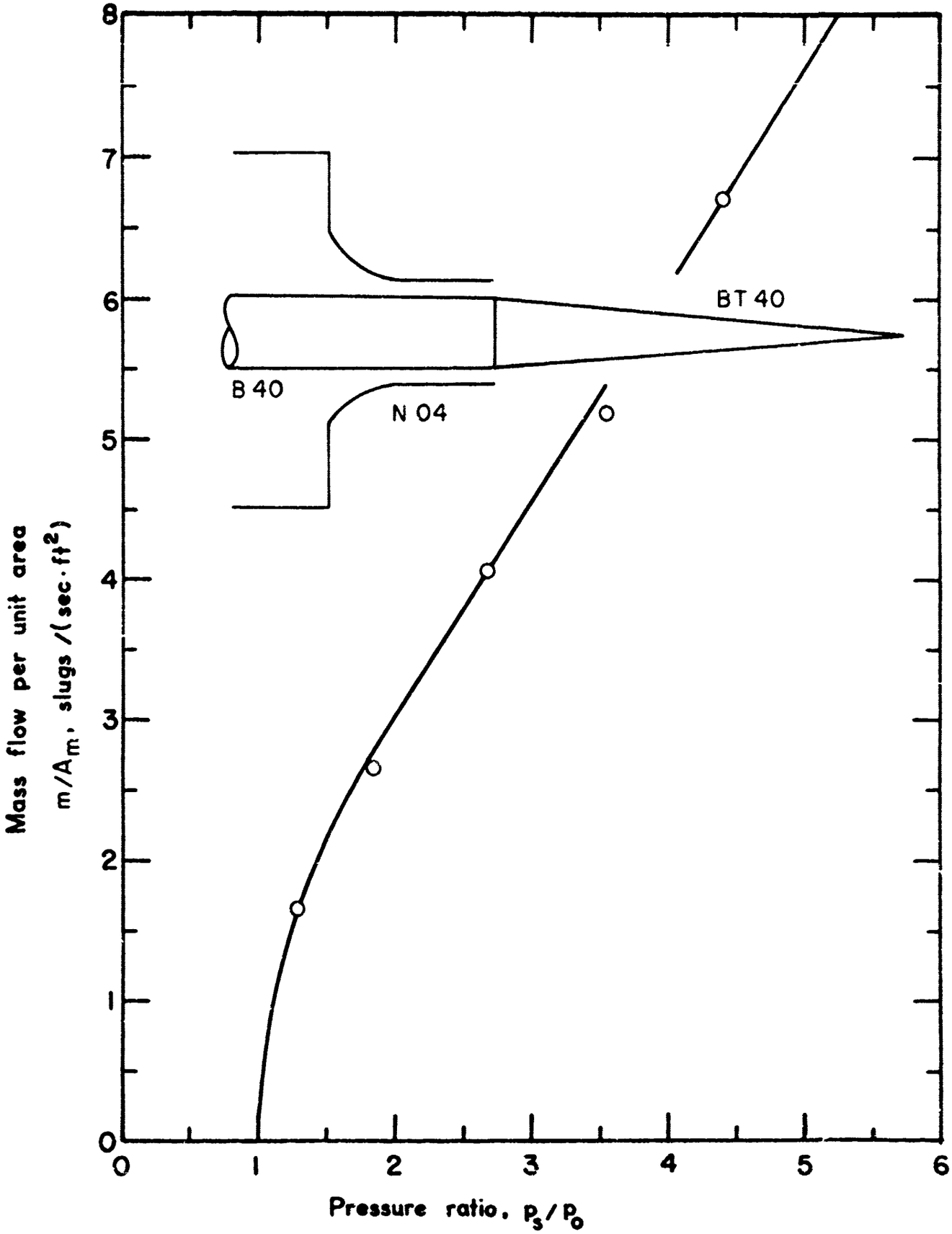

Figure 3. Flow Performance of Nozzles
(d) Plug Nozzle No. 1:04:40:40:0

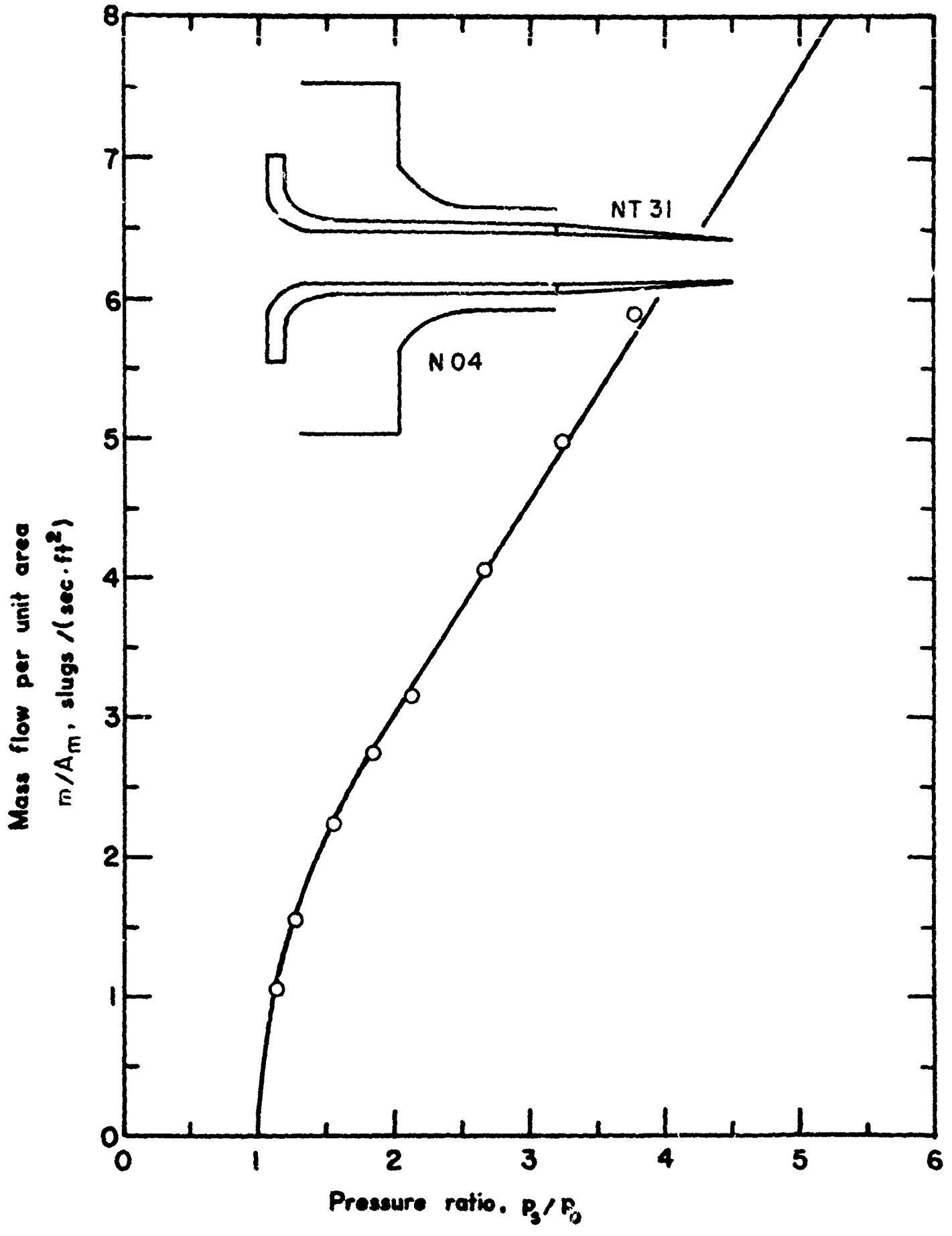

Figure 3. Flow Performance of Nozzles
(e) Center Core Flow Nozzle No. 2:04:51:3[illegible] + 0

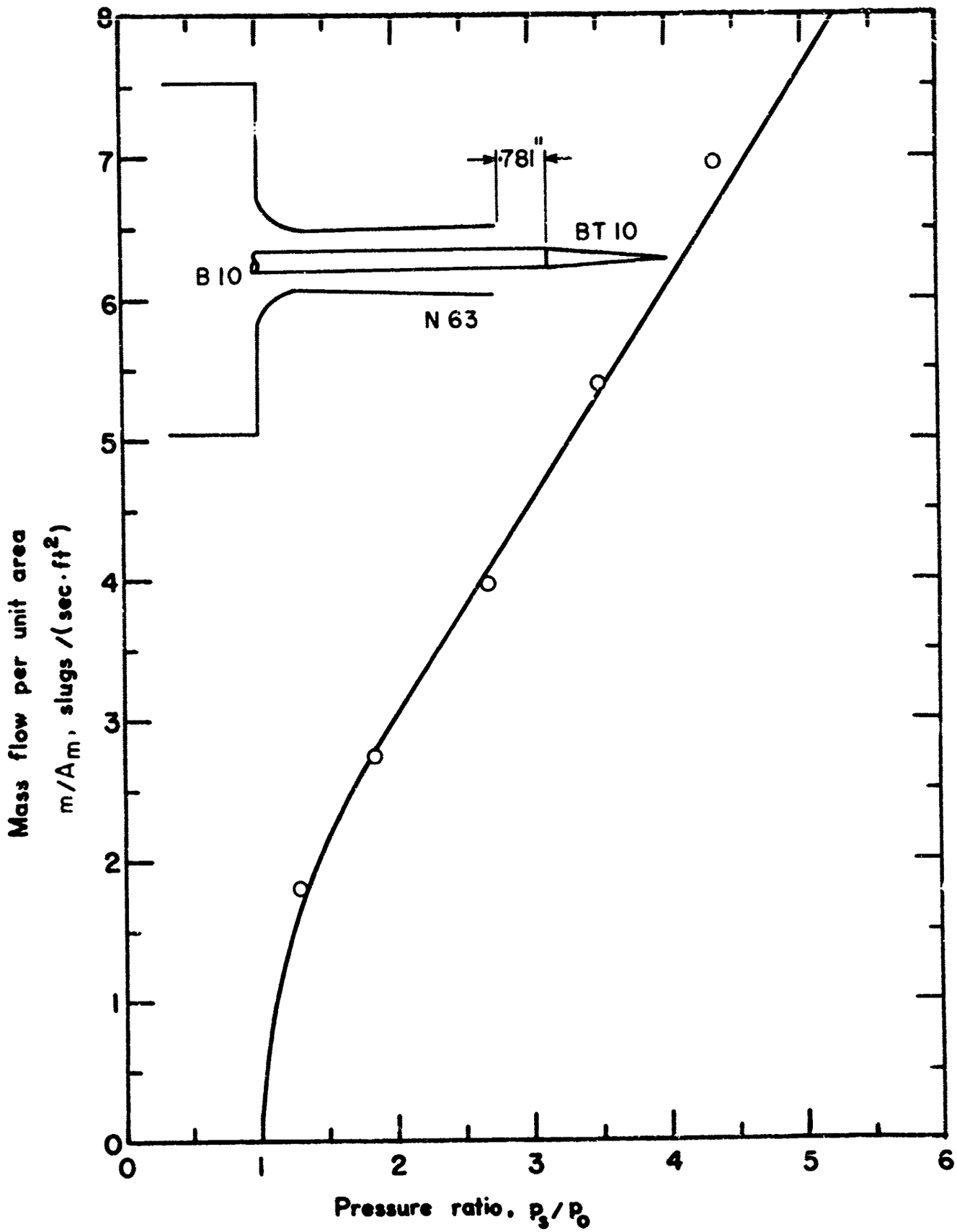

Figure 3. Flow Performance of Nozzles
(f) Converging-Diverging Plug Nozzle No. 1:63:10:10 + 0.781

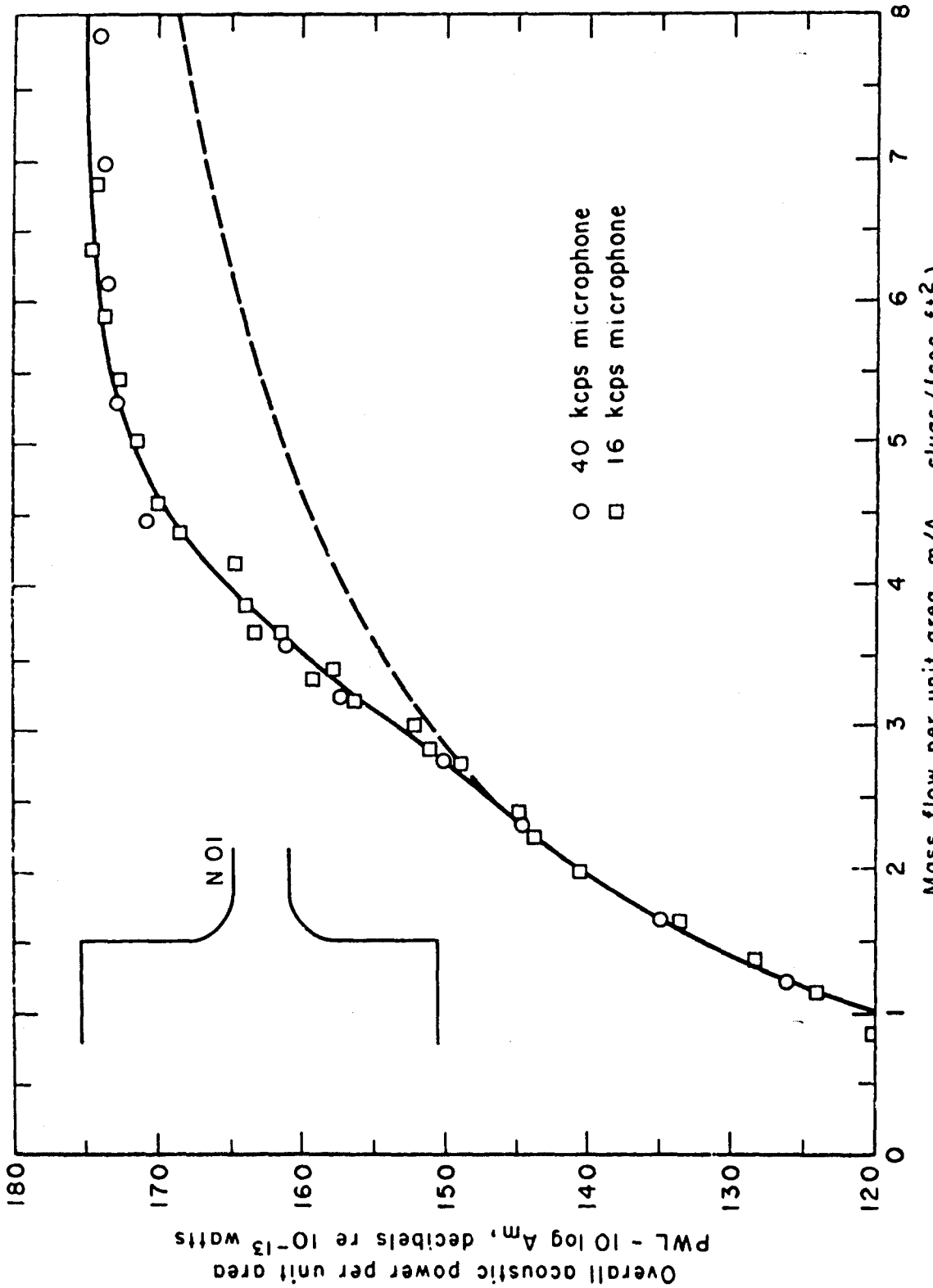

Figure 4. Acoustic Performance of Basic Nozzles
(a) Nozzle No. NO1

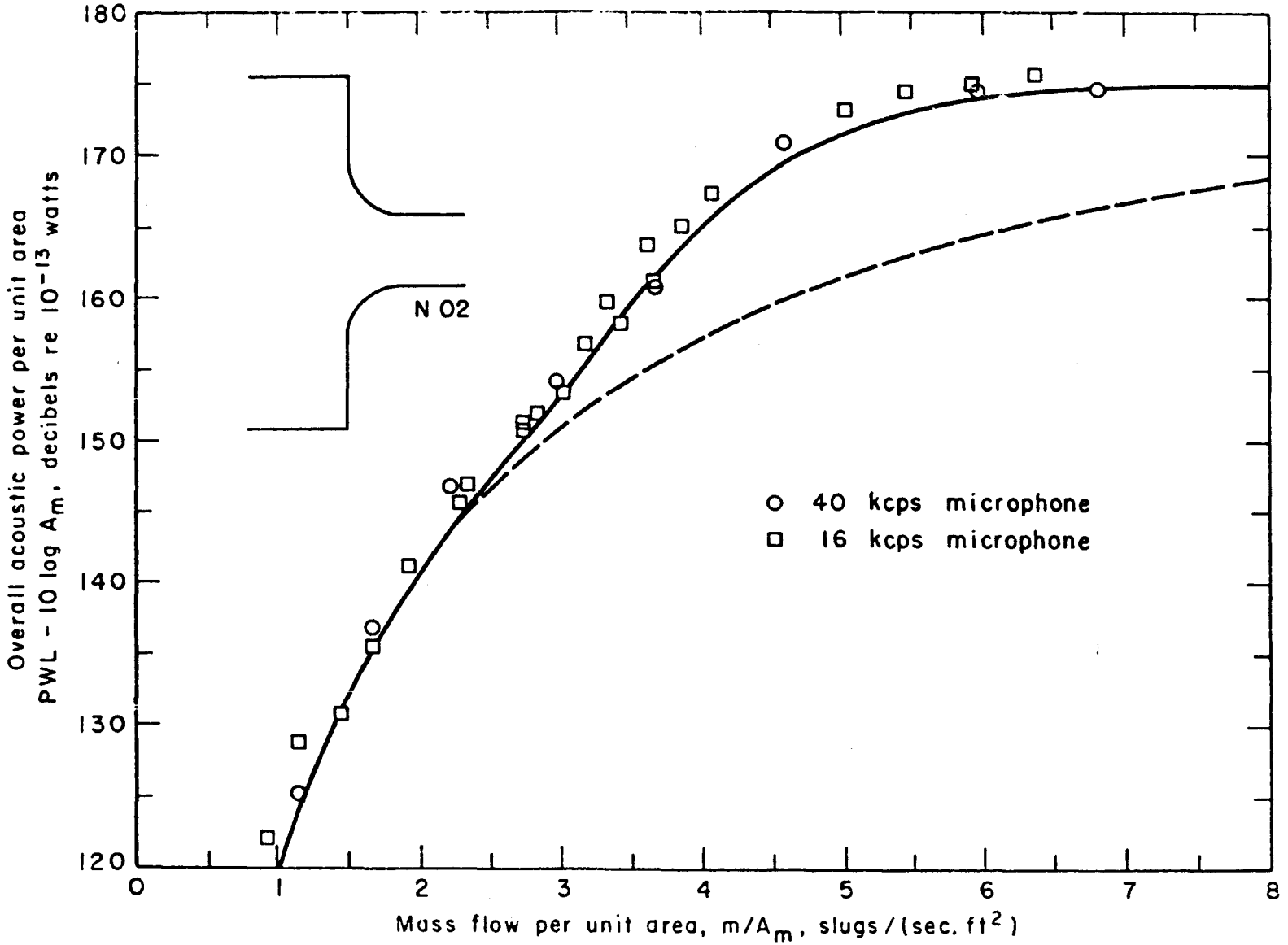

Figure 4. Acoustic Performance of Basic Nozzles
(b) Nozzle No. N02

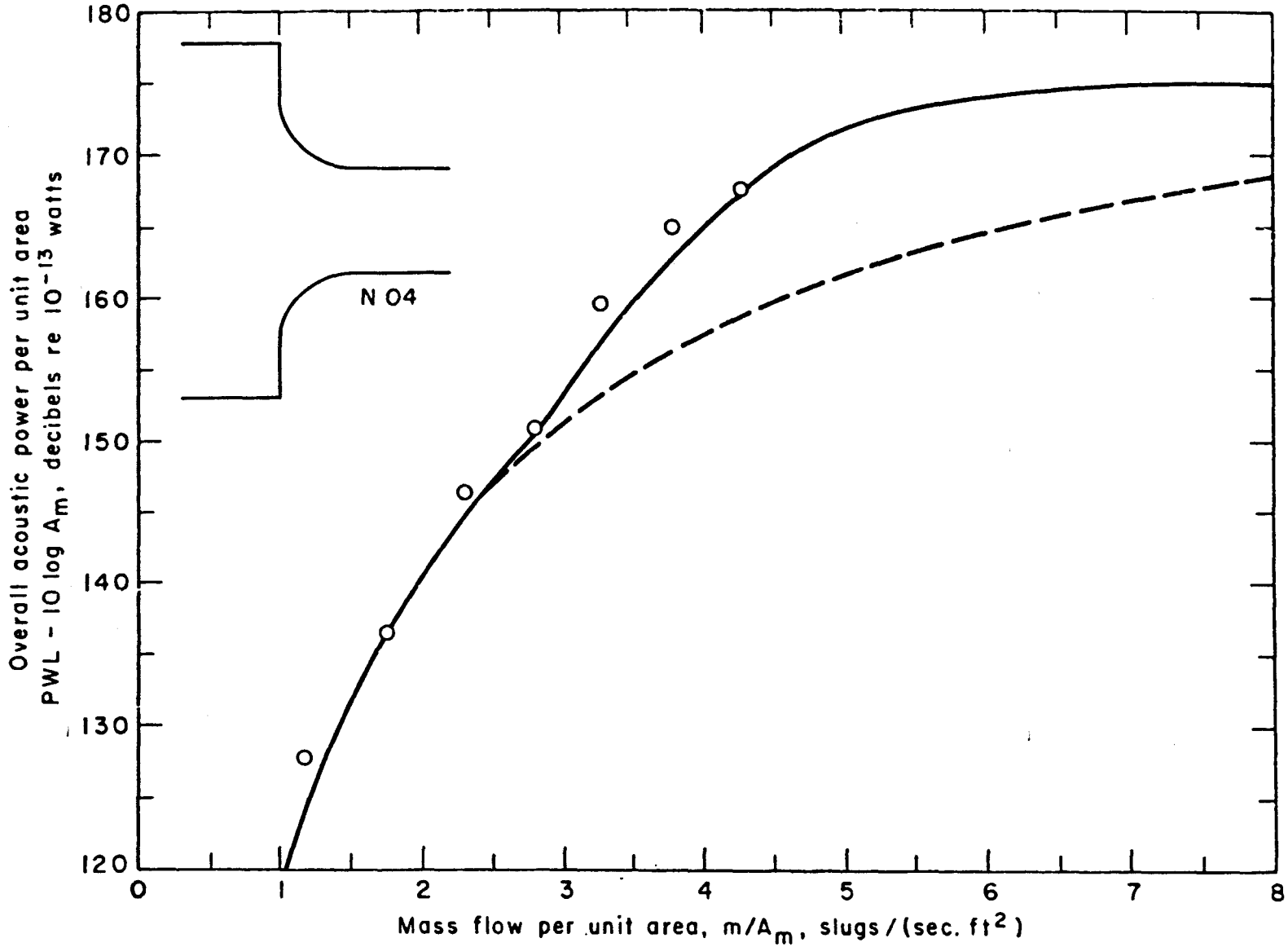

Figure 4. Acoustic Performance of Basic Nozzles
(c) Nozzle No. N04

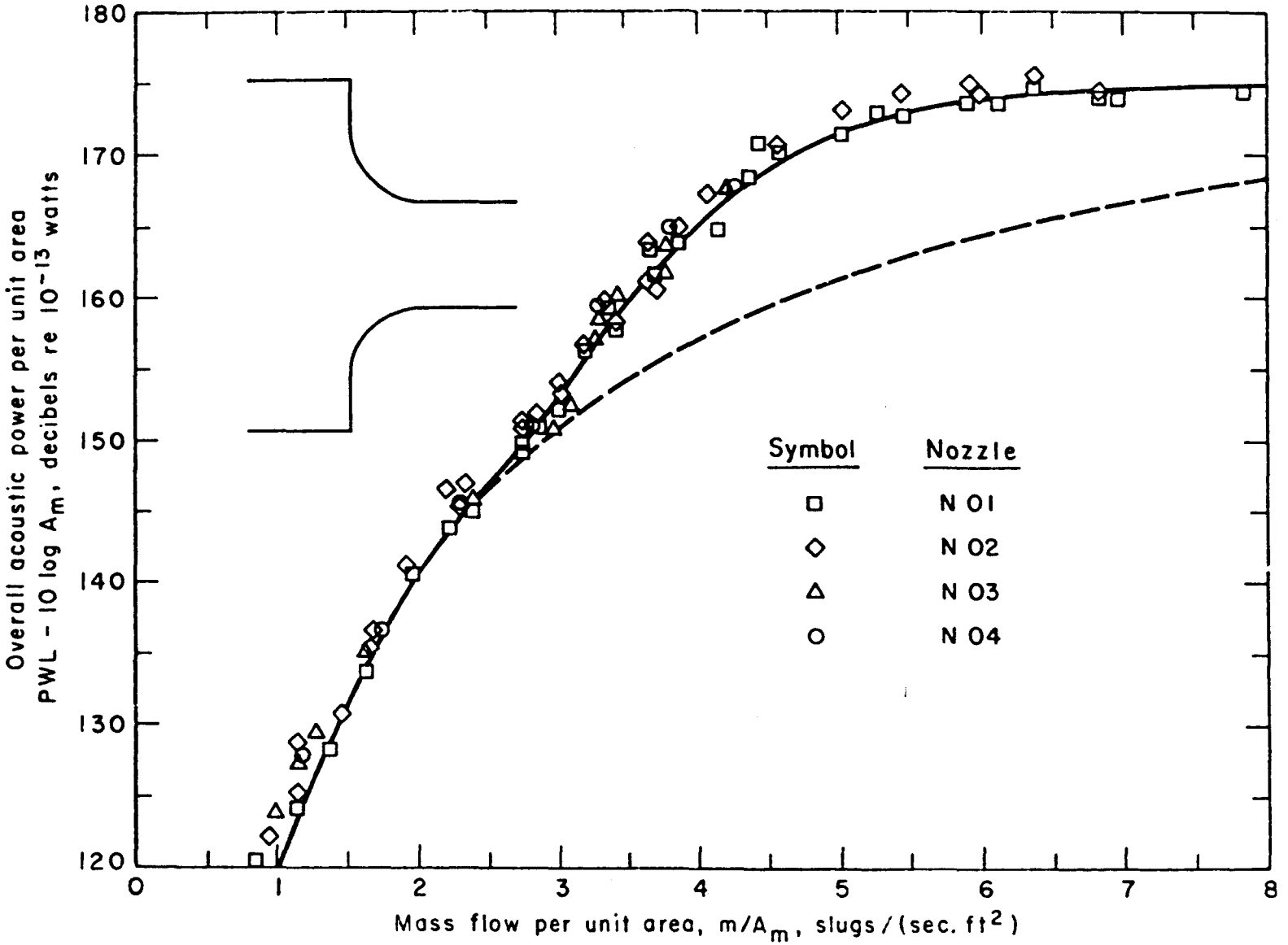

Figure 4. Acoustic Performance of Basic Nozzles
(d) Nozzles Nos. N01, N02, N03, and N04

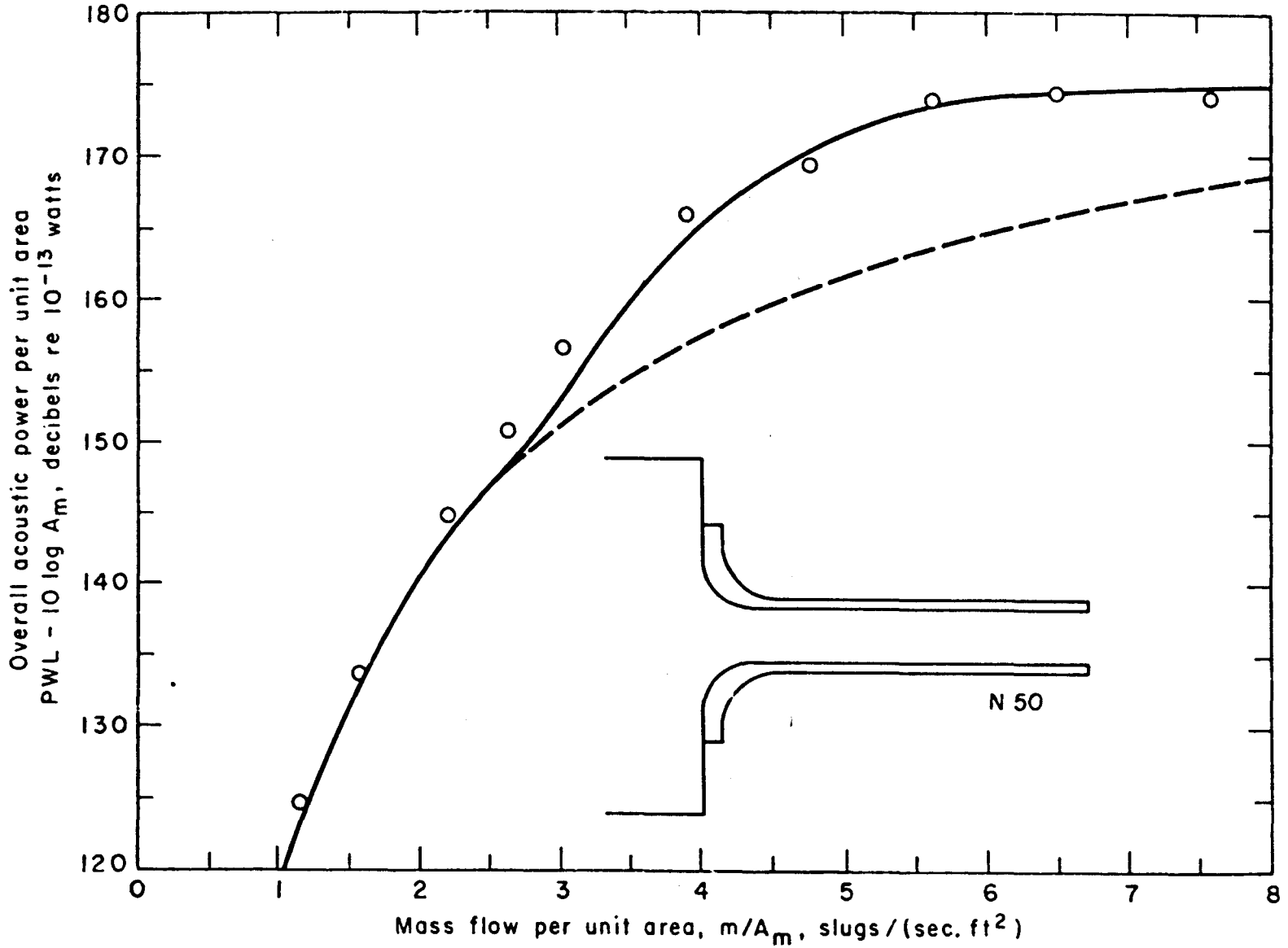

Figure 4. Acoustic Performance of Basic Nozzles
(e) Nozzle No. N50

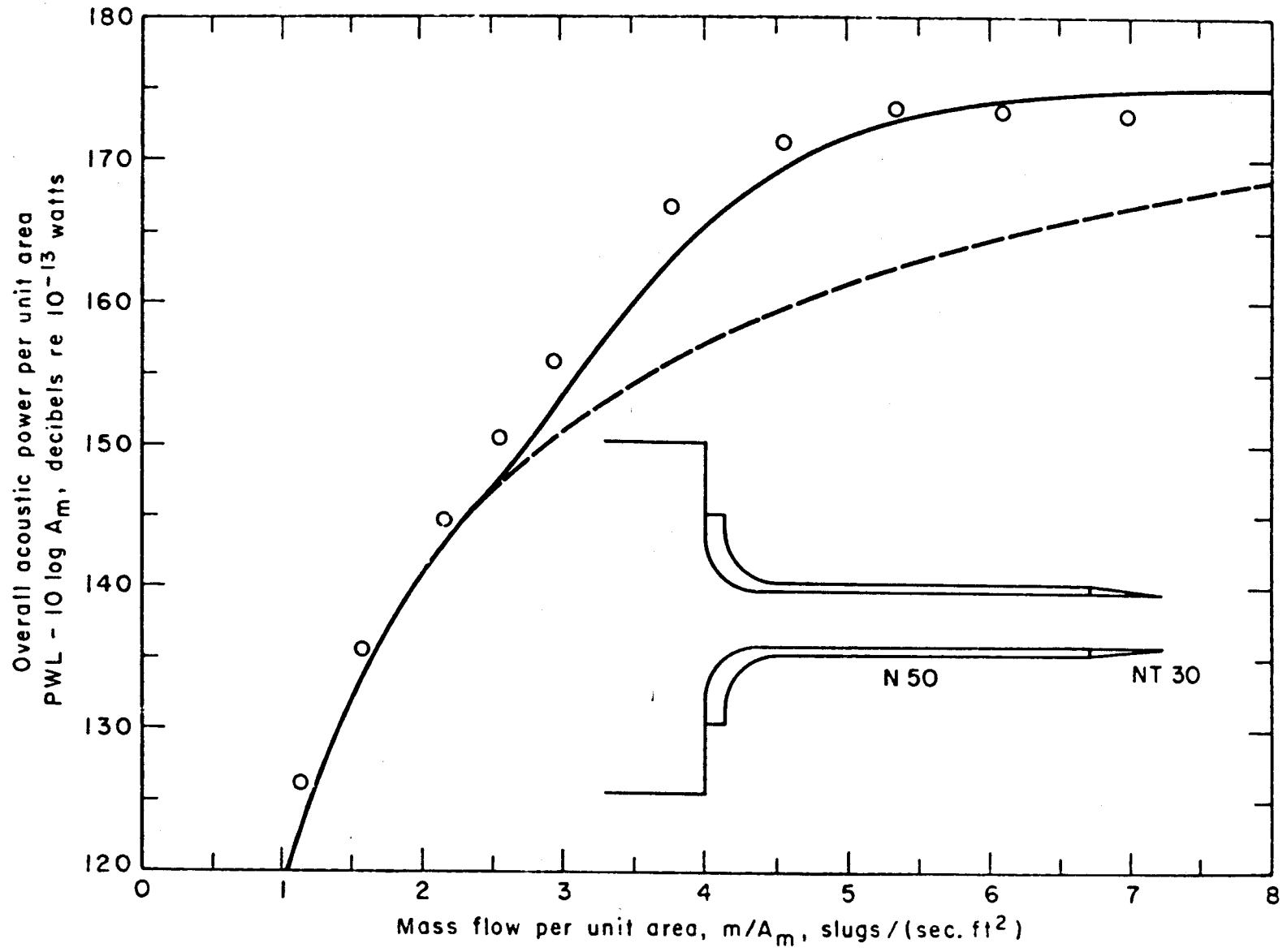

Figure 4. Acoustic Performance of Basic Nozzles
(f) Nozzle No. N50:NT30

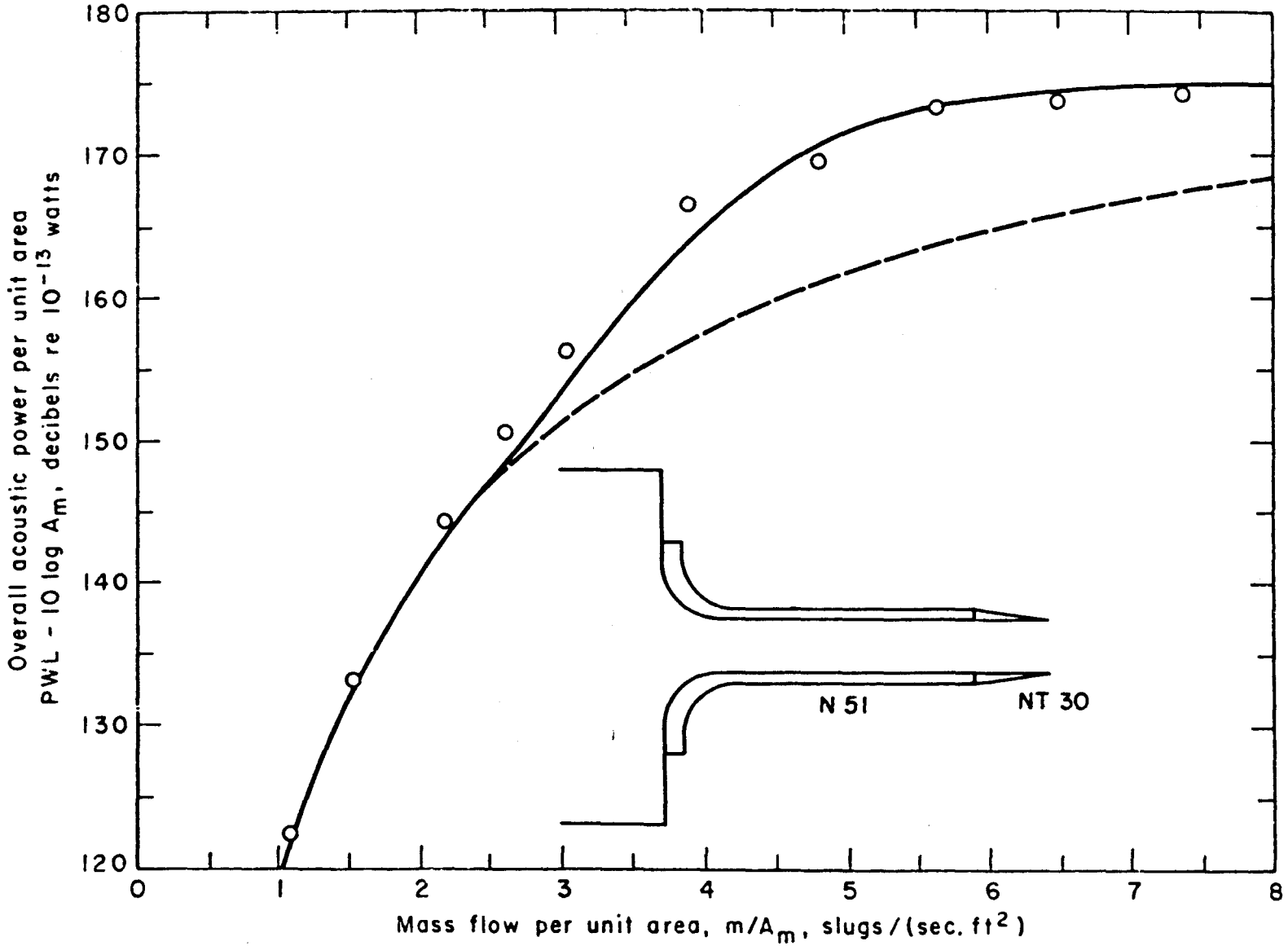

Figure 4. Acoustic Performance of Basic Nozzles
(g) Nozzle No. N51:NT30

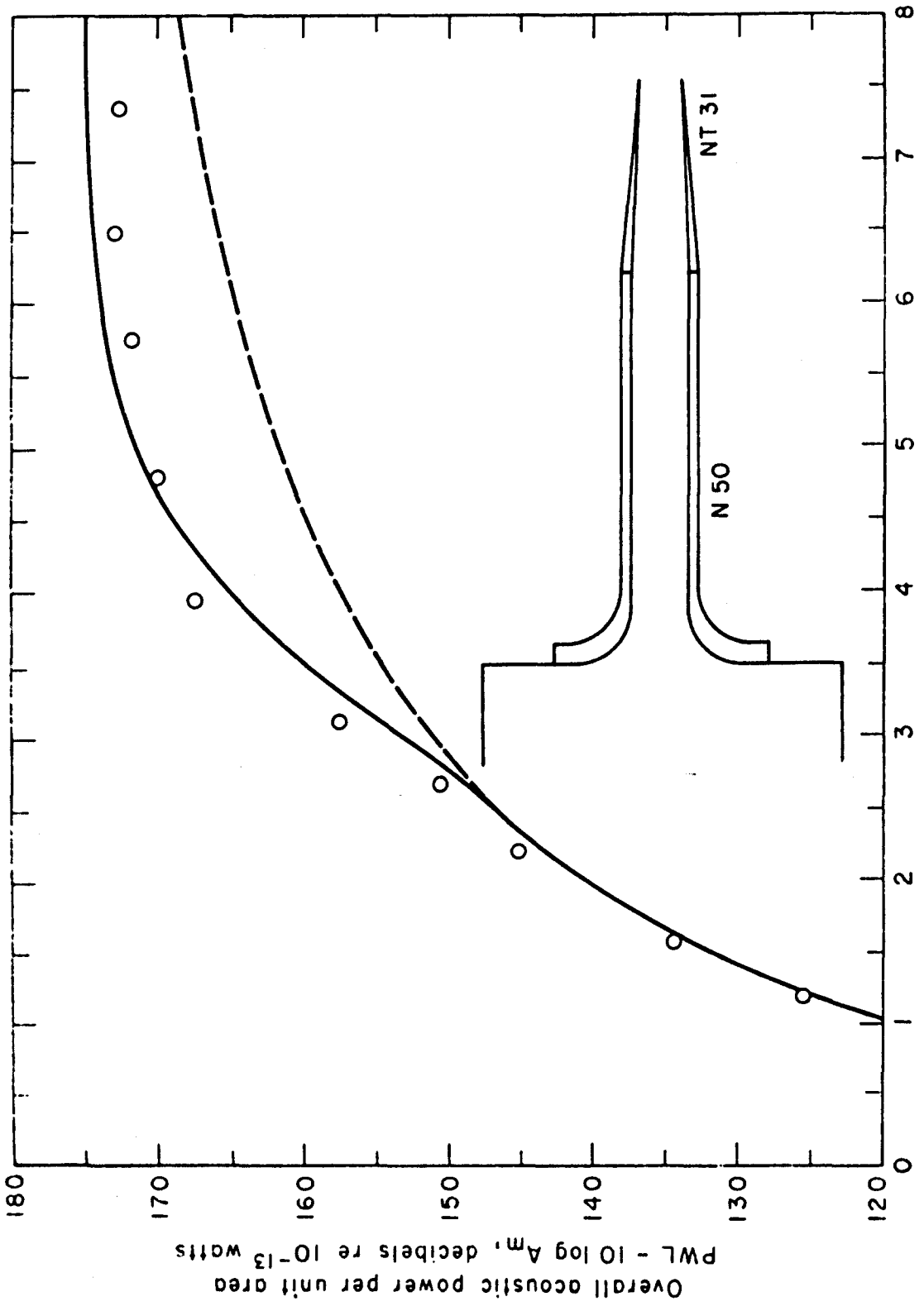

Figure 4. Acoustic Performance of Basic Nozzles
(h) Nozzle No. N50:NT31

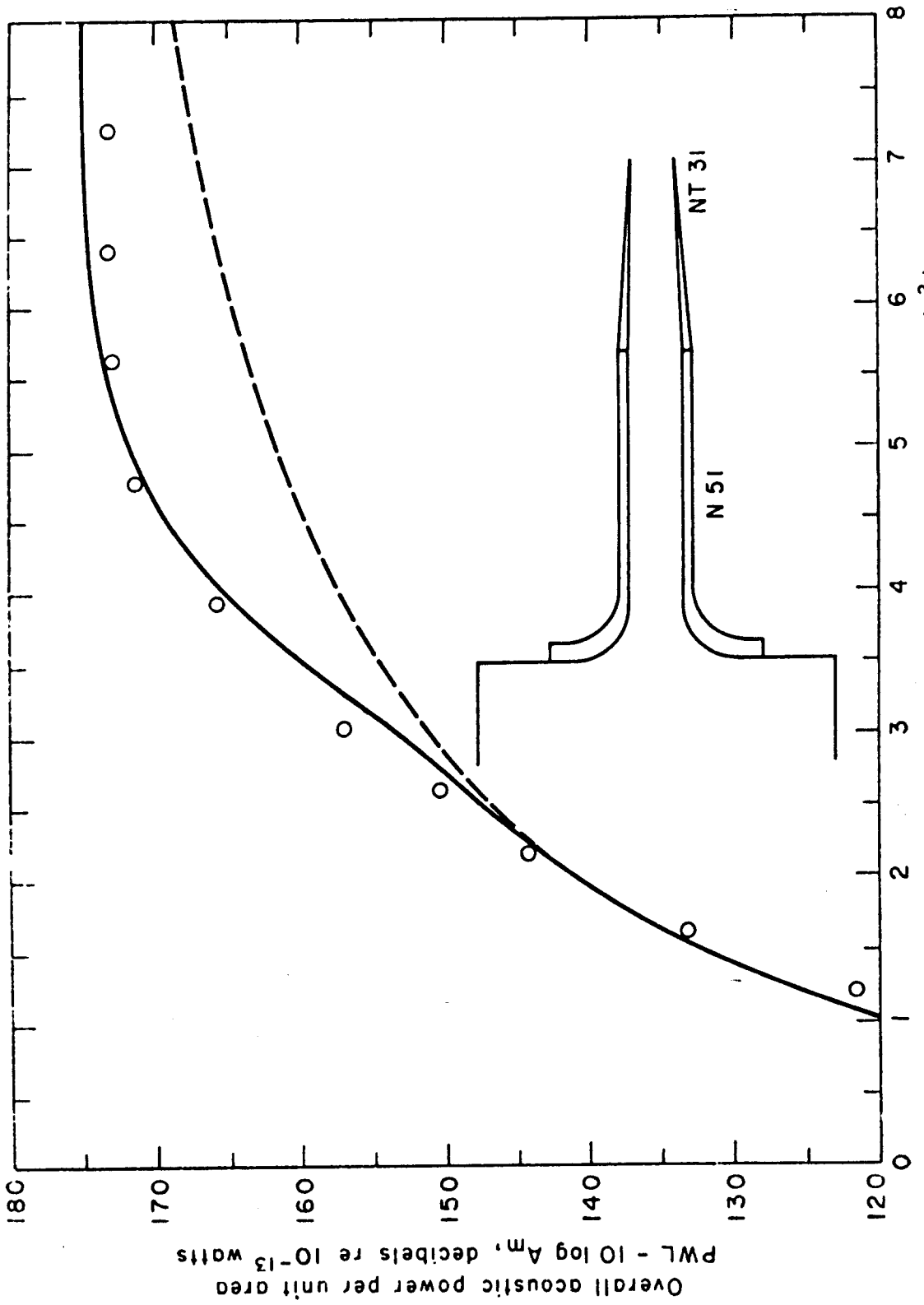

Figure 4. Acoustic Performance of Basic Nozzles
(i) Nozzle No. N51:NT31

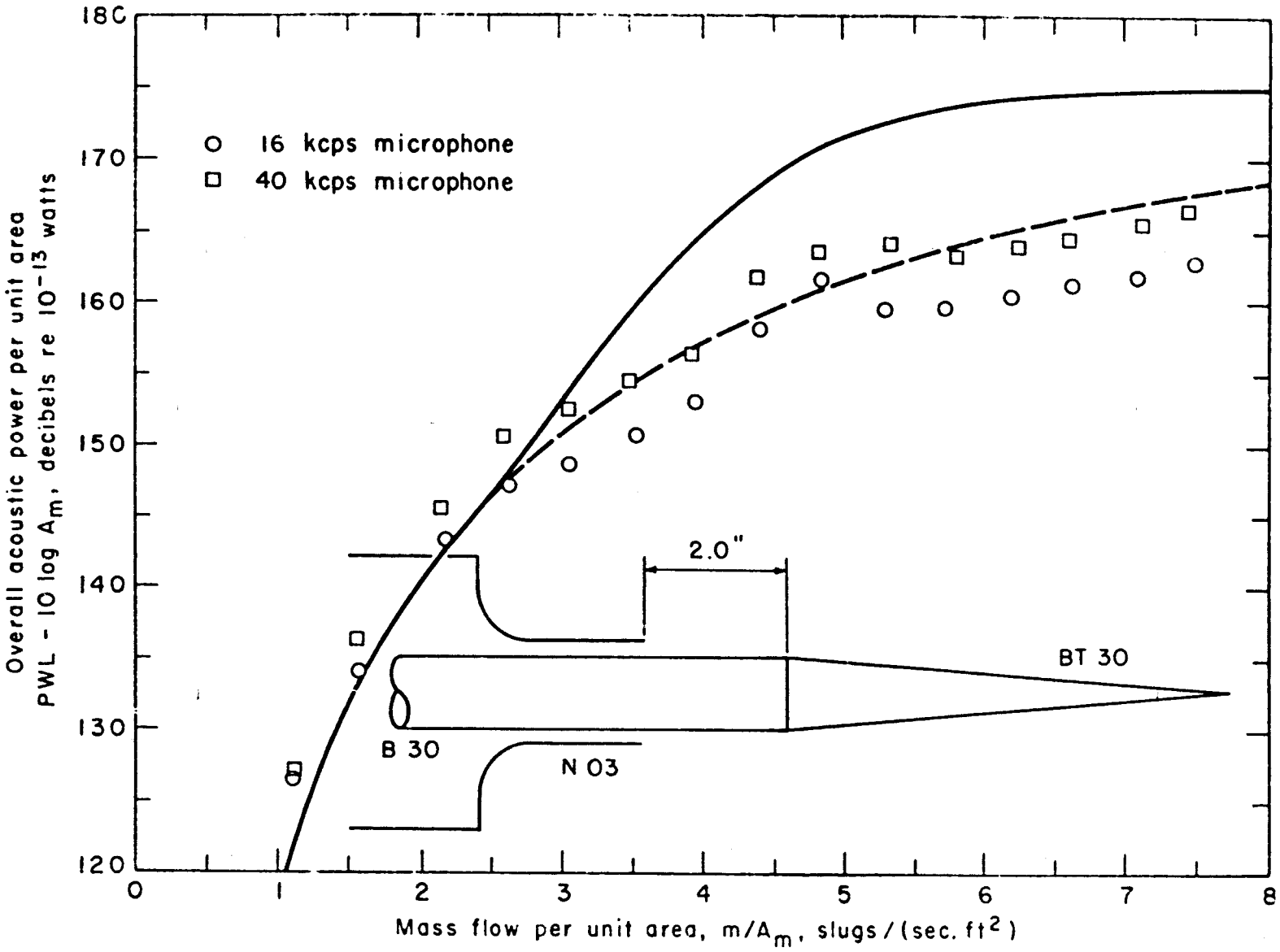

Figure 5. Acoustic Performance of Plug Nozzles
(a) Nozzle No. 1:03:30:30 + 2

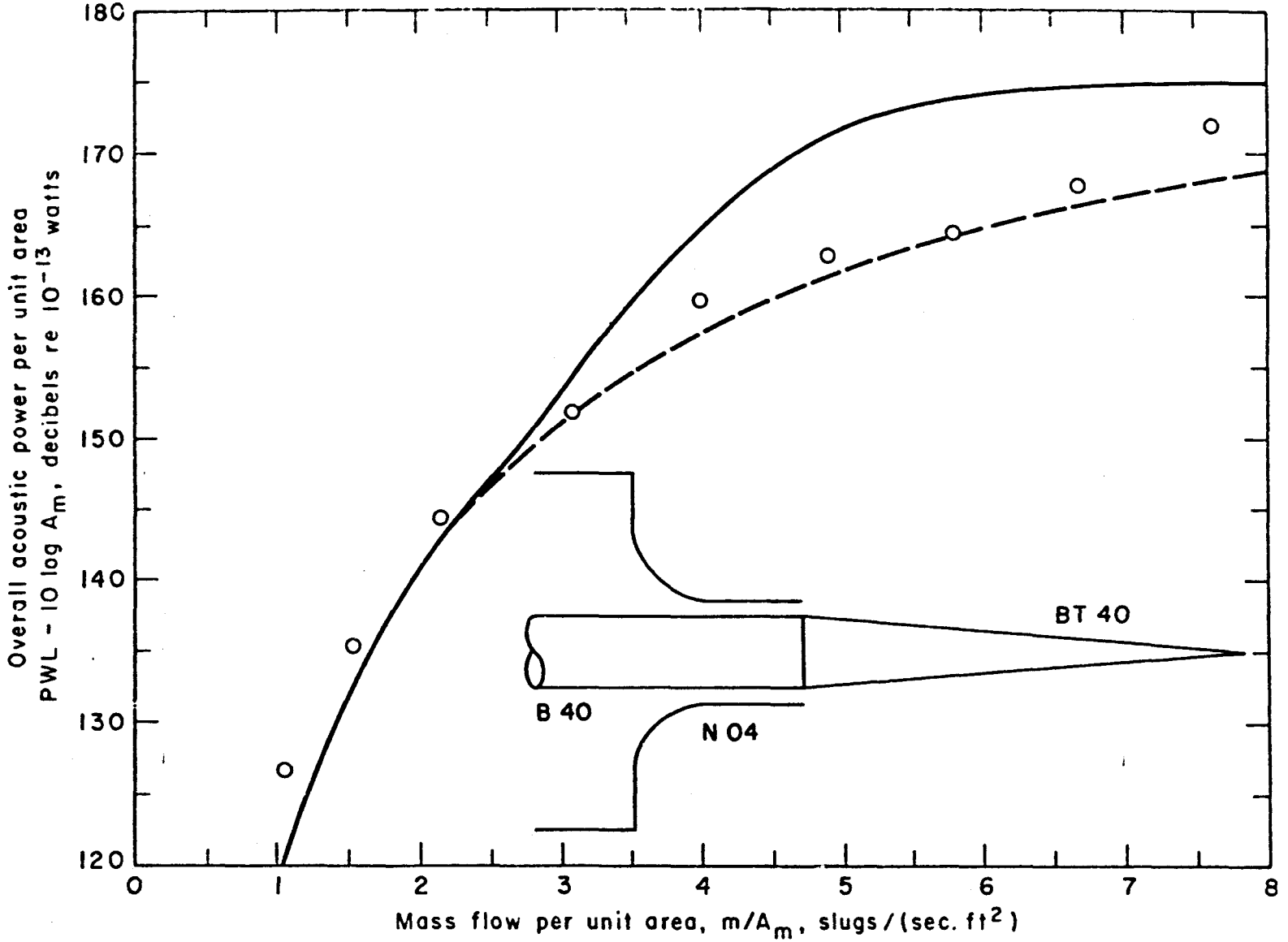

Figure 5. Acoustic Performance of Plug Nozzles
(b) Nozzle No. 1:04:40:40 + 0

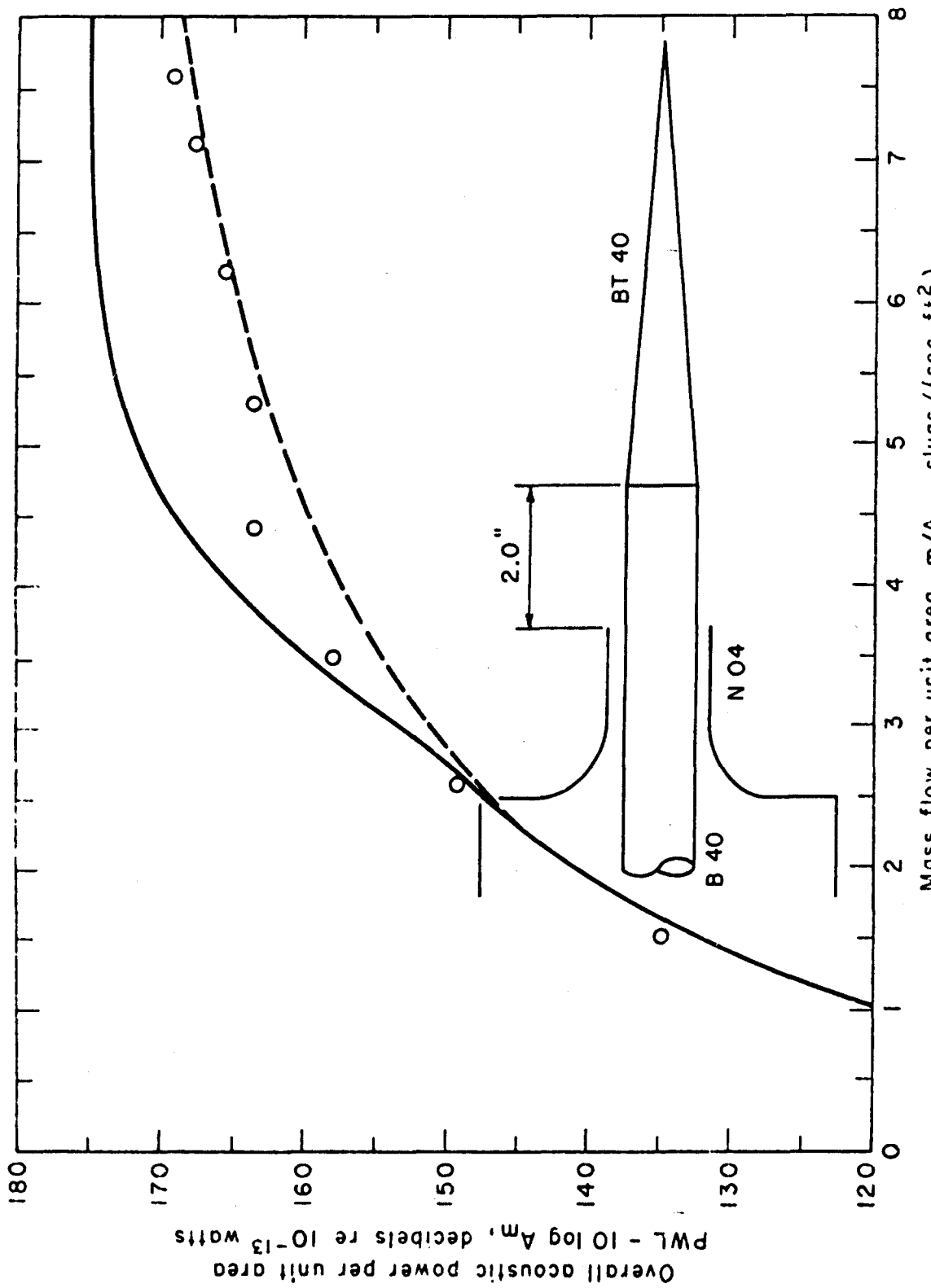

Figure 5. Acoustic Performance of Plug Nozzles
(c) Nozzle No. 1:04:40:40 + 2

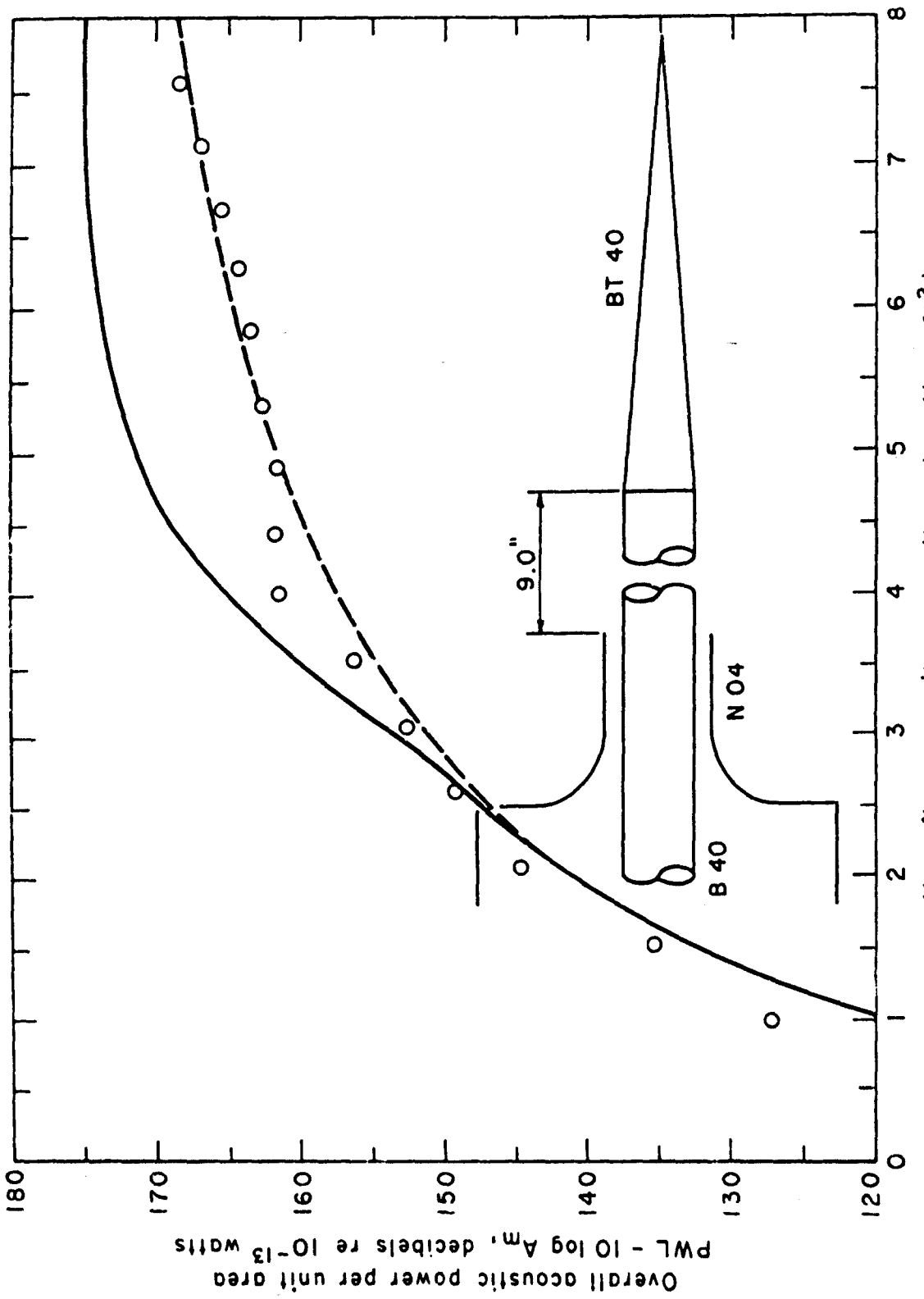

Figure 5. Acoustic Performance of Plug Nozzles
(d) Nozzle No. 1:04:40:40 + 9

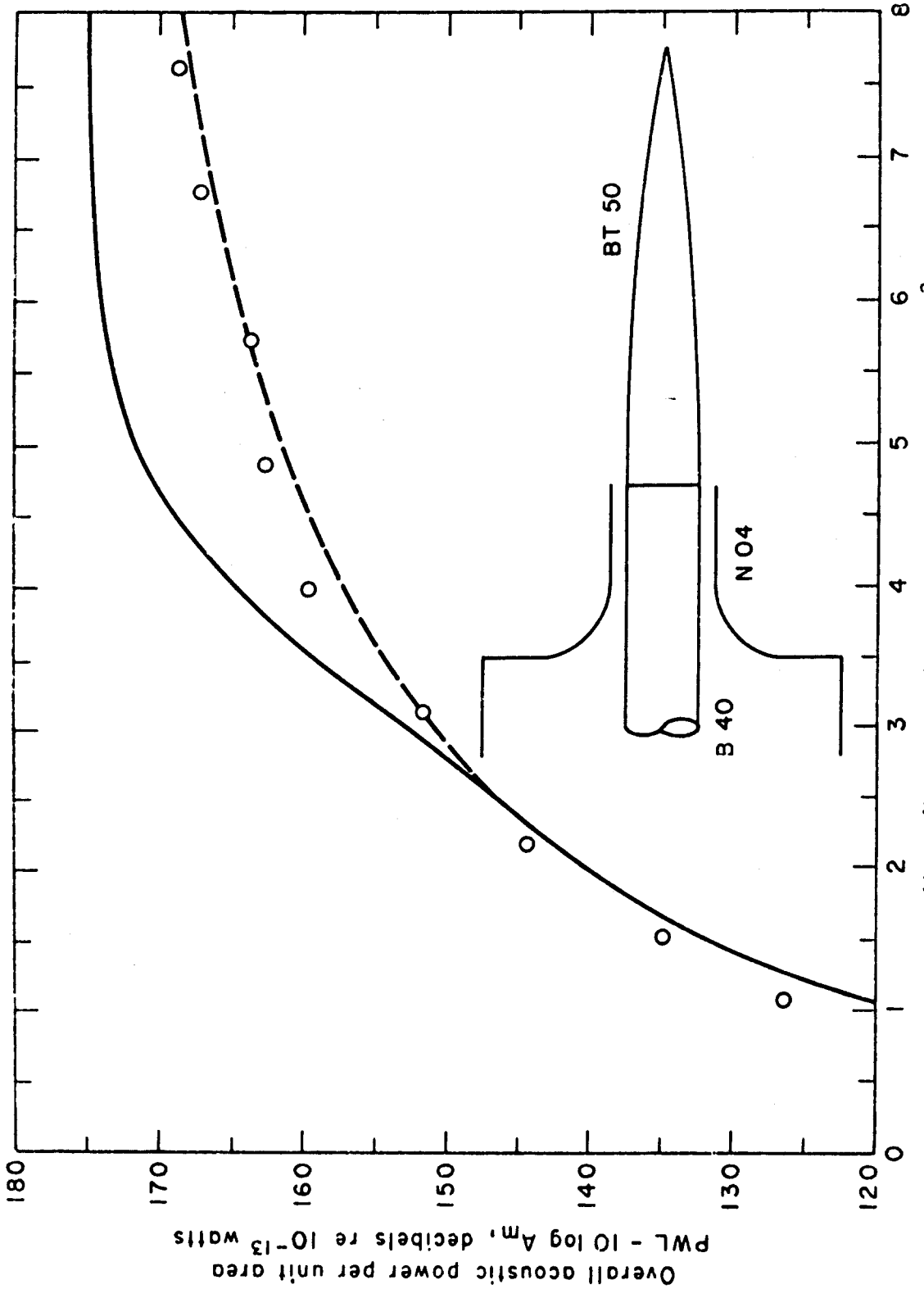

Figure 5. Acoustic Performance of Plug Nozzles
(e) Nozzle No. 1:04:40:50 + 0

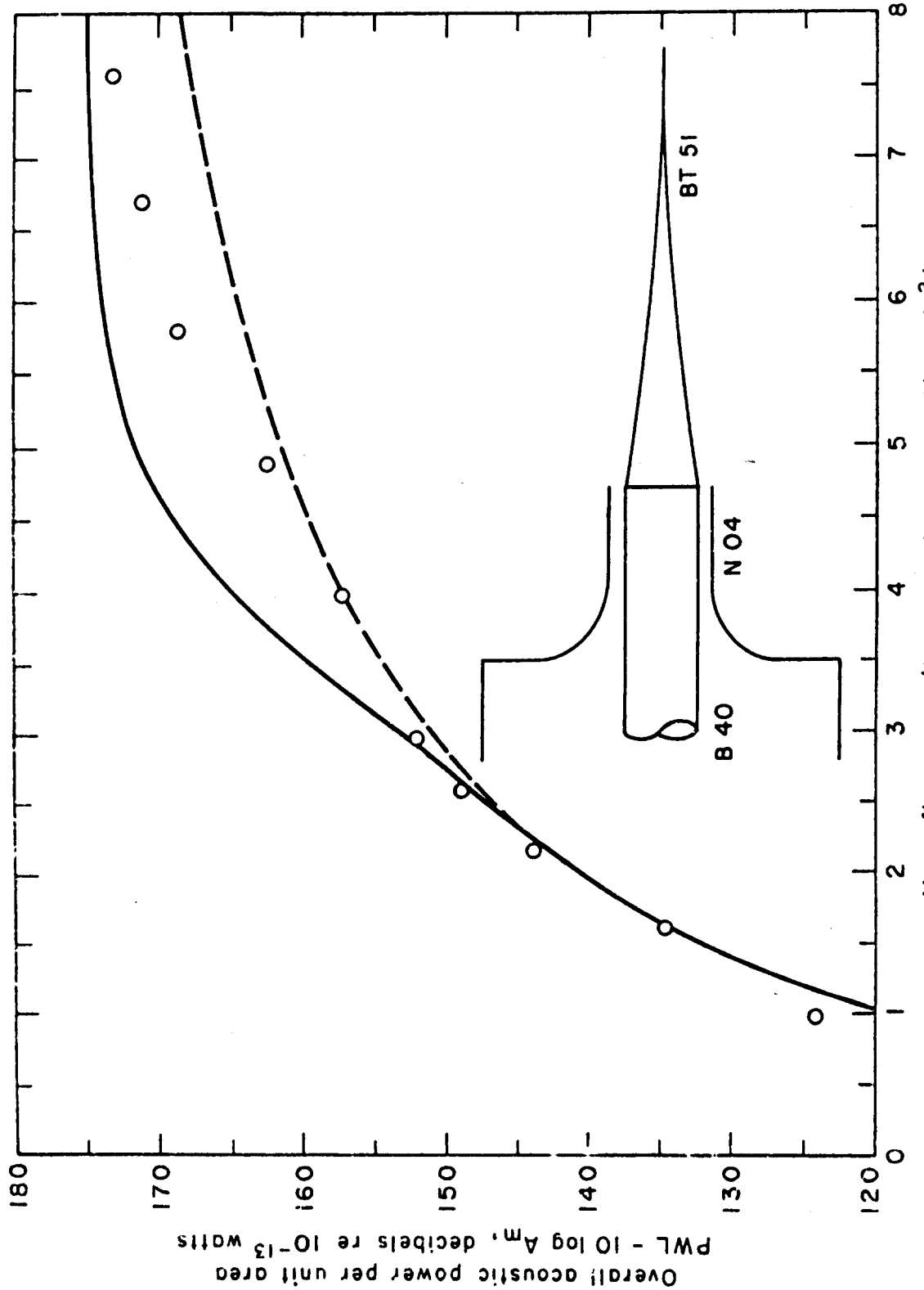

Figure 5. Acoustic Performance of Plug Nozzles
(f) Nozzle No. 1:04:40:51 + 0

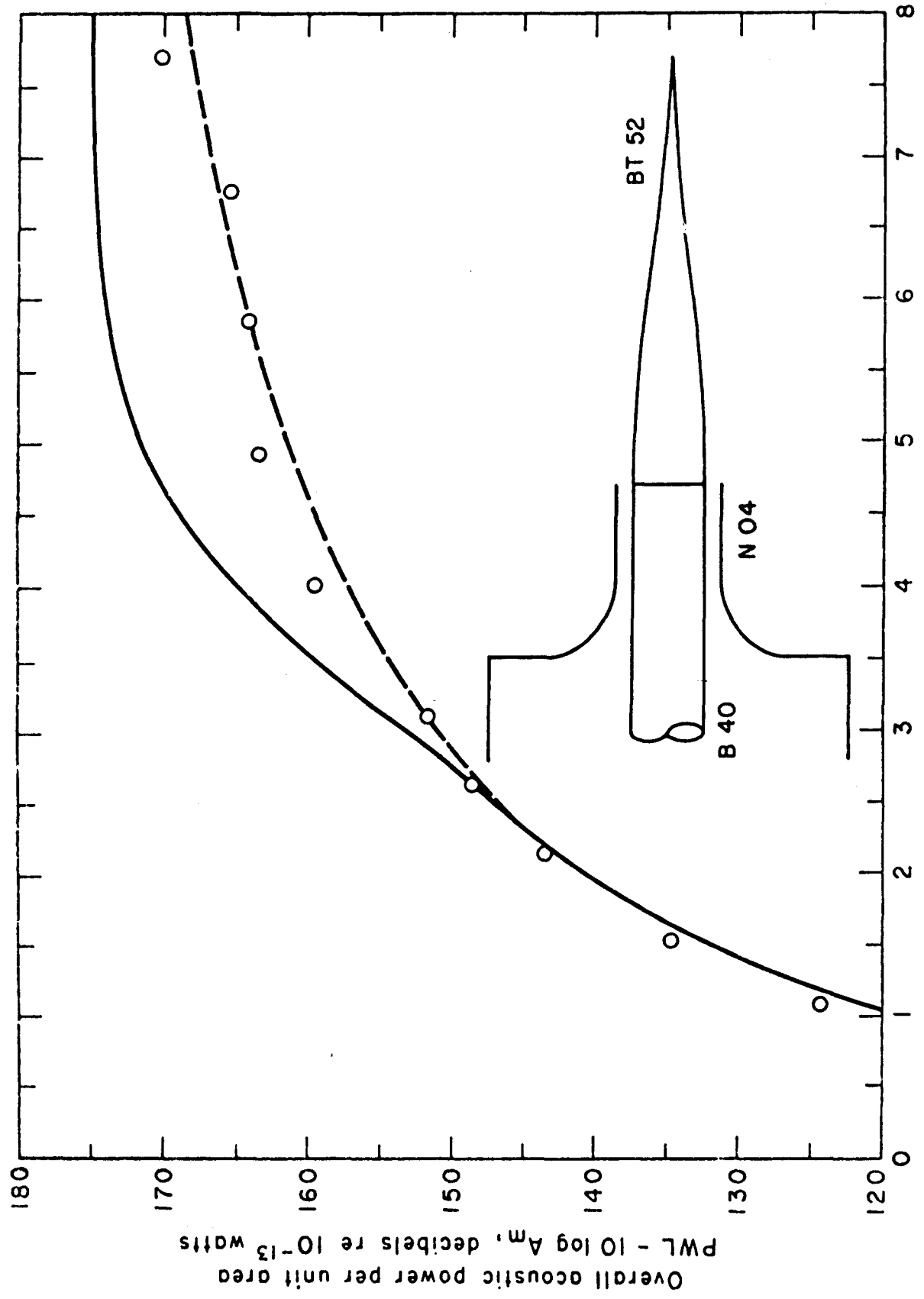

Figure 5. Acoustic Performance of Plug Nozzles
(g) Nozzle No. 1:04:40:52 + 0

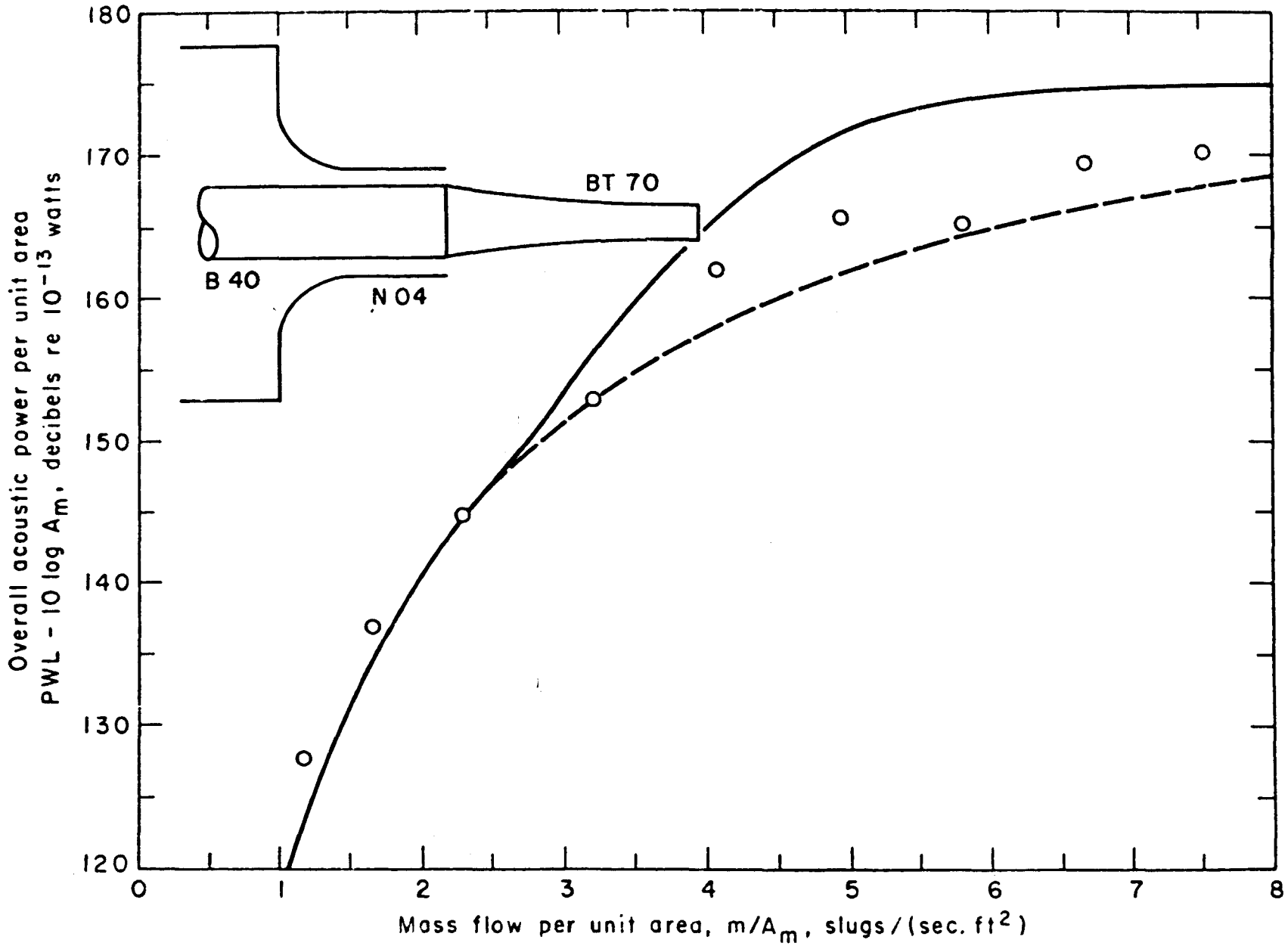

Figure 5. Acoustic Performance of Plug Nozzles
(h) Nozzle No. 1:04:40:70 + 0

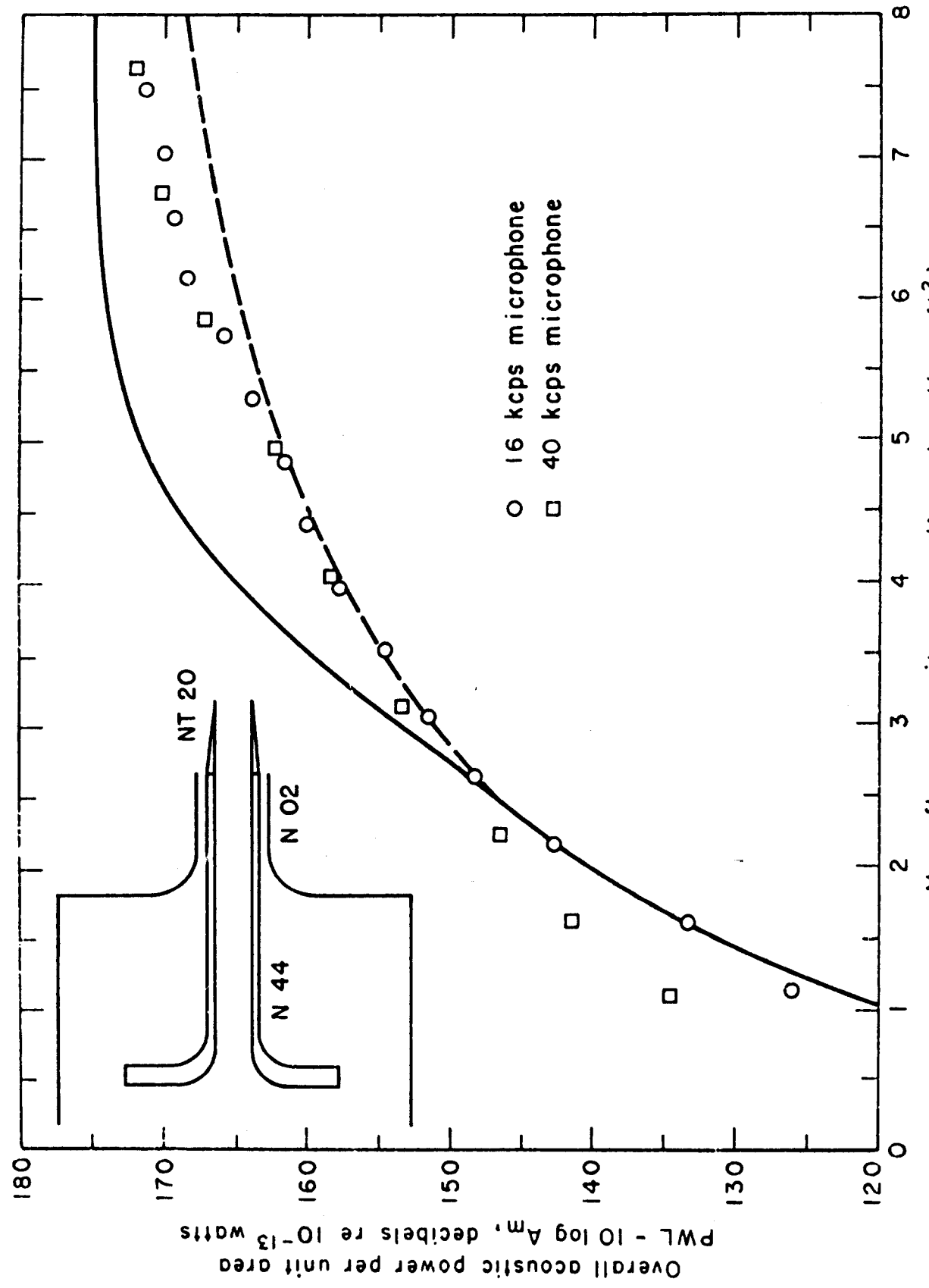

Figure 6. Acoustic Performance of Center Core Flow Nozzles
(a) Nozzle No. 2:02:44:20 + 0

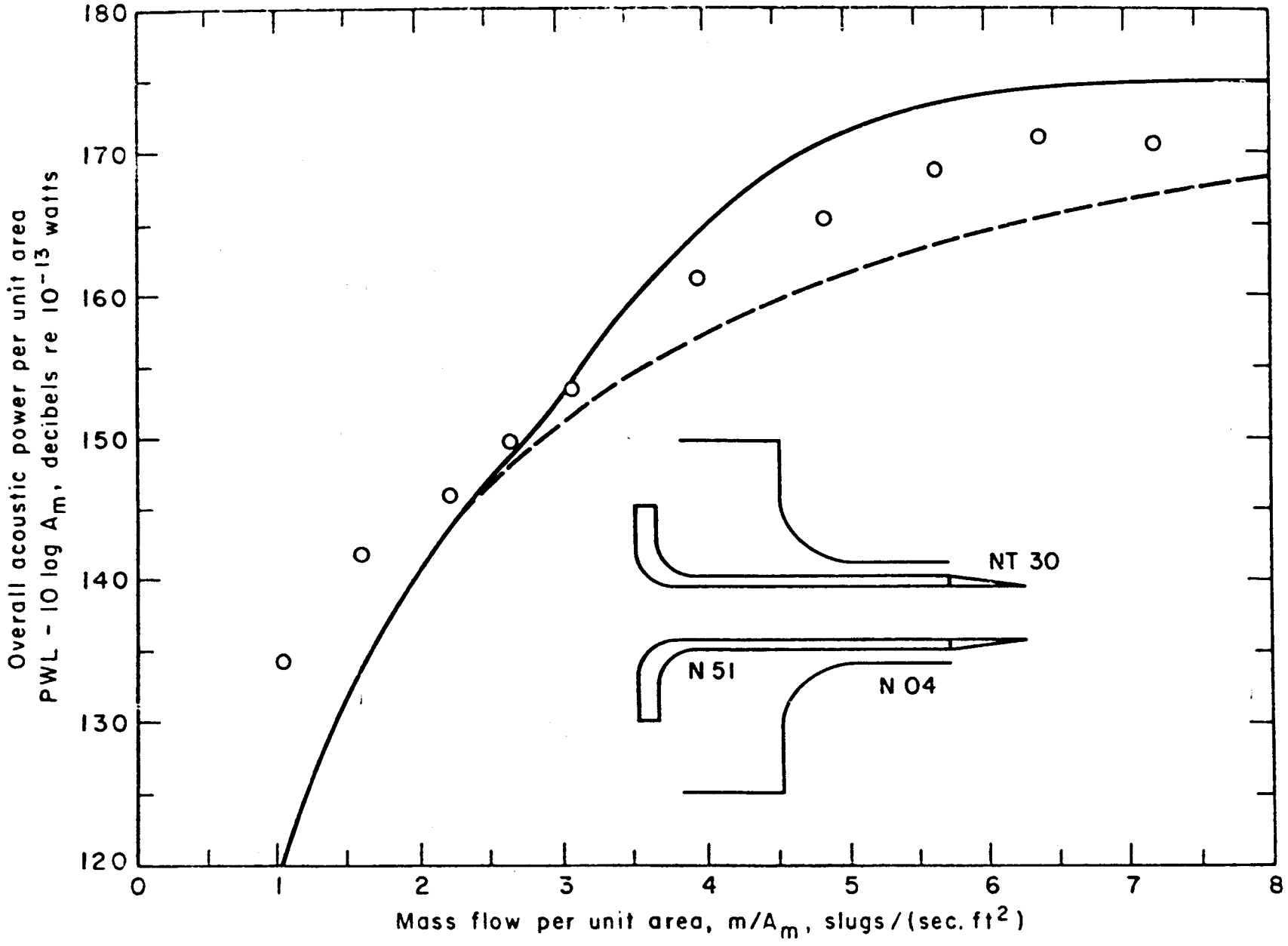

Figure 6. Acoustic Performance of Center Core Flow Nozzles
(b) Nozzle No. 2:04:51:30 + 0

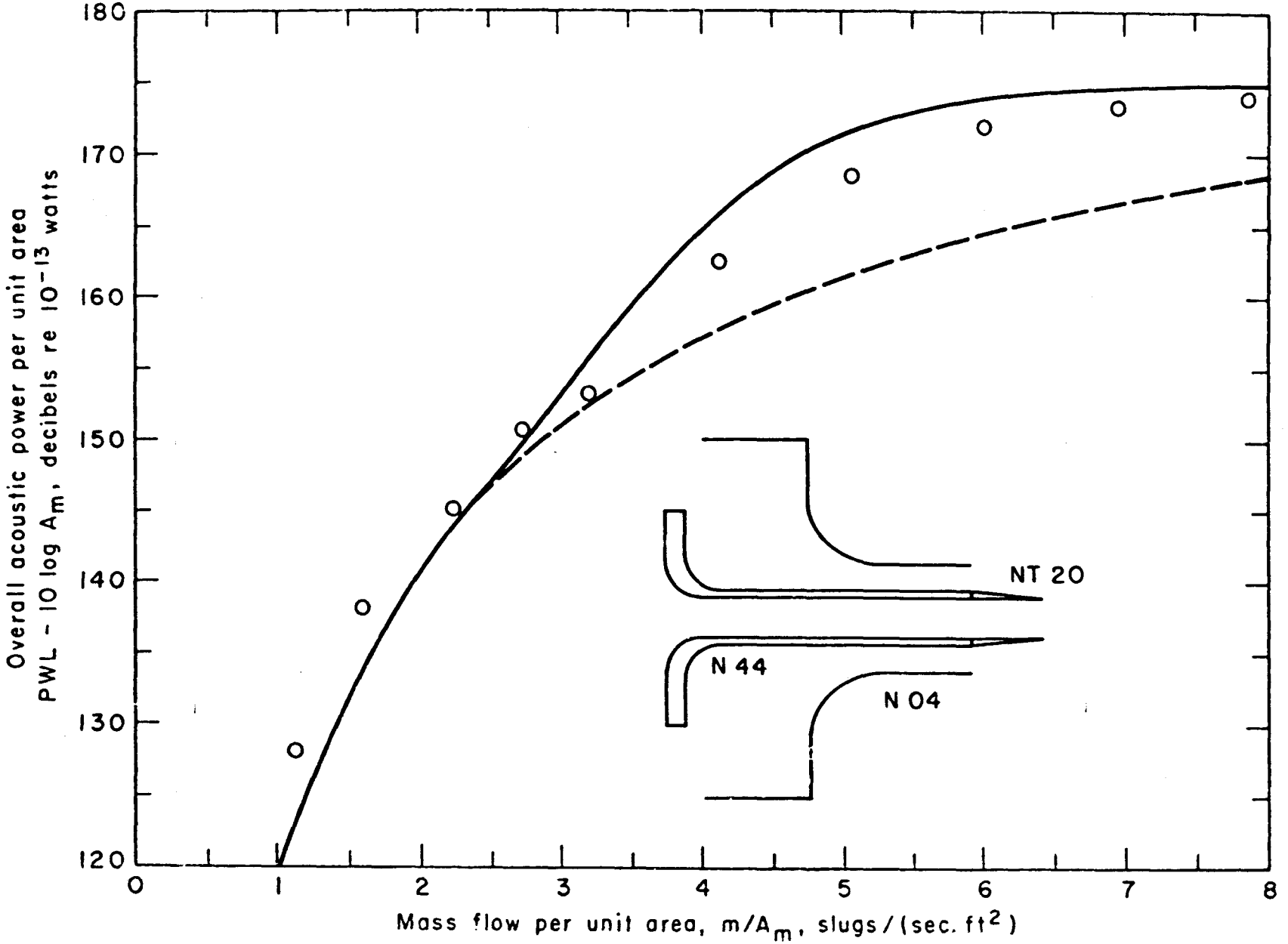

Figure 6. Acoustic Performance of Center Core Flow Nozzles
(c) Nozzle No. 2:04:44:20 + 0

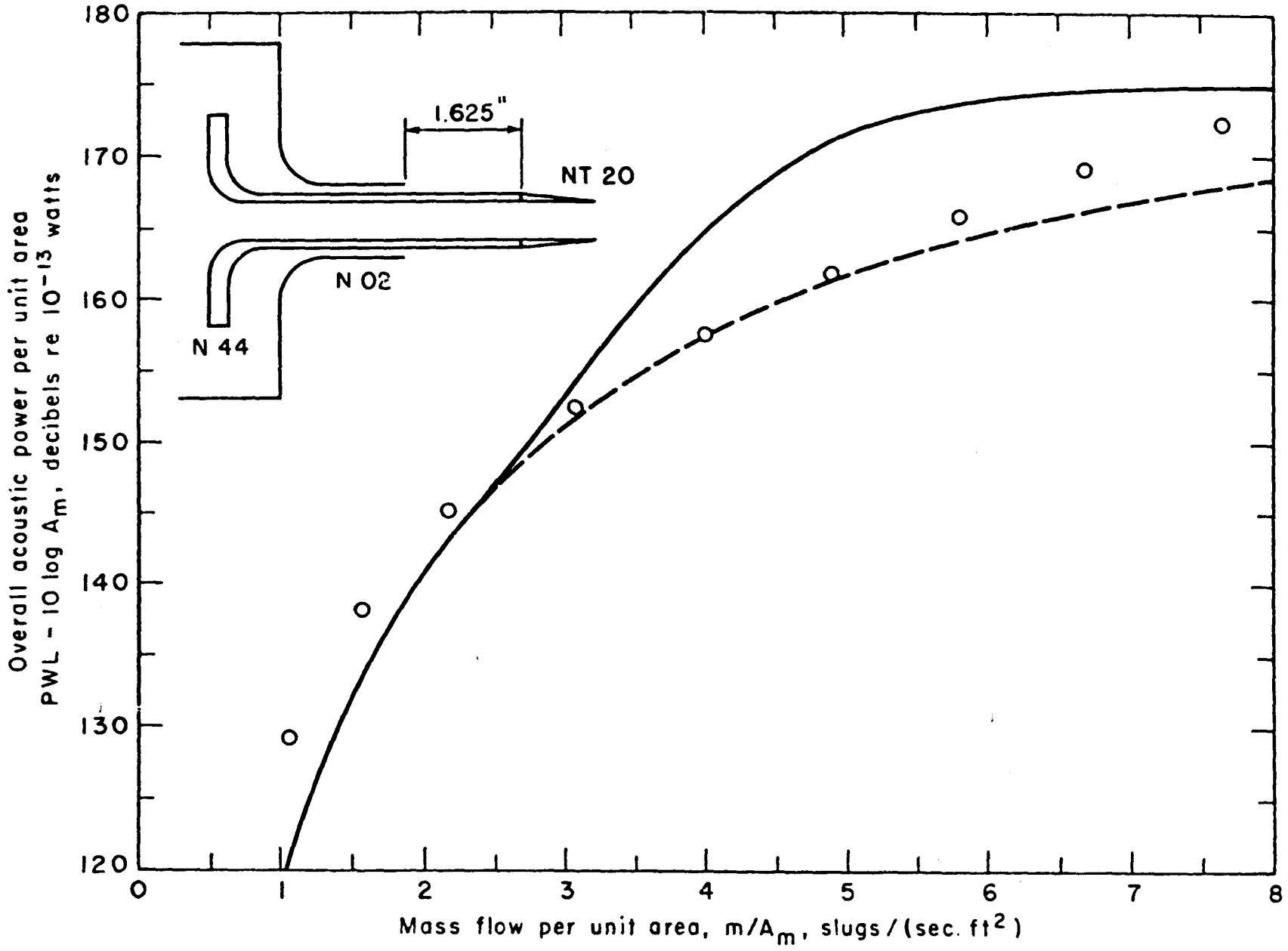

Figure 6. Acoustic Performance of Center Core Flow Nozzles
(d) Nozzle No. 2:02:44:20 + 1.625

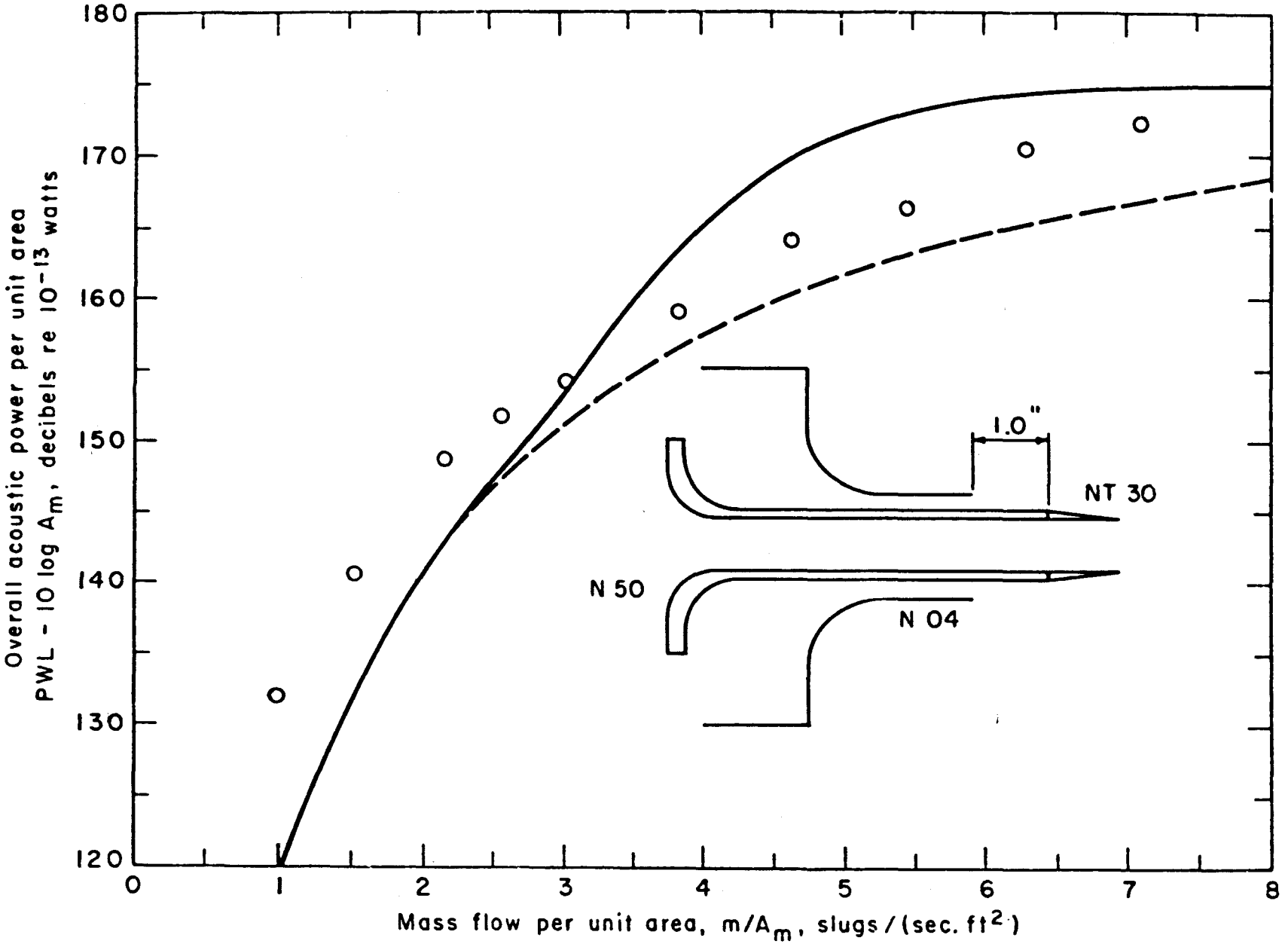

Figure 6. Acoustic Performance of Center Core Flow Nozzles
(e) Nozzle No. 2:04:50:30 + 1.0

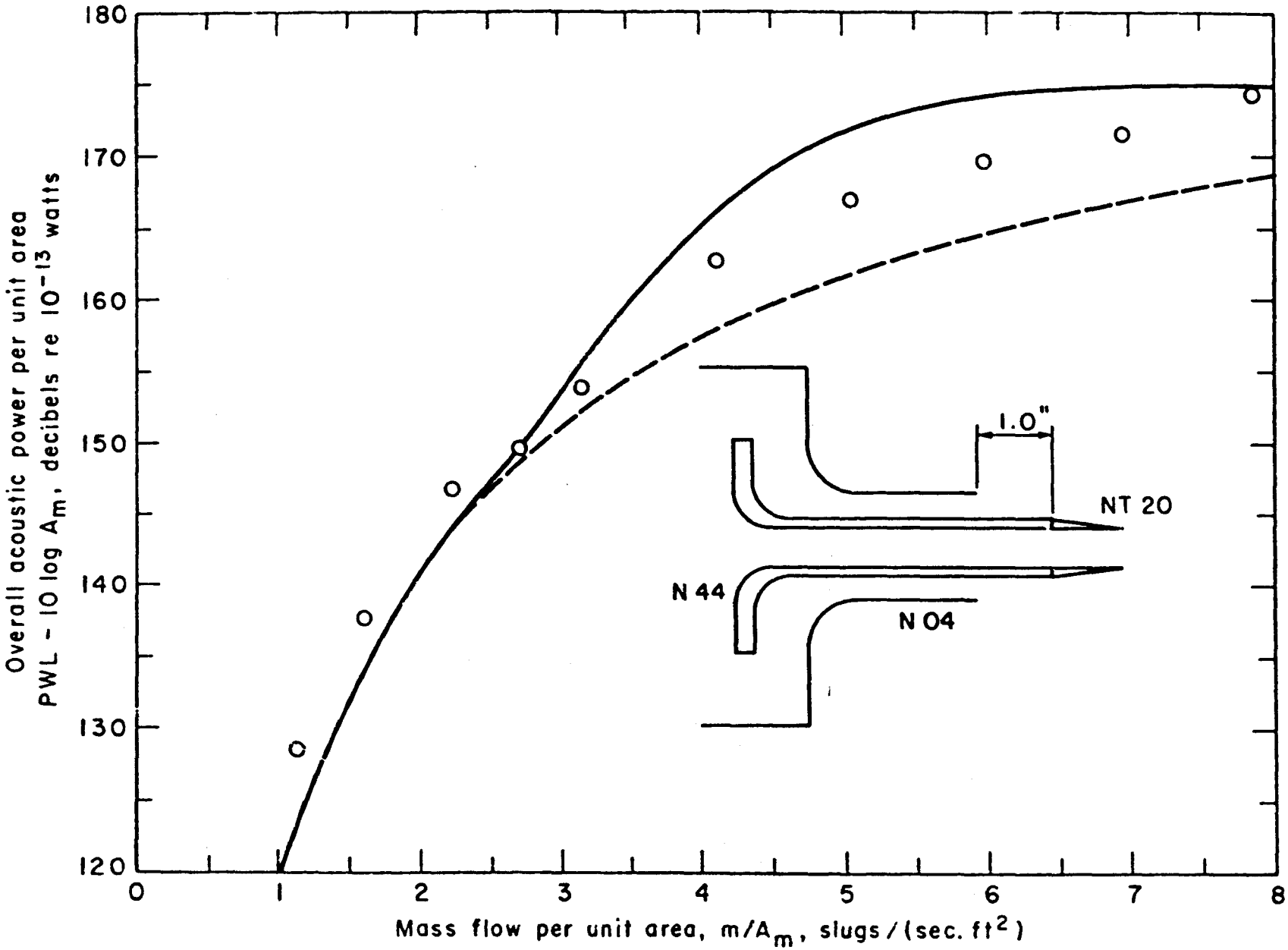

Figure 6. Acoustic Performance of Center Core Flow Nozzles
(f) Nozzle No. 2:04:44:20 + 1.0

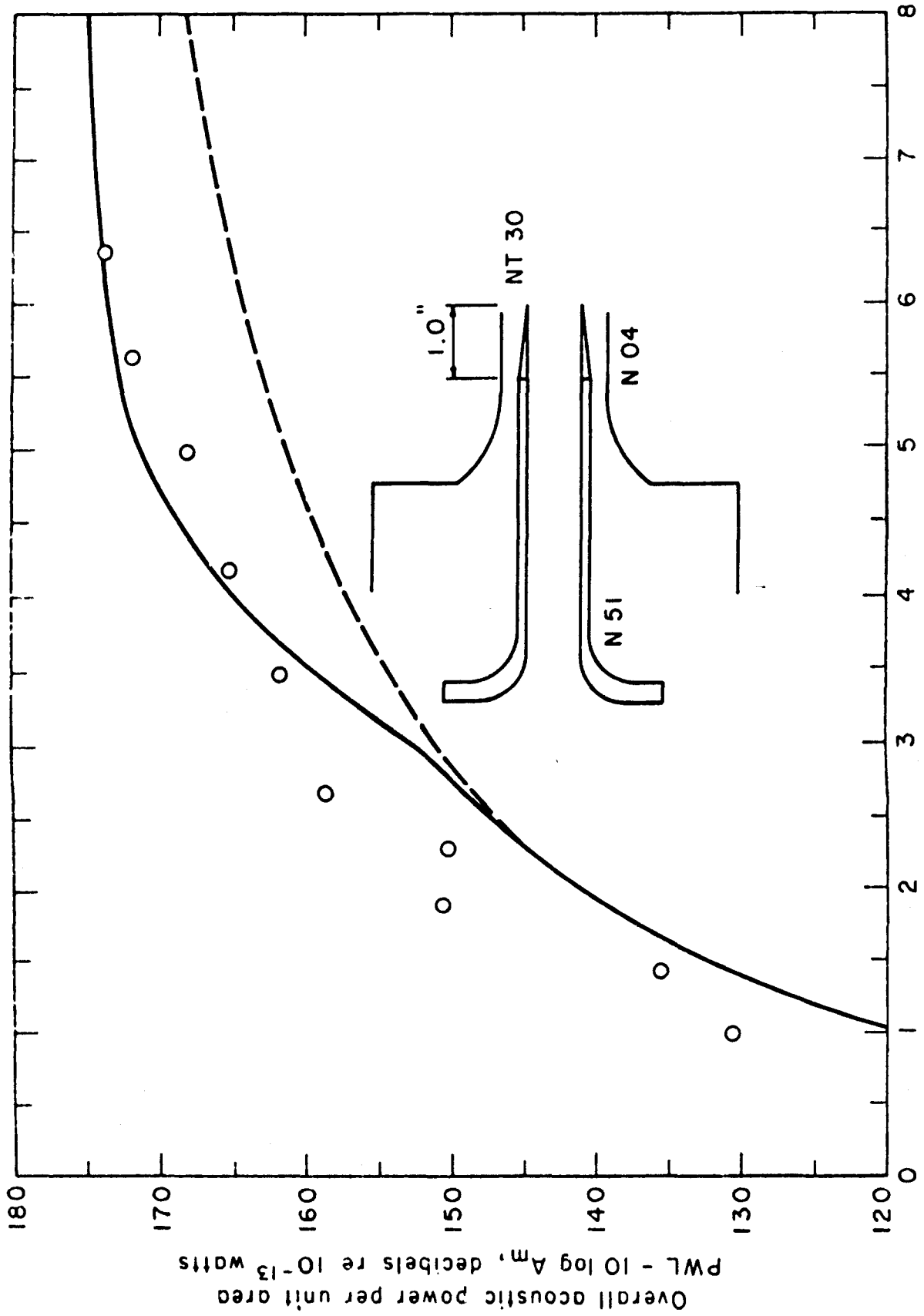

Figure 6. Acoustic Performance of Center Core Flow Nozzles
(g) Nozzle No. 2:04:51:30 - 1.0

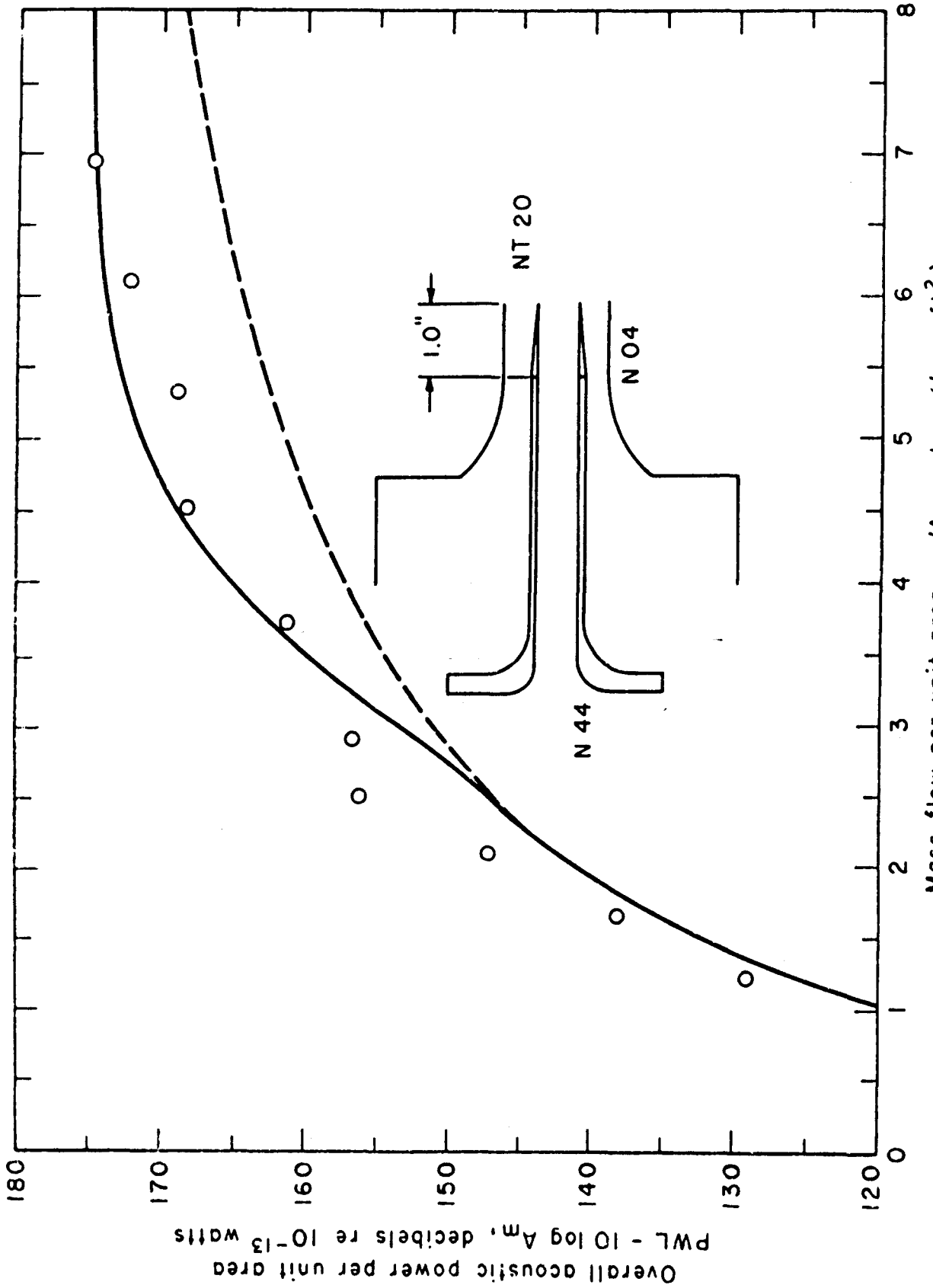

Figure 6. Acoustic Performance of Center Core Flow Nozzles
(h) Nozzle No. 2:04:44:20 - 1.0

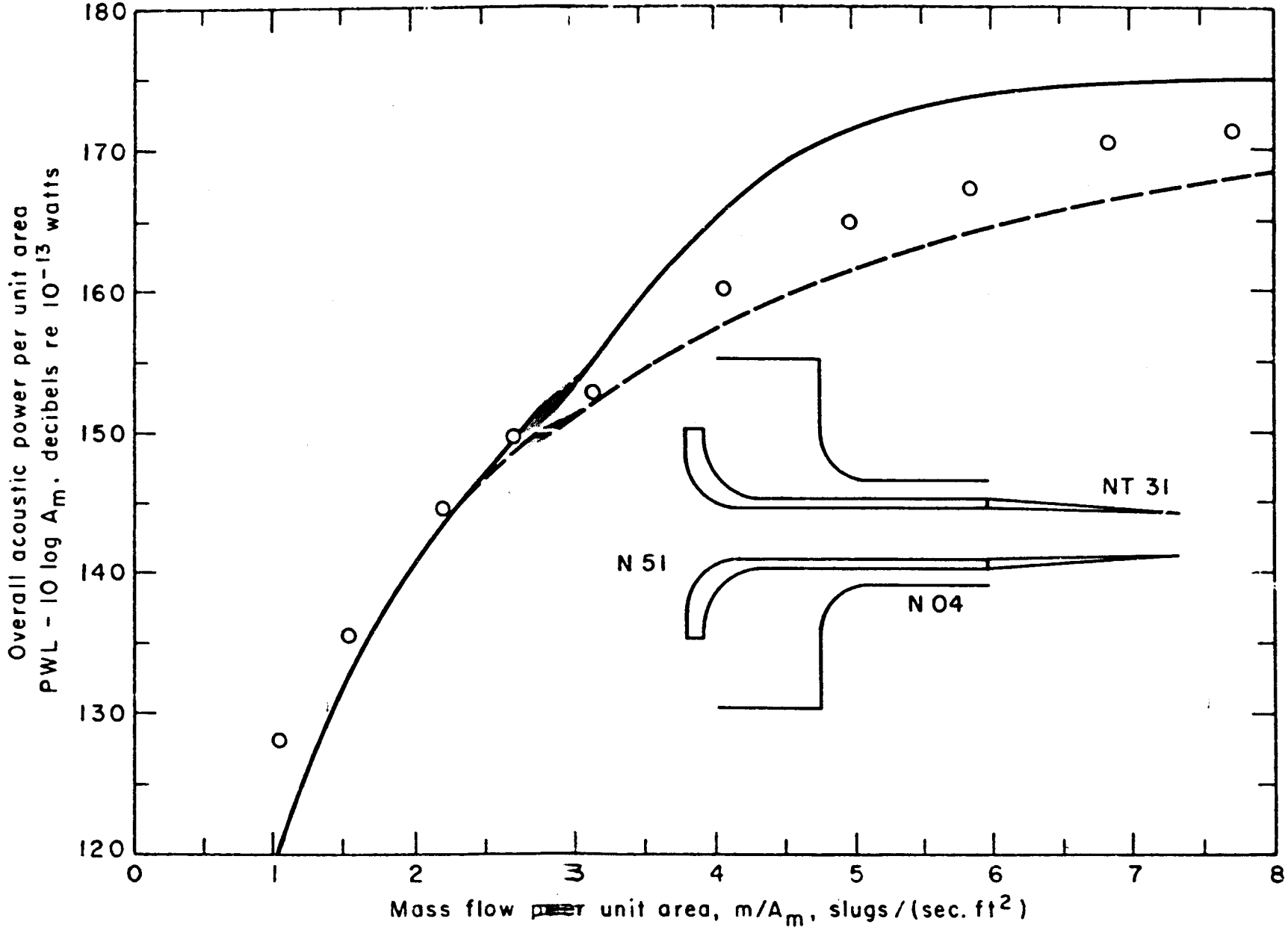

Figure 6. Acoustic Performance of Center Core Flow Nozzles
(i) Nozzle No. 2D4:51:31 + 0

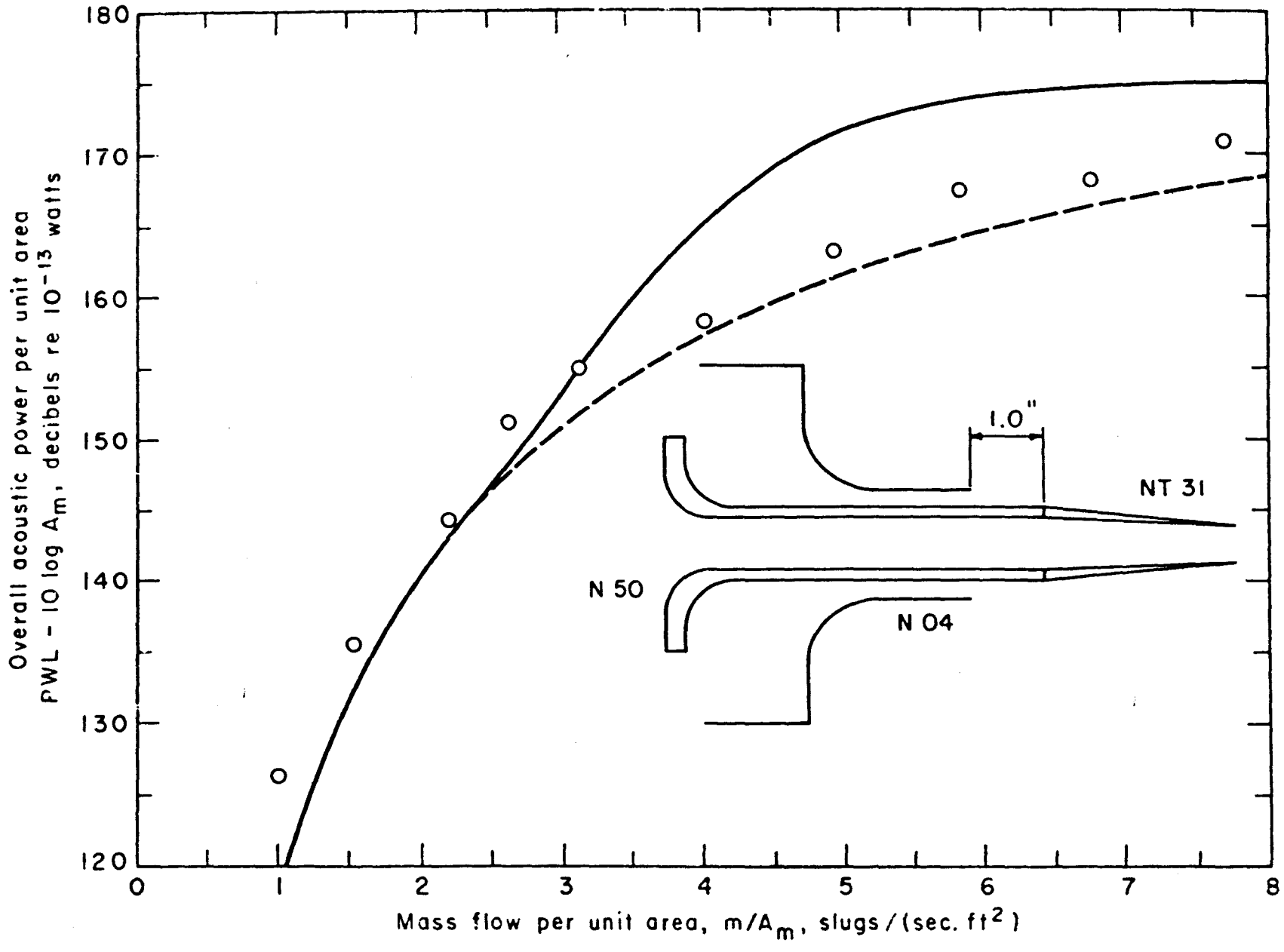

Figure 6. Acoustic Performance of Center Core Flow Nozzles
(j) Nozzle No. 2:04:50:31 + 1.0

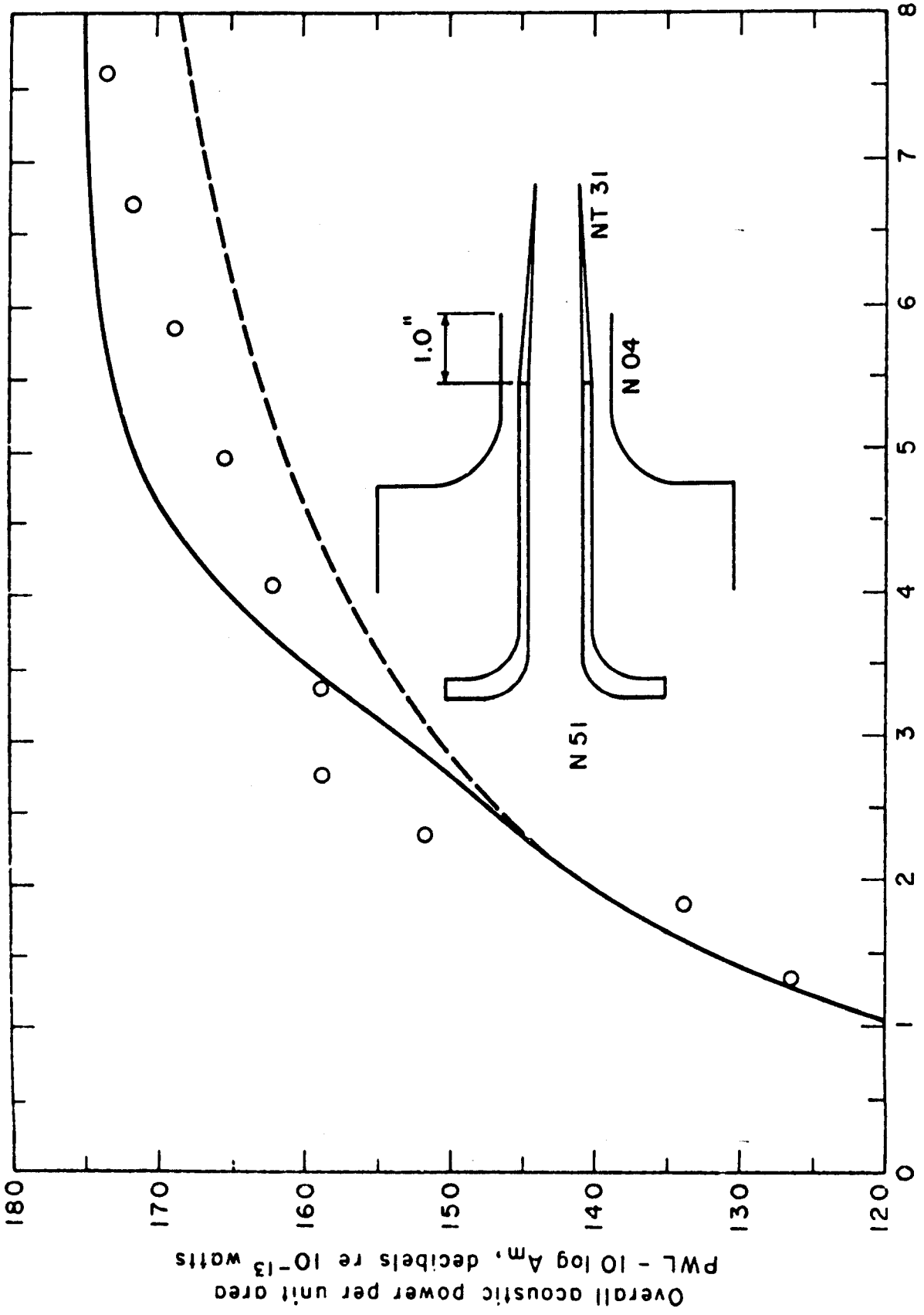

Figure 6. Acoustic Performance of Center Core Flow Nozzles
(k) Nozzle No. 2:04:51:31 - 1.0

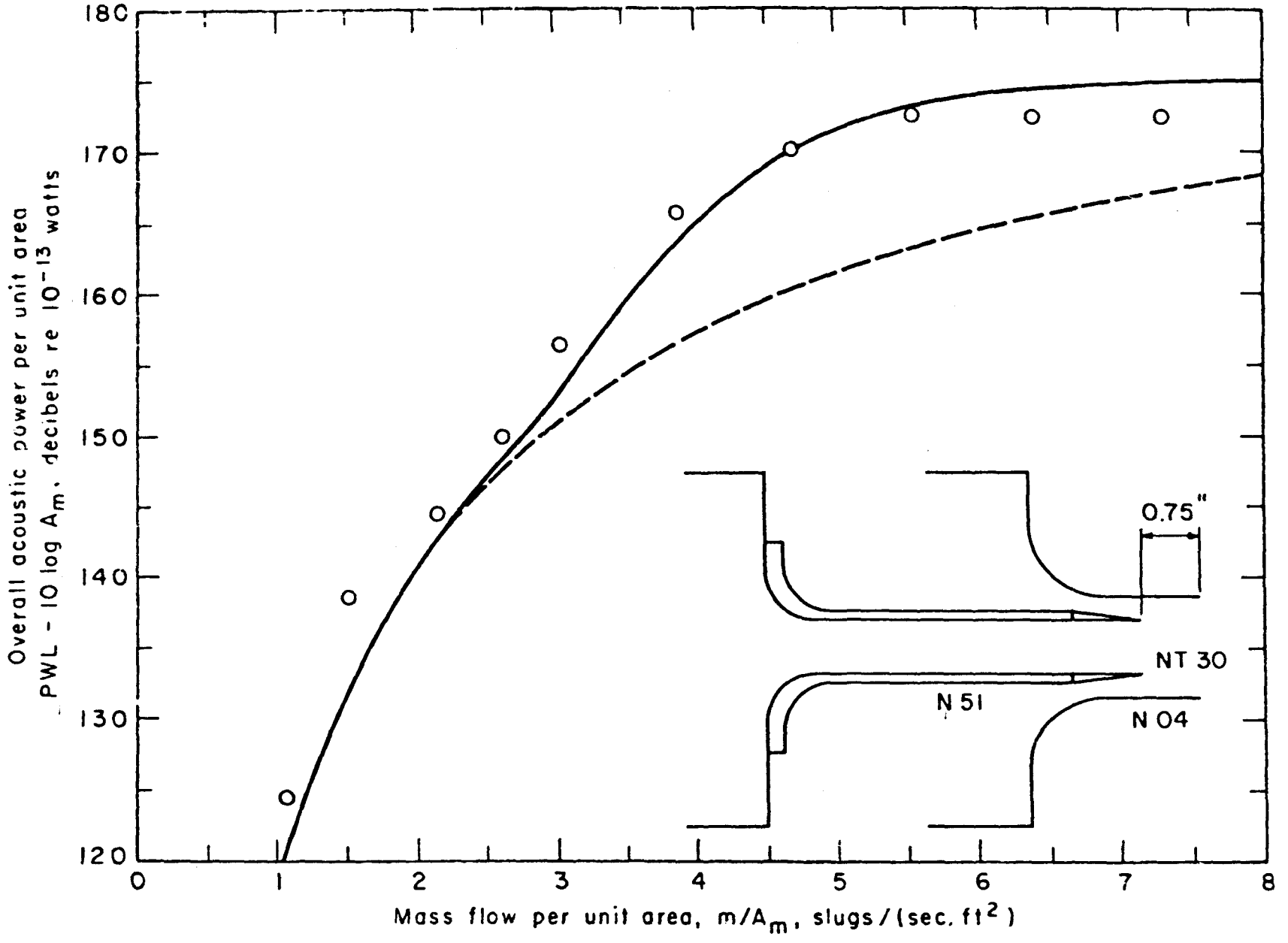

Figure 7. Acoustic Performance of Ejector Nozzles
(a) Nozzle No. 3:51:30:04 + 0.75

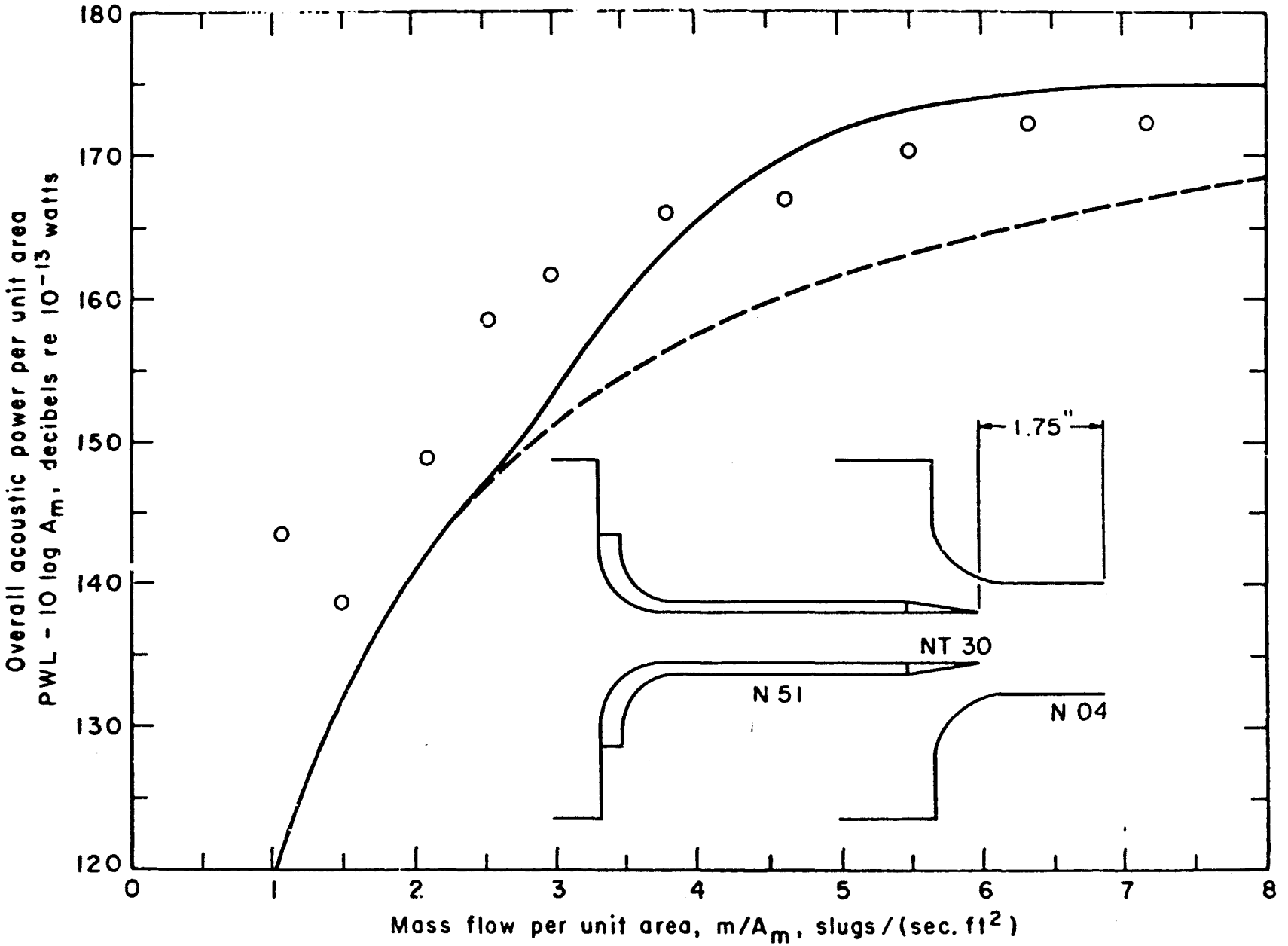

Figure 7. Acoustic Performance of Ejector Nozzles
(b) Nozzle No. 3:51:30:04 + 1.75

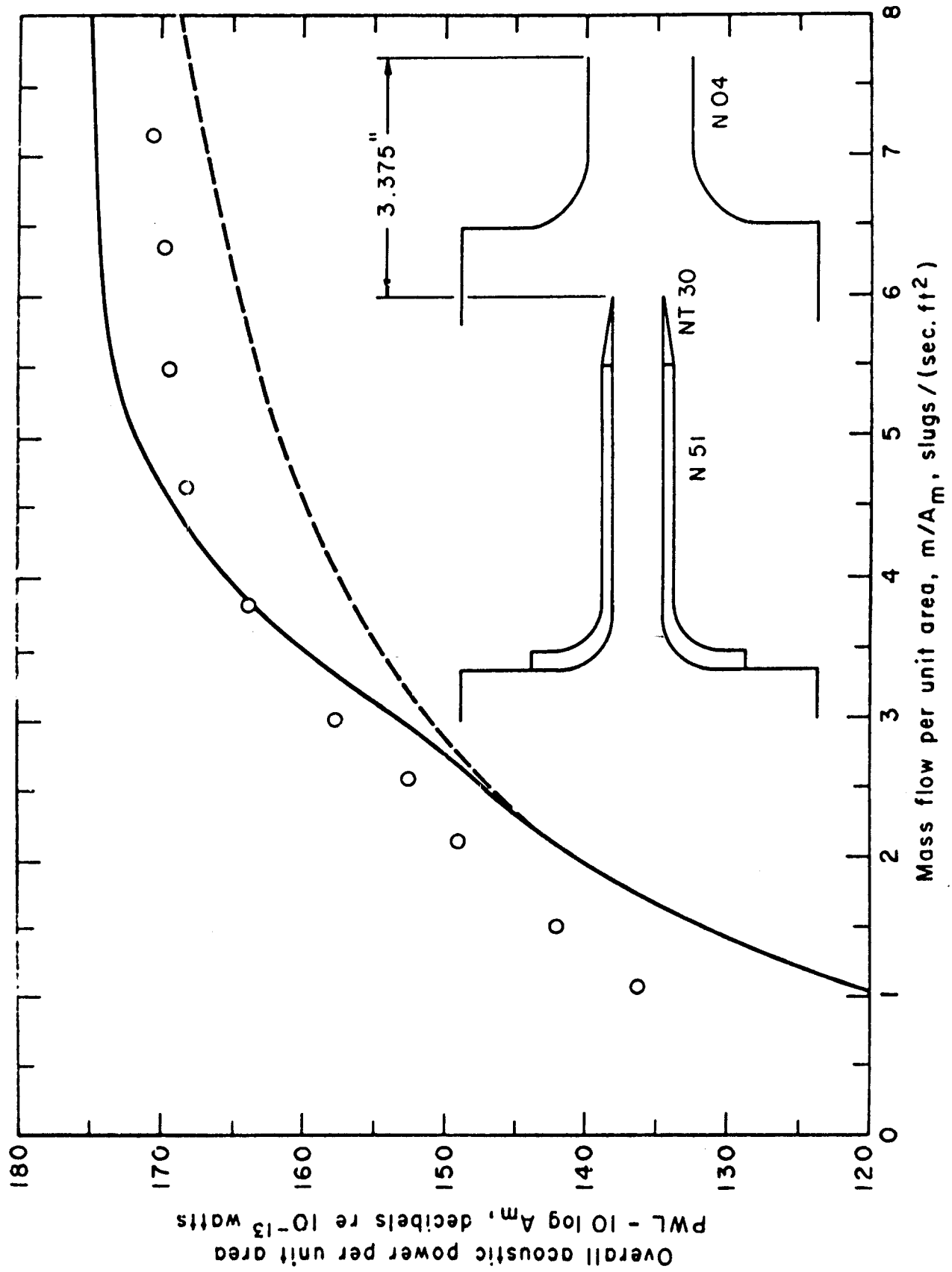

Figure 7. Acoustic Performance of Ejector Nozzles
(c) Nozzle No. 3:51:30:04 + 3.375

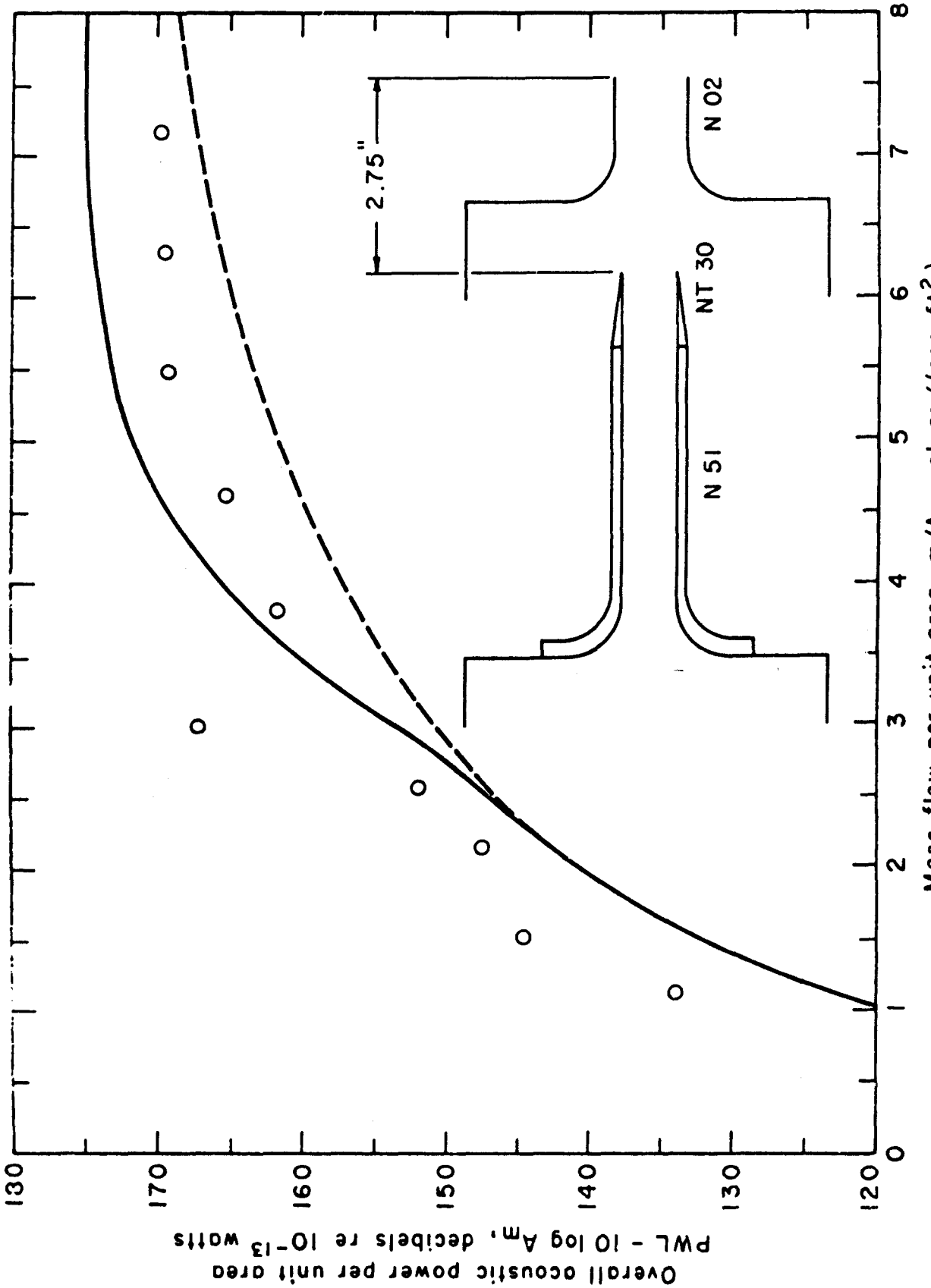

Figure 7. Acoustic Performance of Ejector Nozzles
(d) Nozzle No. 3:51:30:02 + 2.75

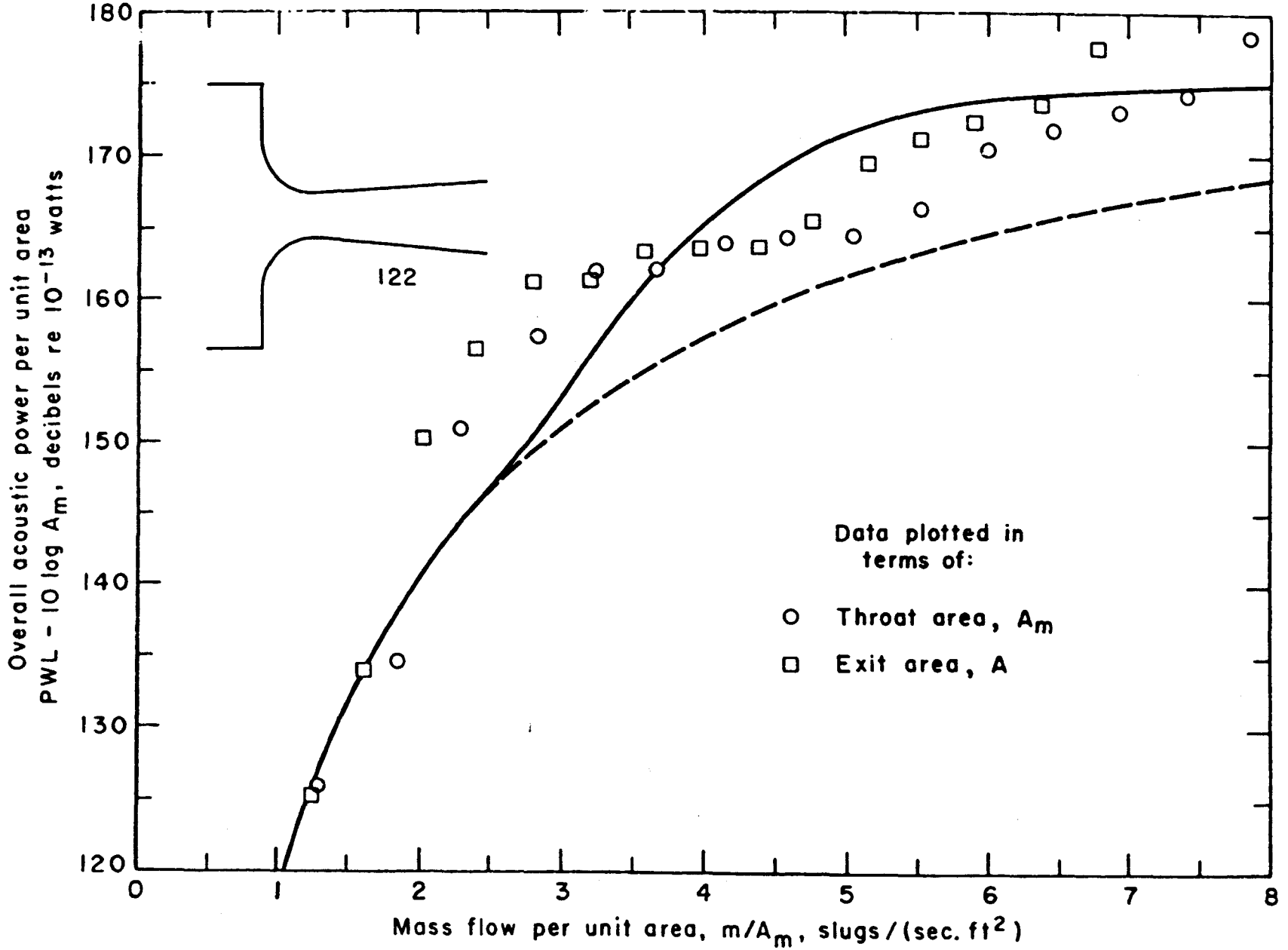

Figure 8. Acoustic Performance of Converging-Diverging Nozzles
(a) Nozzle No. 122 (N62)

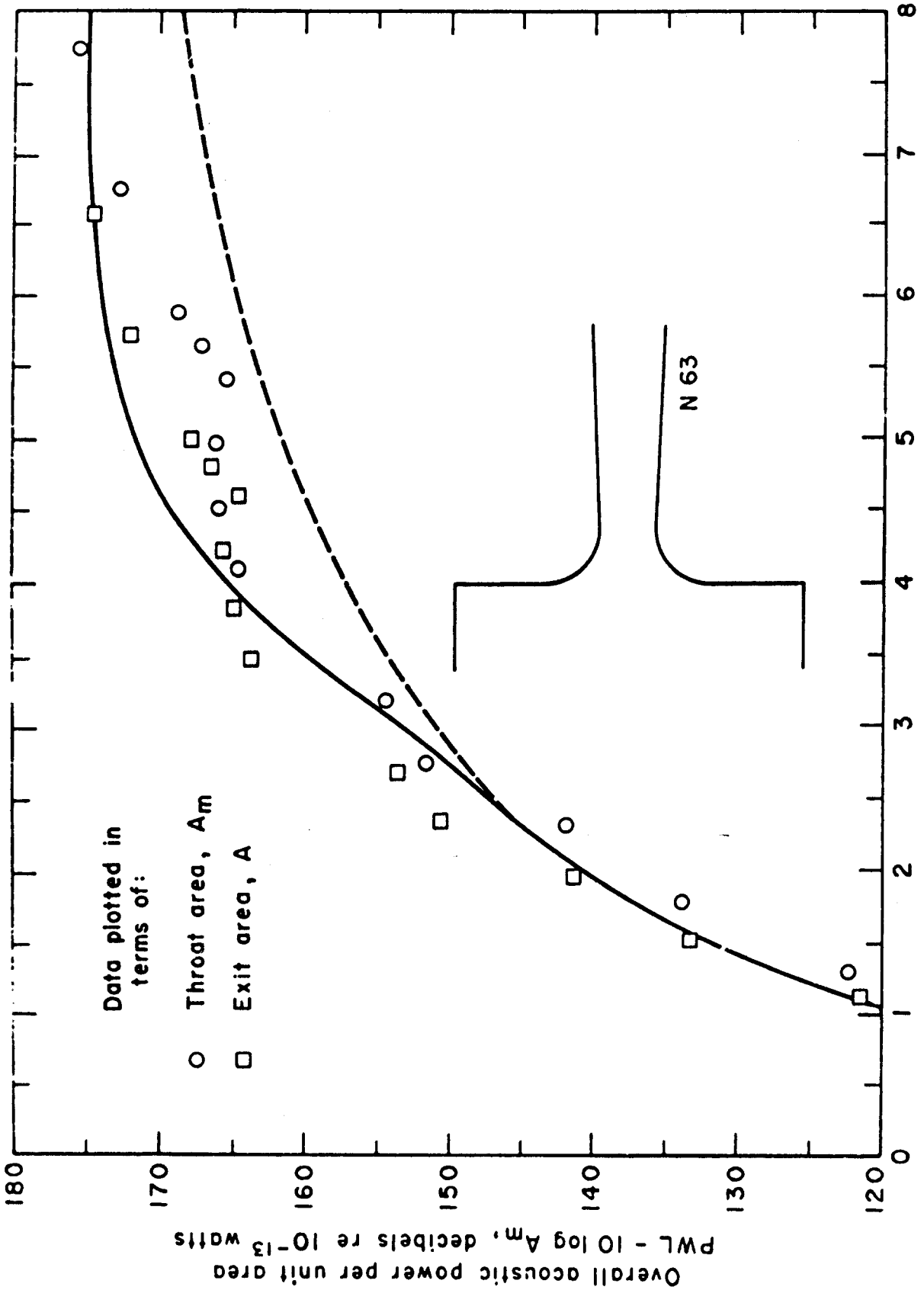

Figure 8. Acoustic Performance of Converging-Diverging Nozzles
(b) Nozzle No. N63

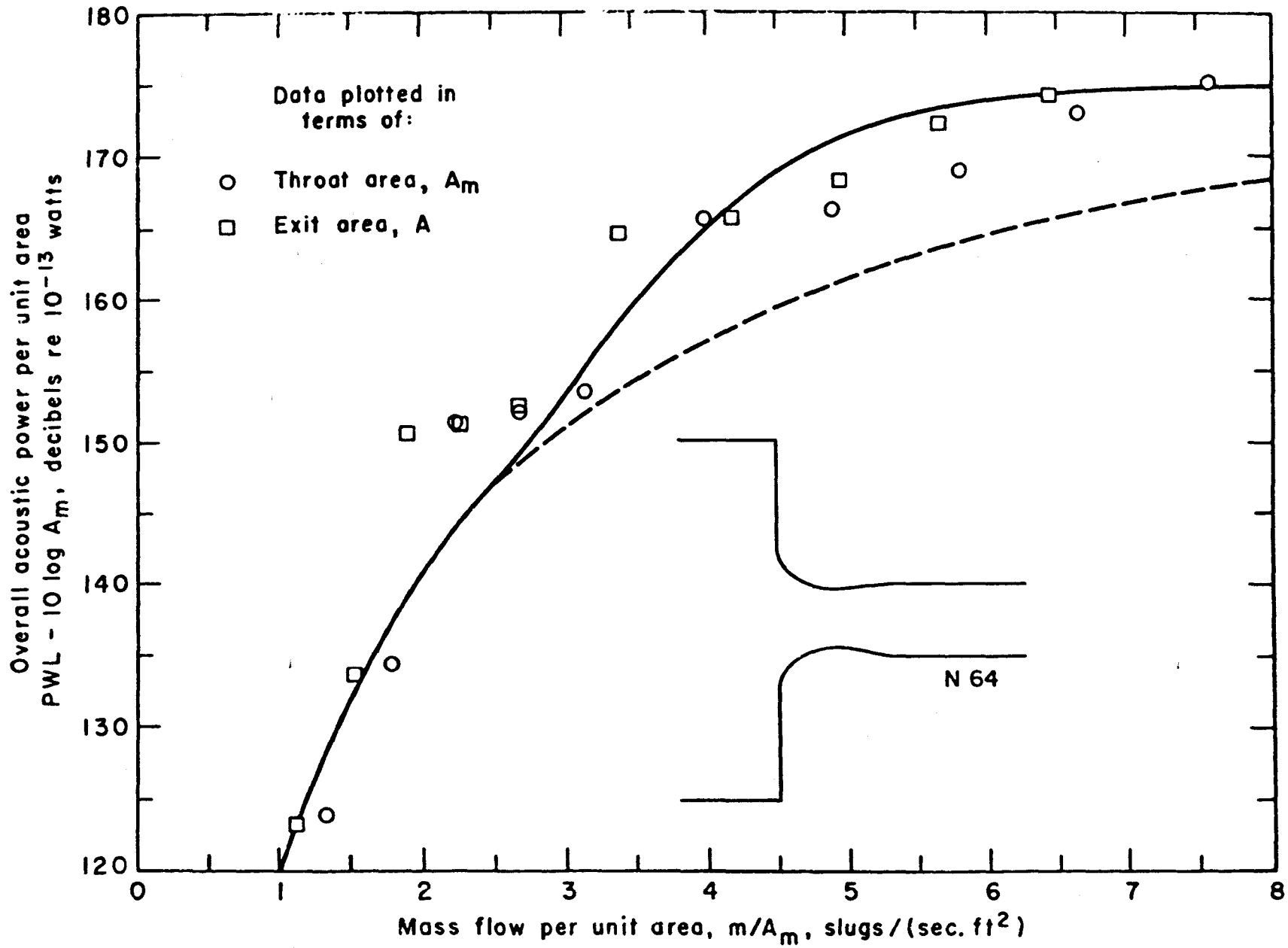

Figure 8. Acoustic Performance of Converging-Diverging Nozzles
(c) Nozzle No. N64

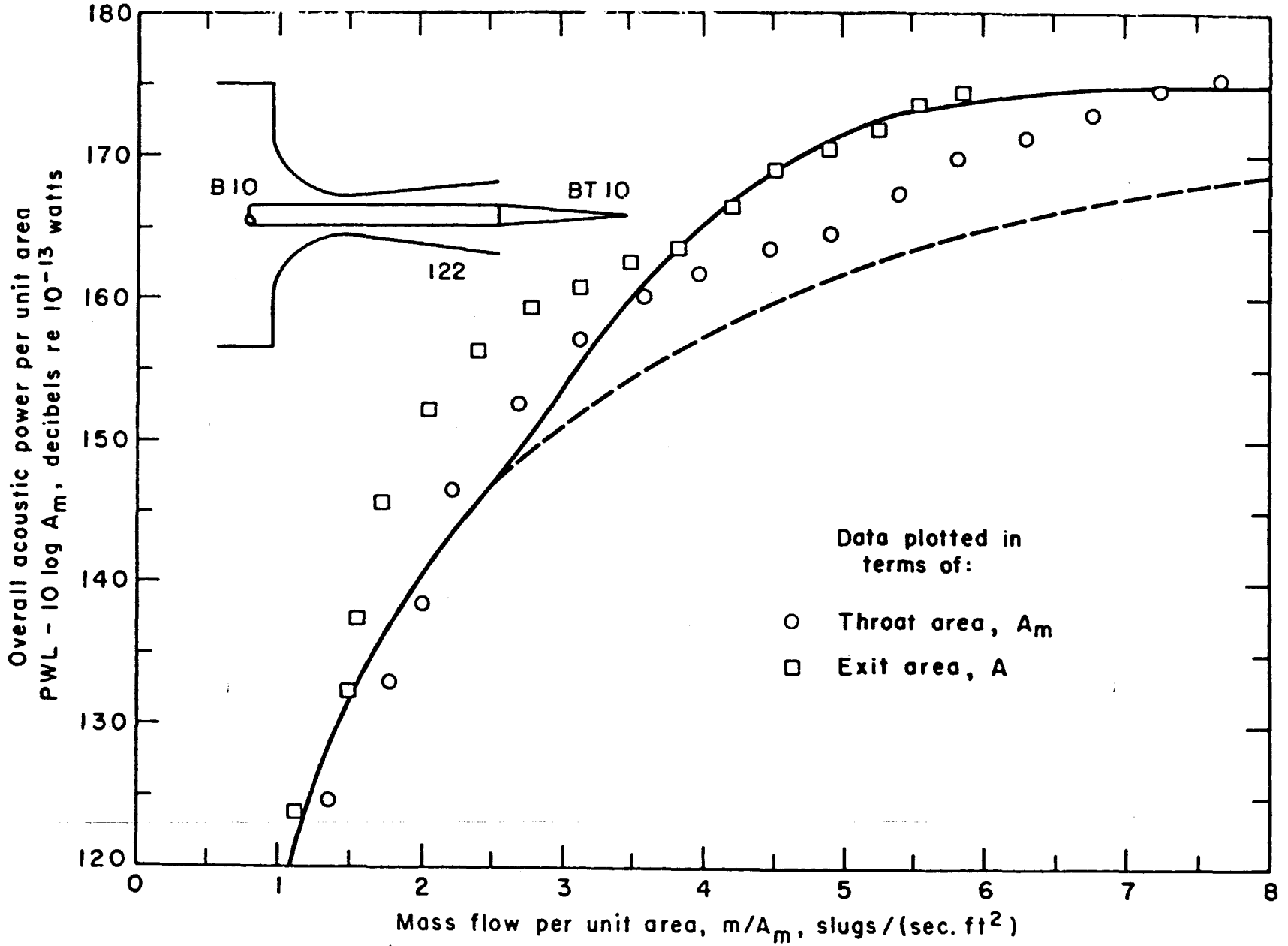

Figure 9. Acoustic Performance of Converging-Diverging Plug Nozzles
(a) Nozzle No. 621 (1:62:10:10 + 0)

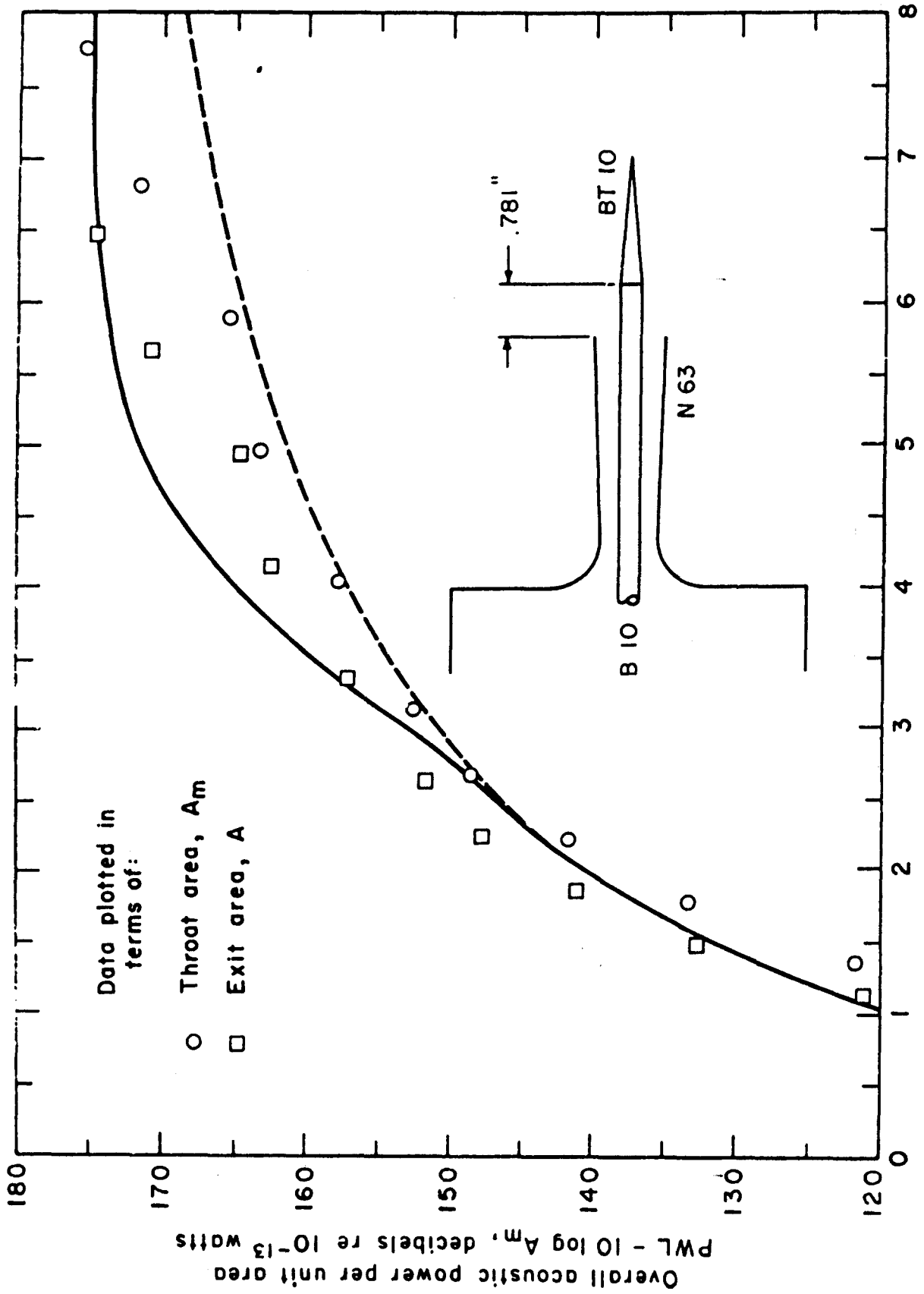

Figure 9. Acoustic Performance of Converging-Diverging Plug Nozzles
(b) Nozzle No. 1:63:10:10 + 0.781

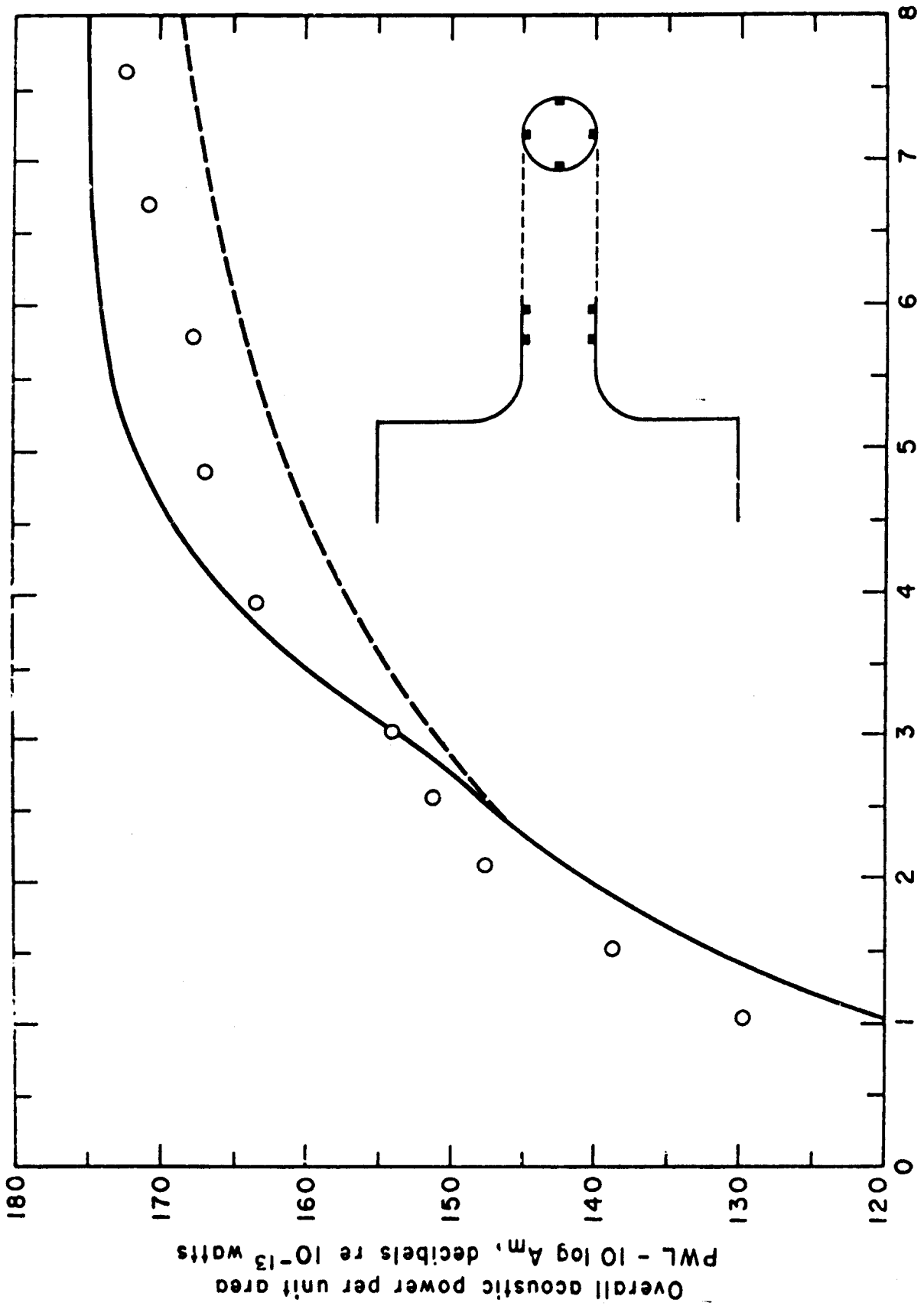

Figure 10. Acoustic Performance of Convergent Nozzle with Roughness
(a) Nozzle No. 4:02

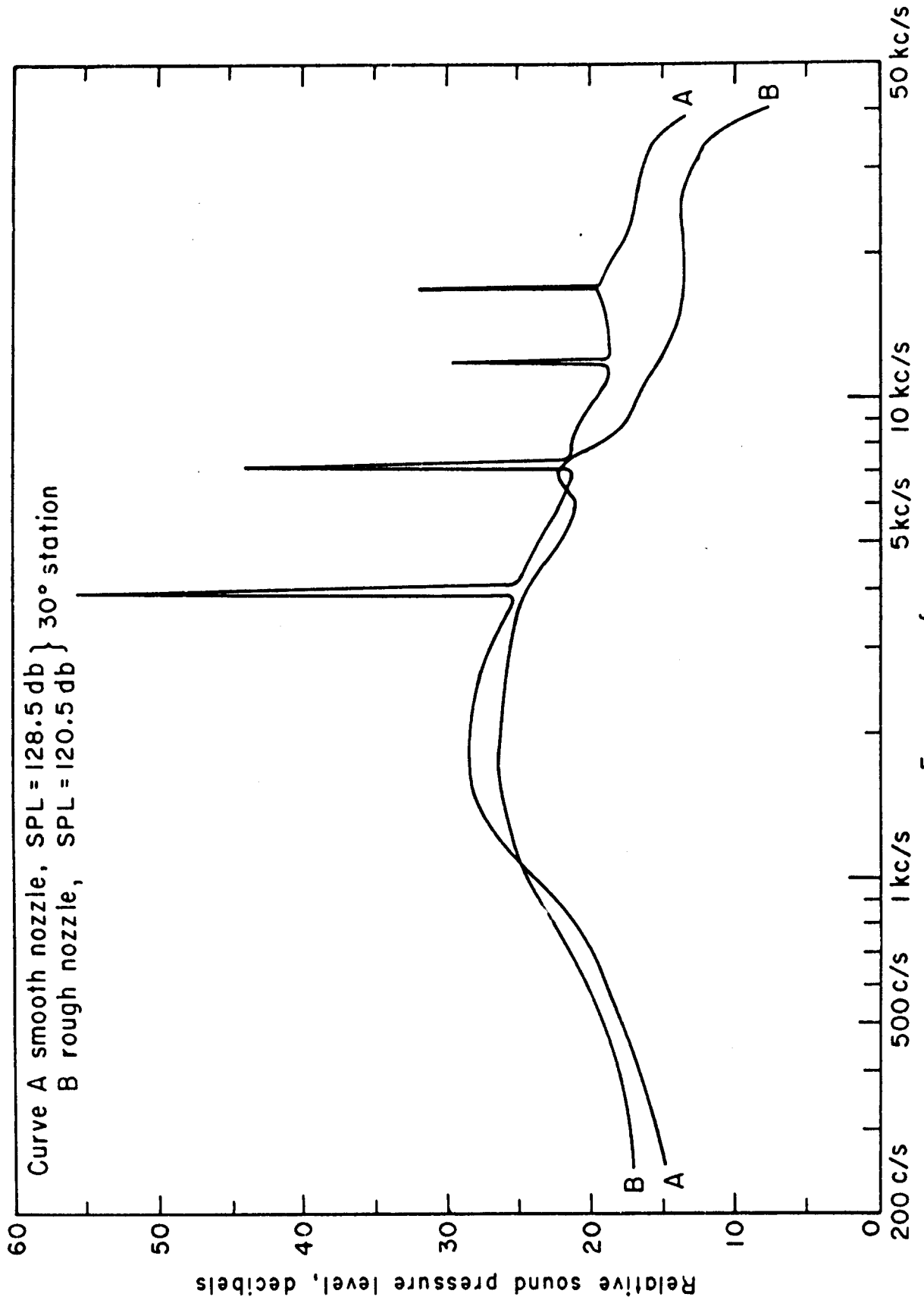

Figure 10. Narrow Band (3 Cycles) Analysis for Rough Converging Nozzle
(b) 30° Station

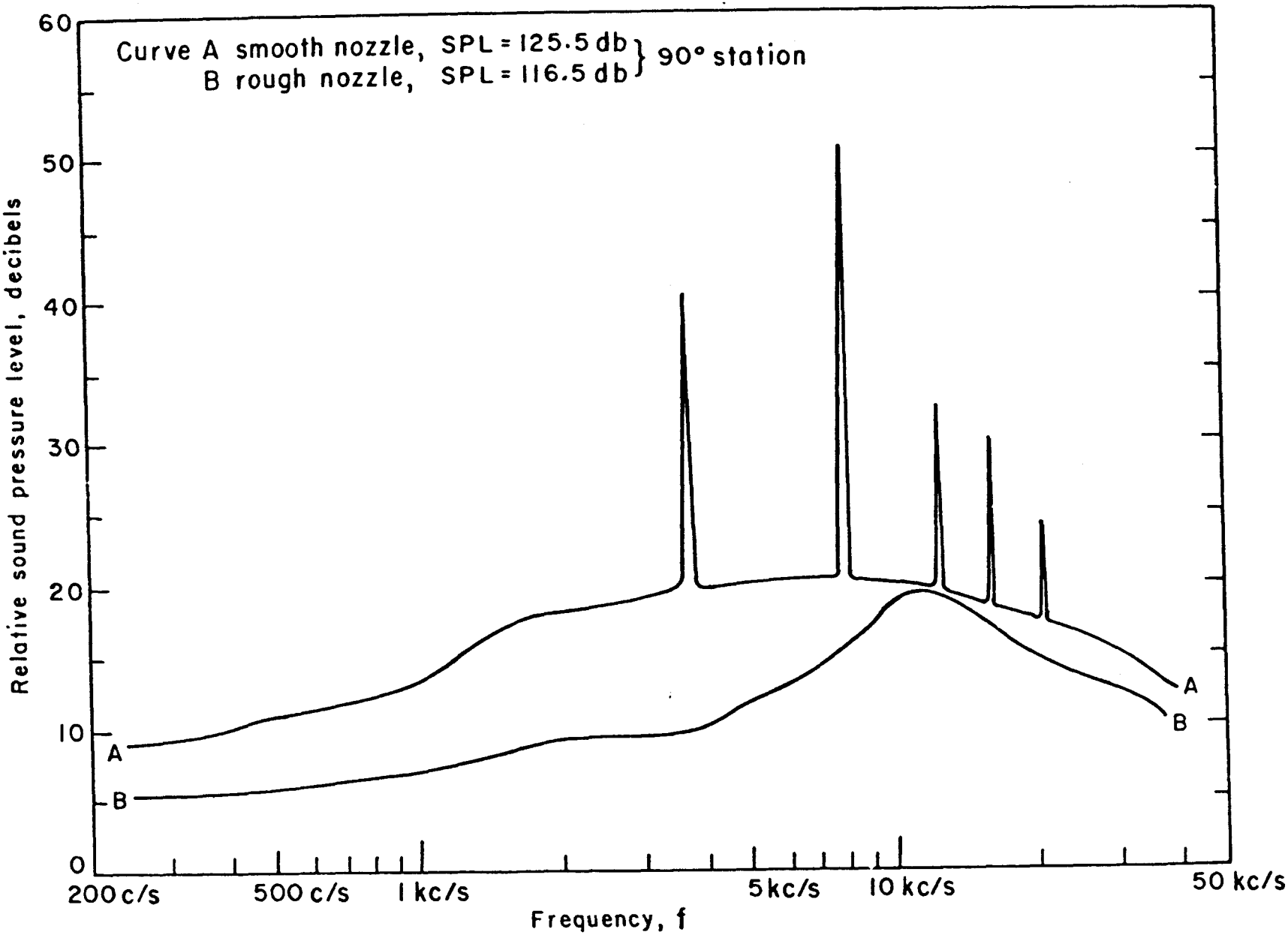

Figure 10. Narrow Band (3 Cycles) Analysis for Rough Converging Nozzle
(c) 90° Station

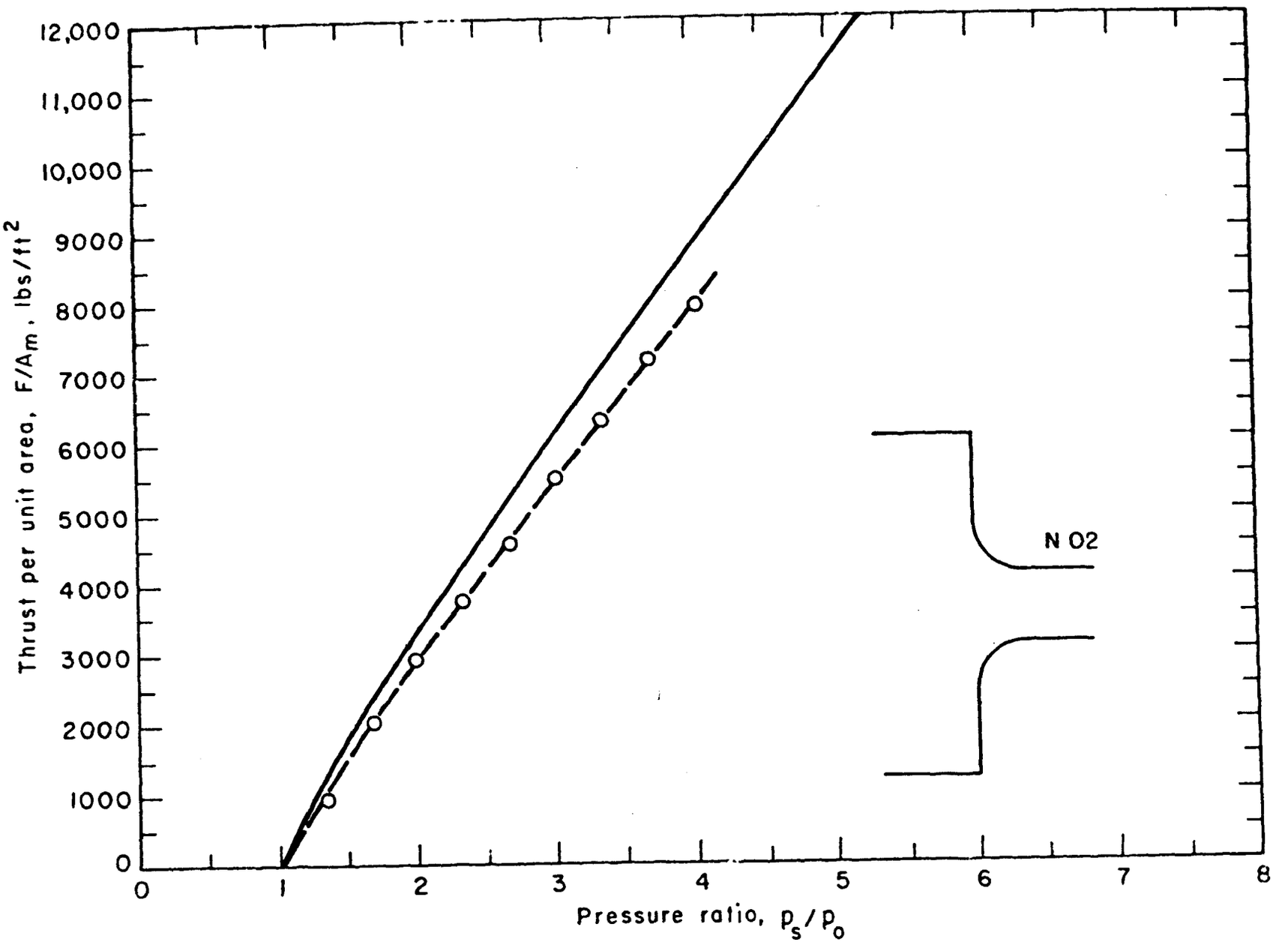

Figure 11. Thrust Performance of Nozzles
(a) Converging Nozzle No. N02

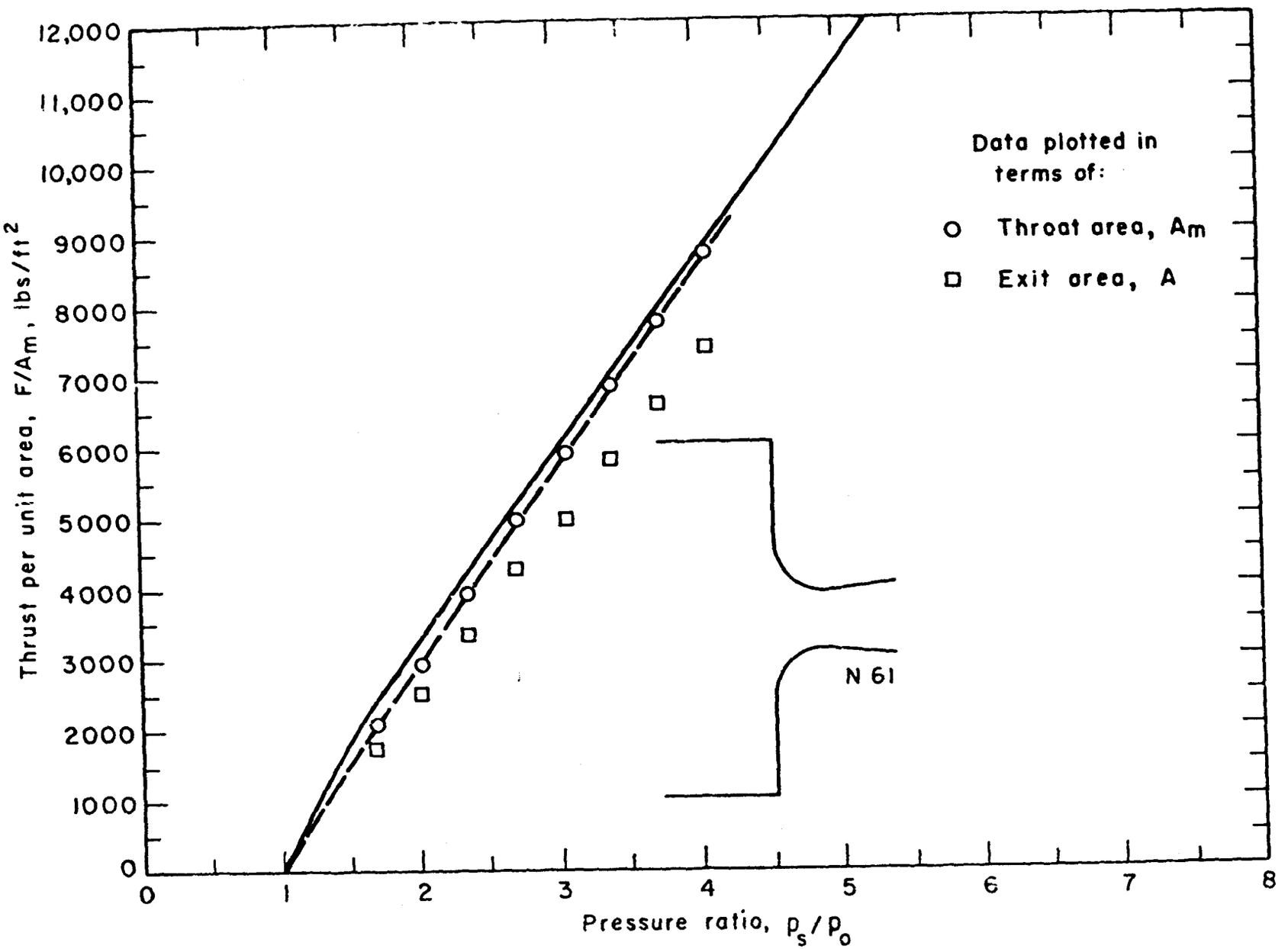

Figure 11. Thrust Performance of Nozzles
(b) Converging-Diverging Nozzle No. 121 (N61)

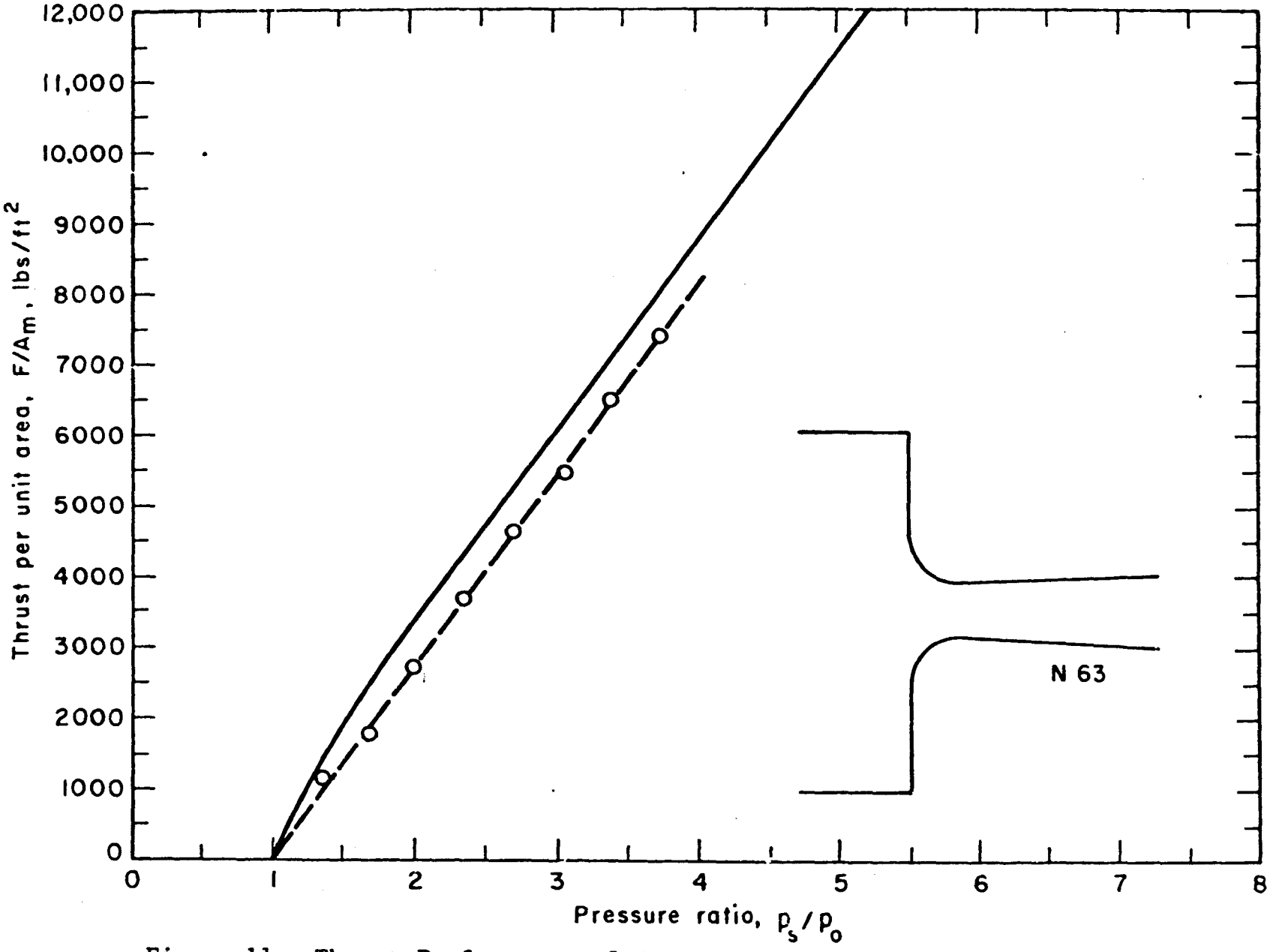

Figure 11. Thrust Performance of Nozzles
(c) Converging-Diverging Nozzle No. N63

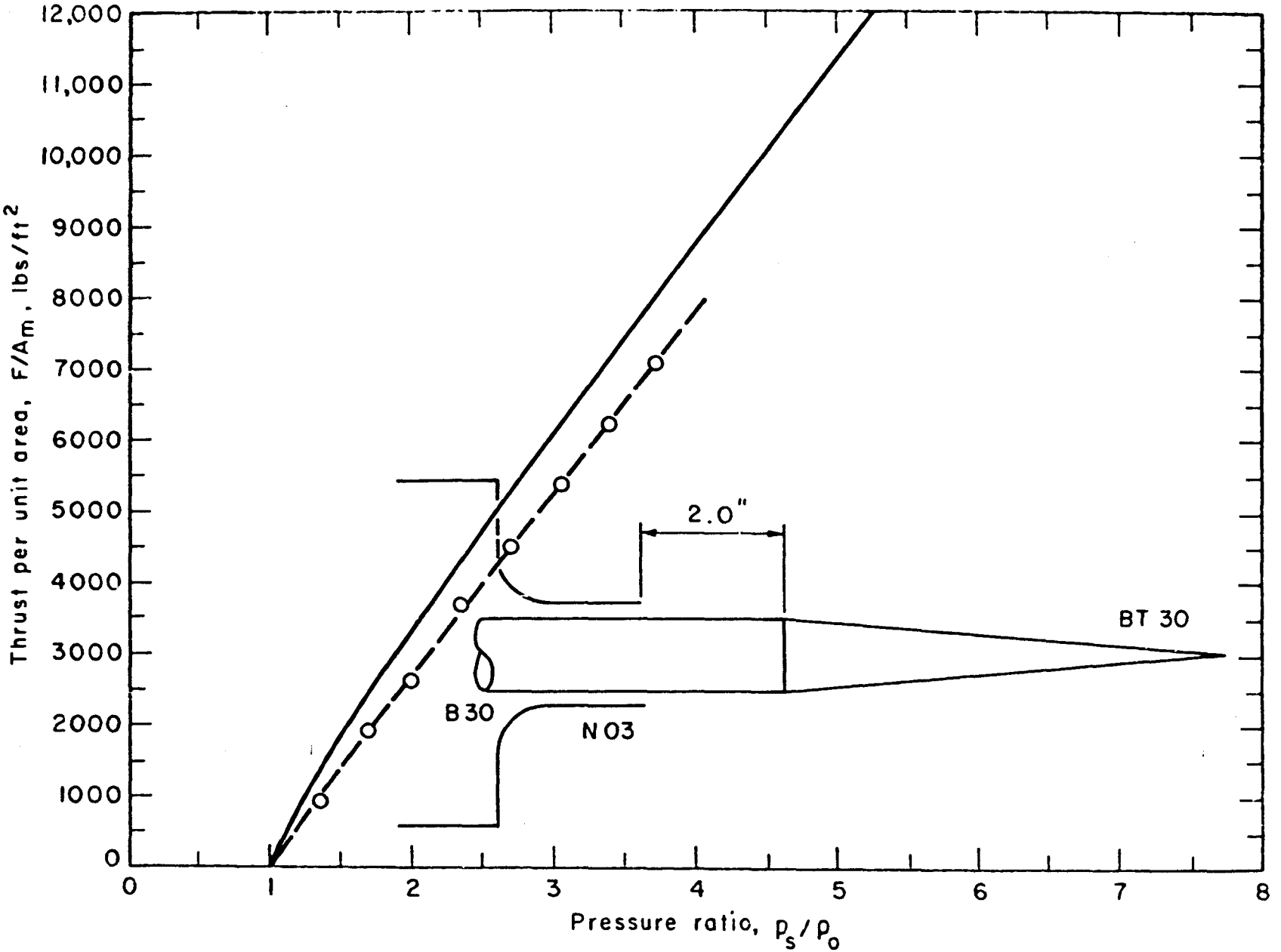

Figure 11. Thrust Performance of Nozzles
(d) Plug Nozzle No. 347 (1:03:30:30 + 2.0)

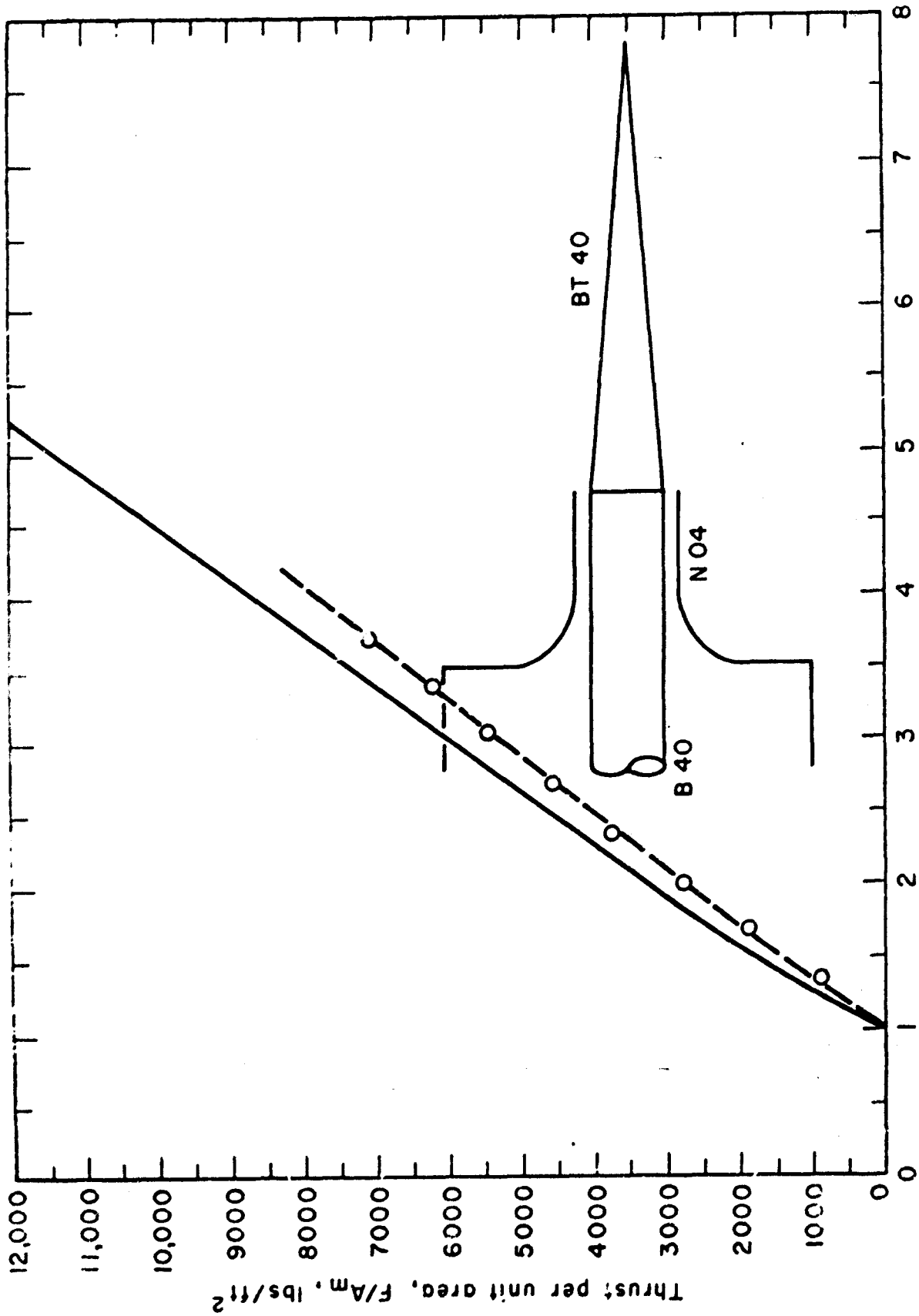

Figure 11. Thrust Performance of Nozzles
(e) Plug Nozzle No. 1:04:40:40 + 0

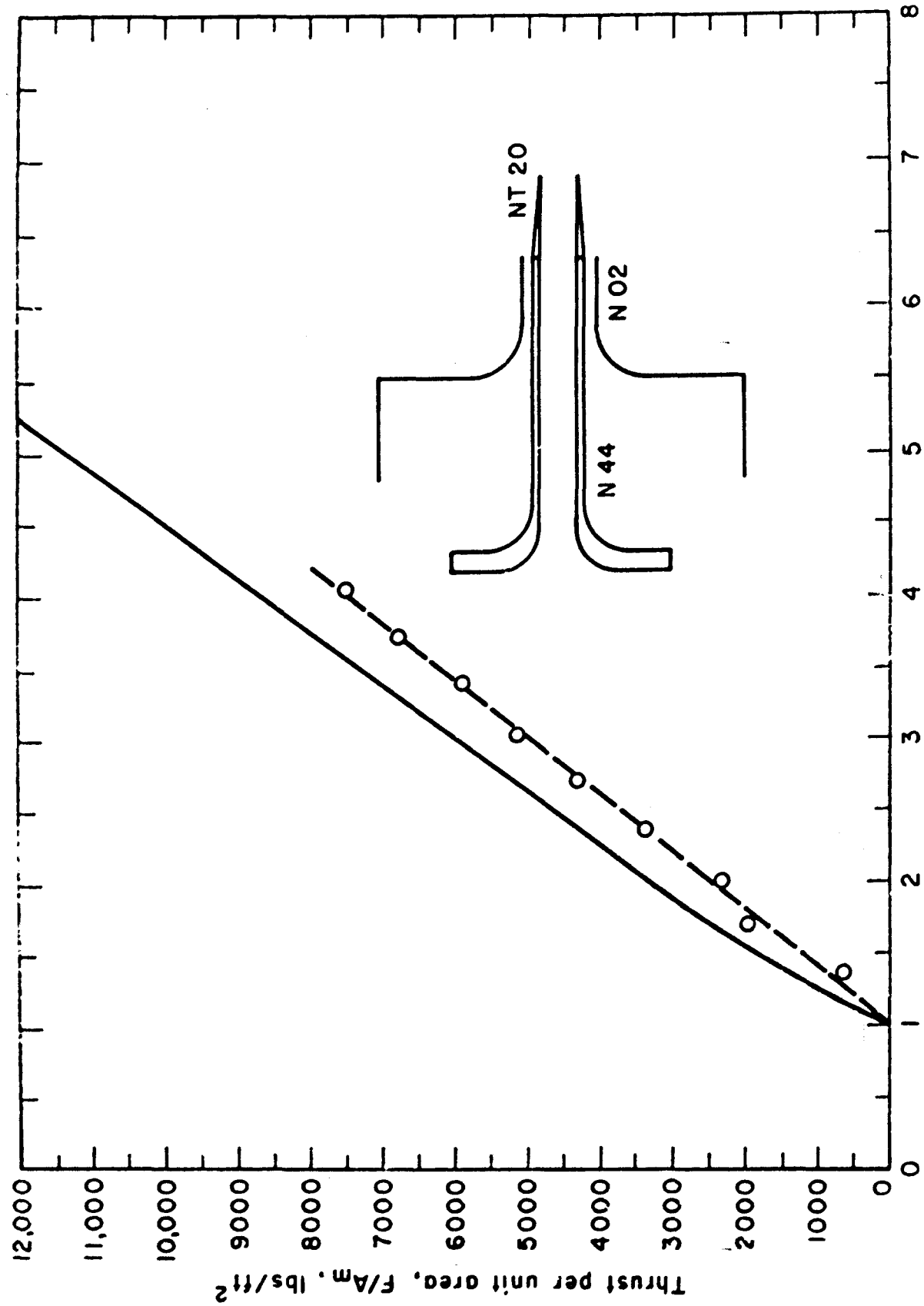

Figure 11. Thrust Performance of Nozzles
(f) Center Core Flow Nozzle No. 2:02:44:20 + 0

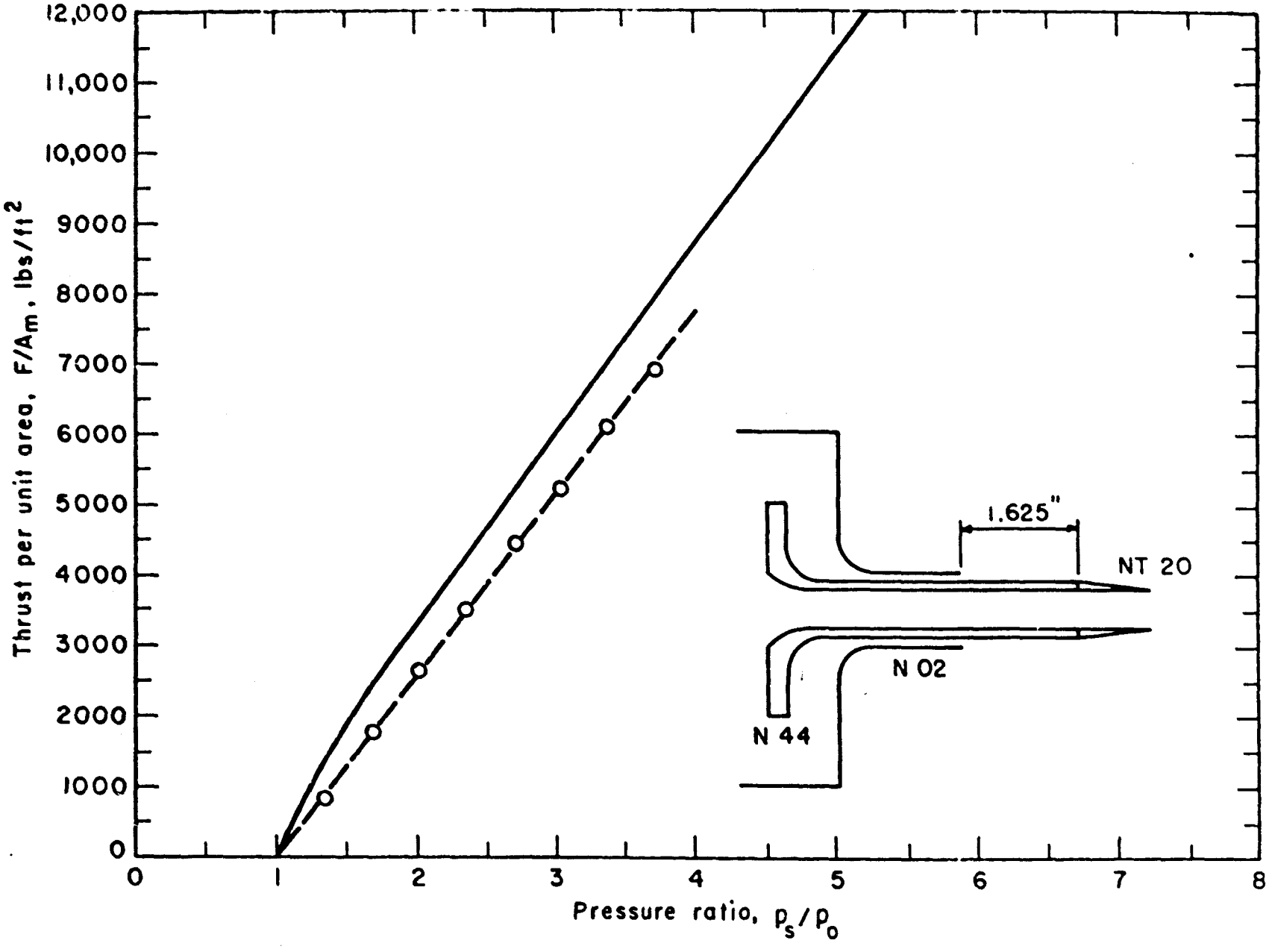

Figure 11. Thrust Performance of Nozzles
(g) Center Core Flow Nozzle No. 2:02:44:20 + 1.625

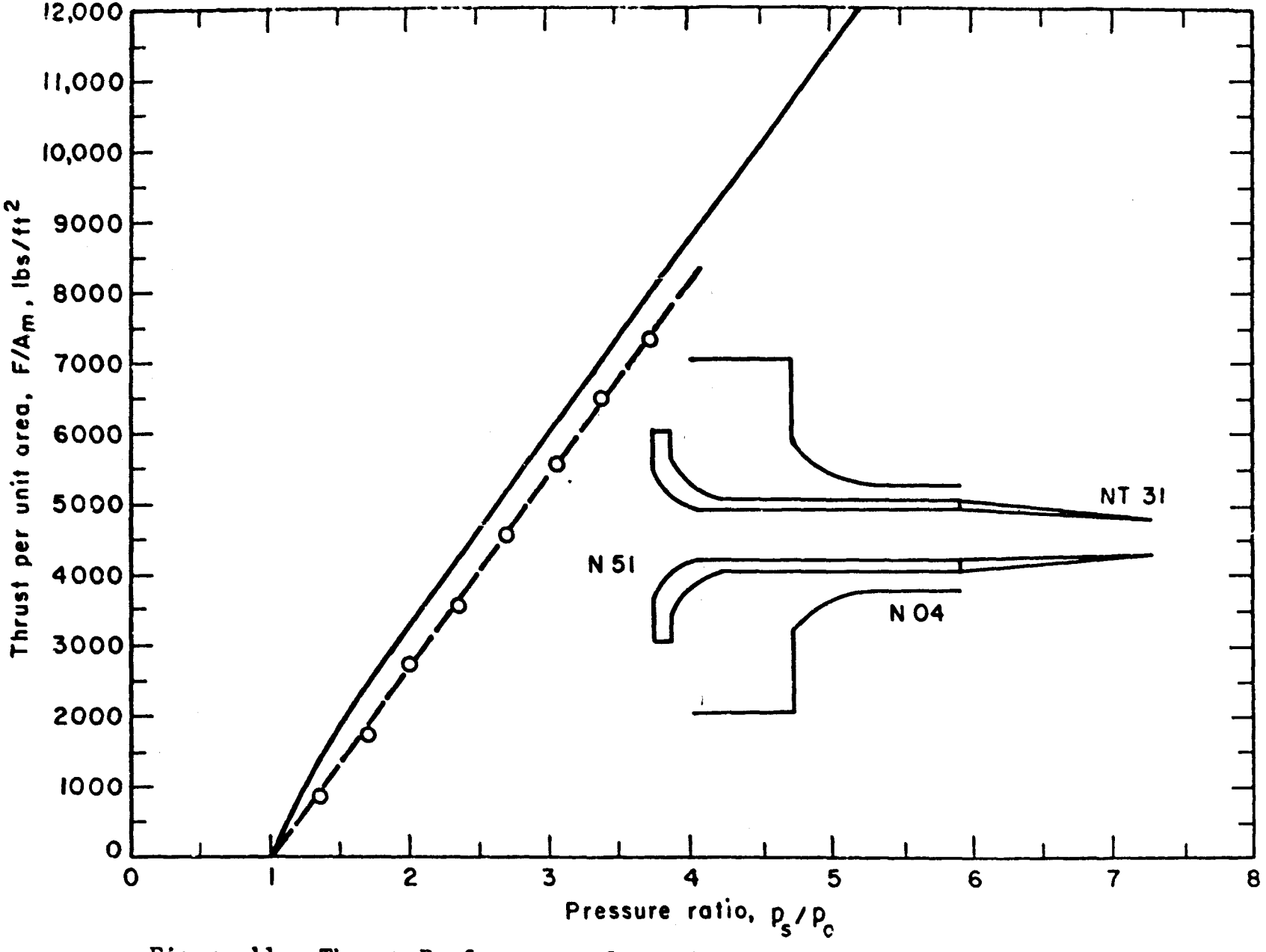

Figure 11. Thrust Performance of Nozzles
(h) Center Core Flow Nozzle No. 2:04:51:31 + 0

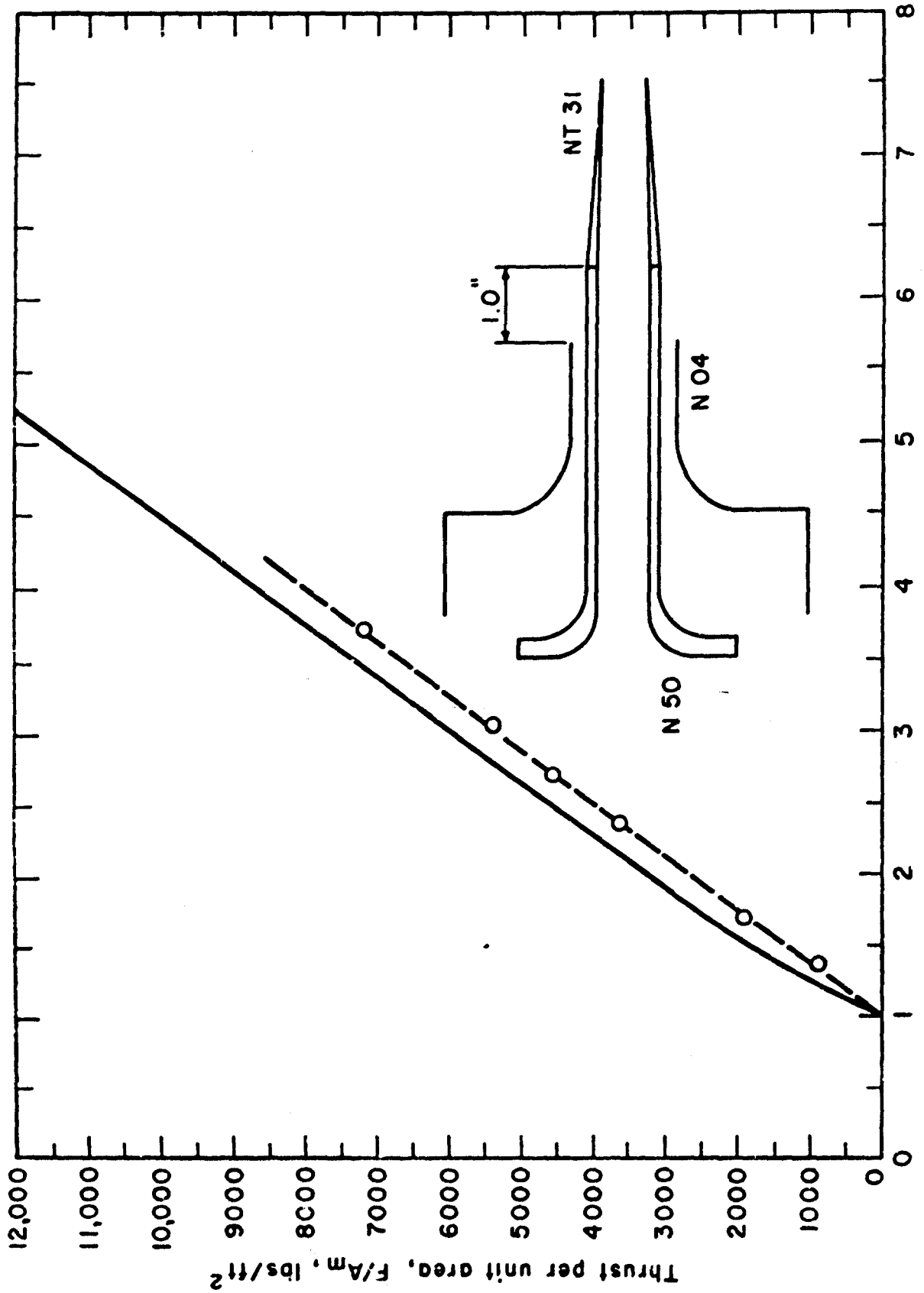

Figure 11. Thrust Performance of Nozzles
(1) Center Core Flow Nozzle No. 2:04:50:31 + 1.0

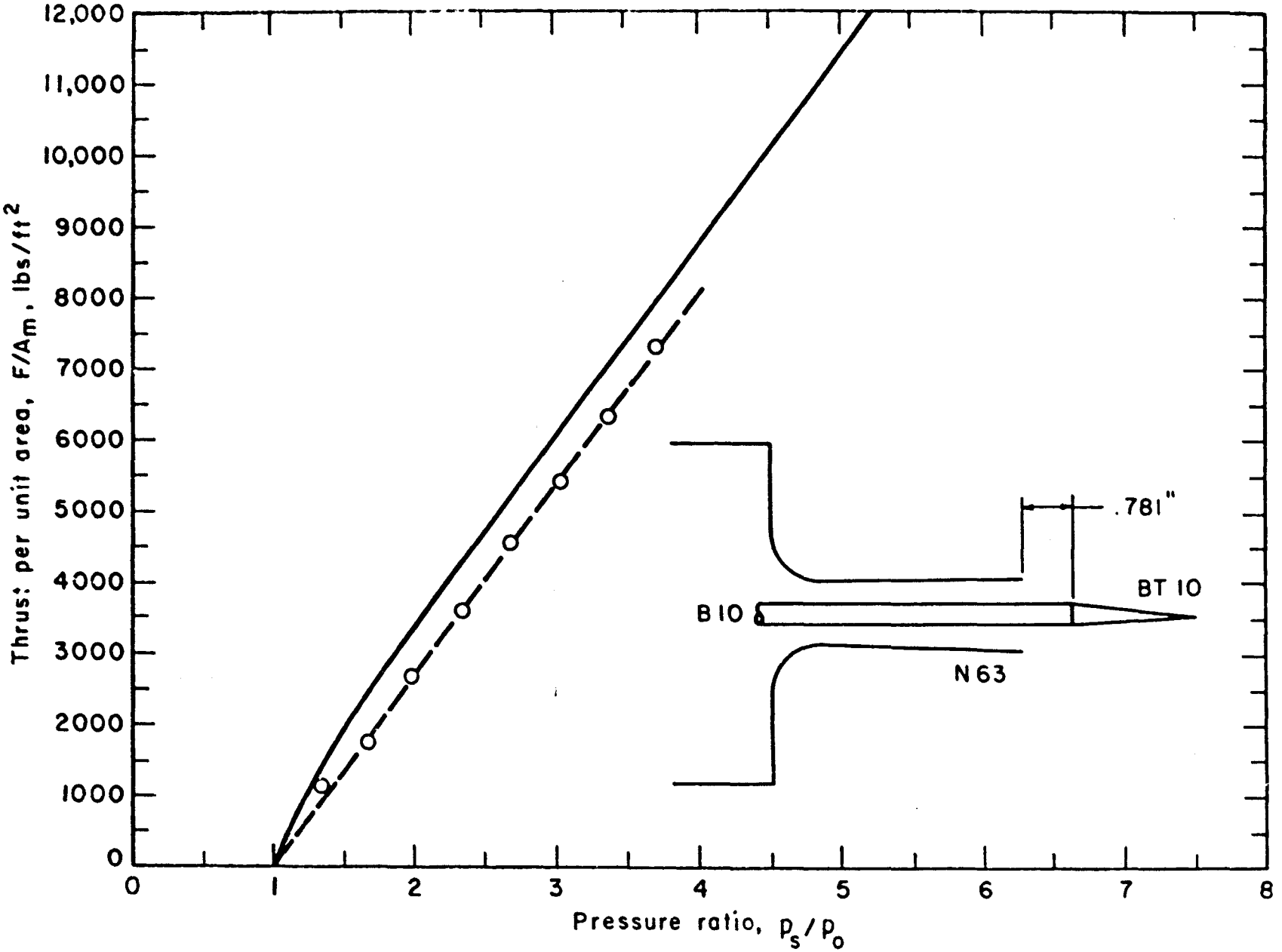

Figure 11. Thrust Performance of Nozzles
(j) Converging-Diverging Plug Nozzle No. 1:63:10:10 + 0.781

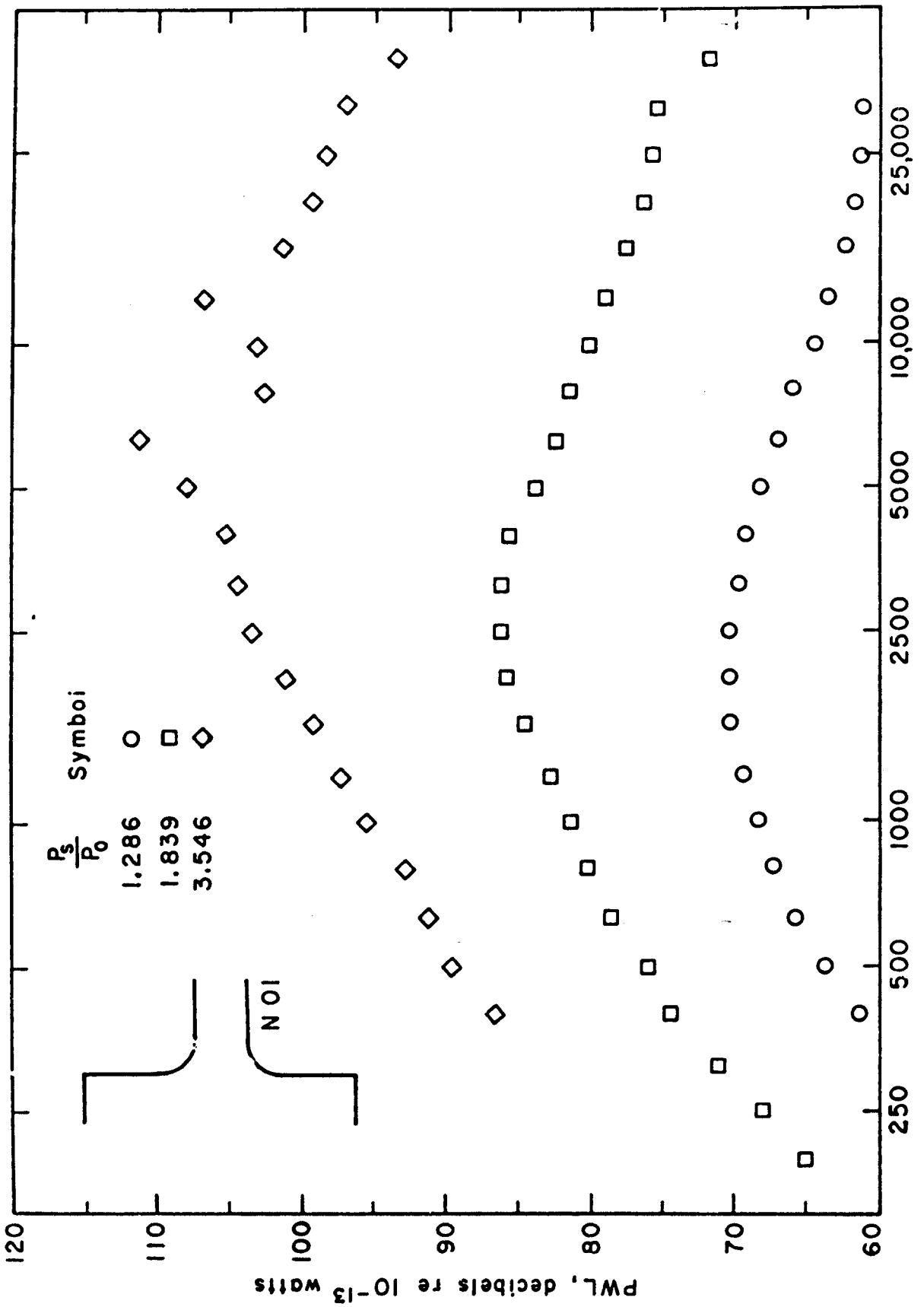

Figure 12. Frequency Analysis of Converging Nozzles
(a) Nozzle No. N01

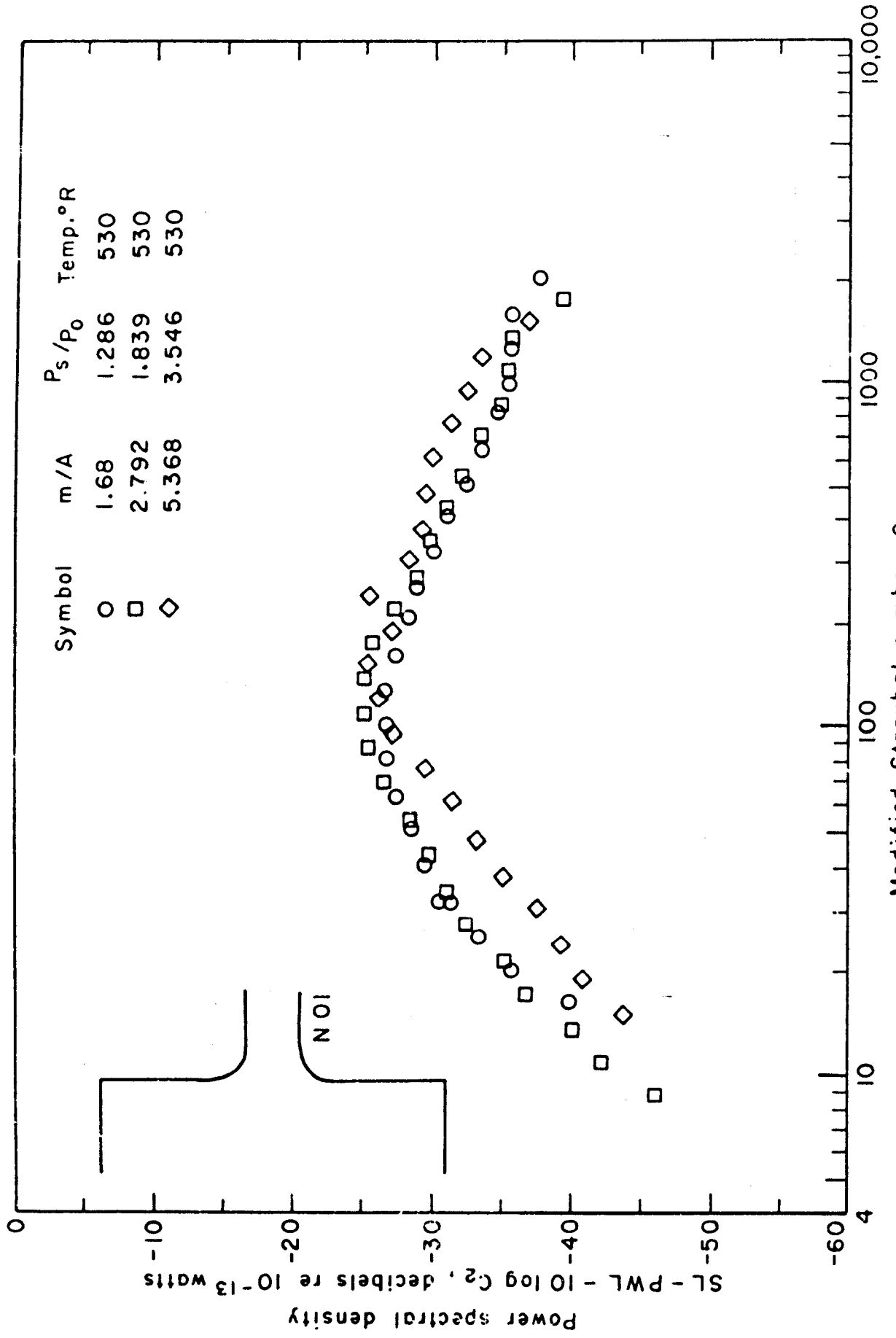

Figure 12. Frequency Analysis of Converging Nozzles
(b) Nozzle No. NOi, Normalized

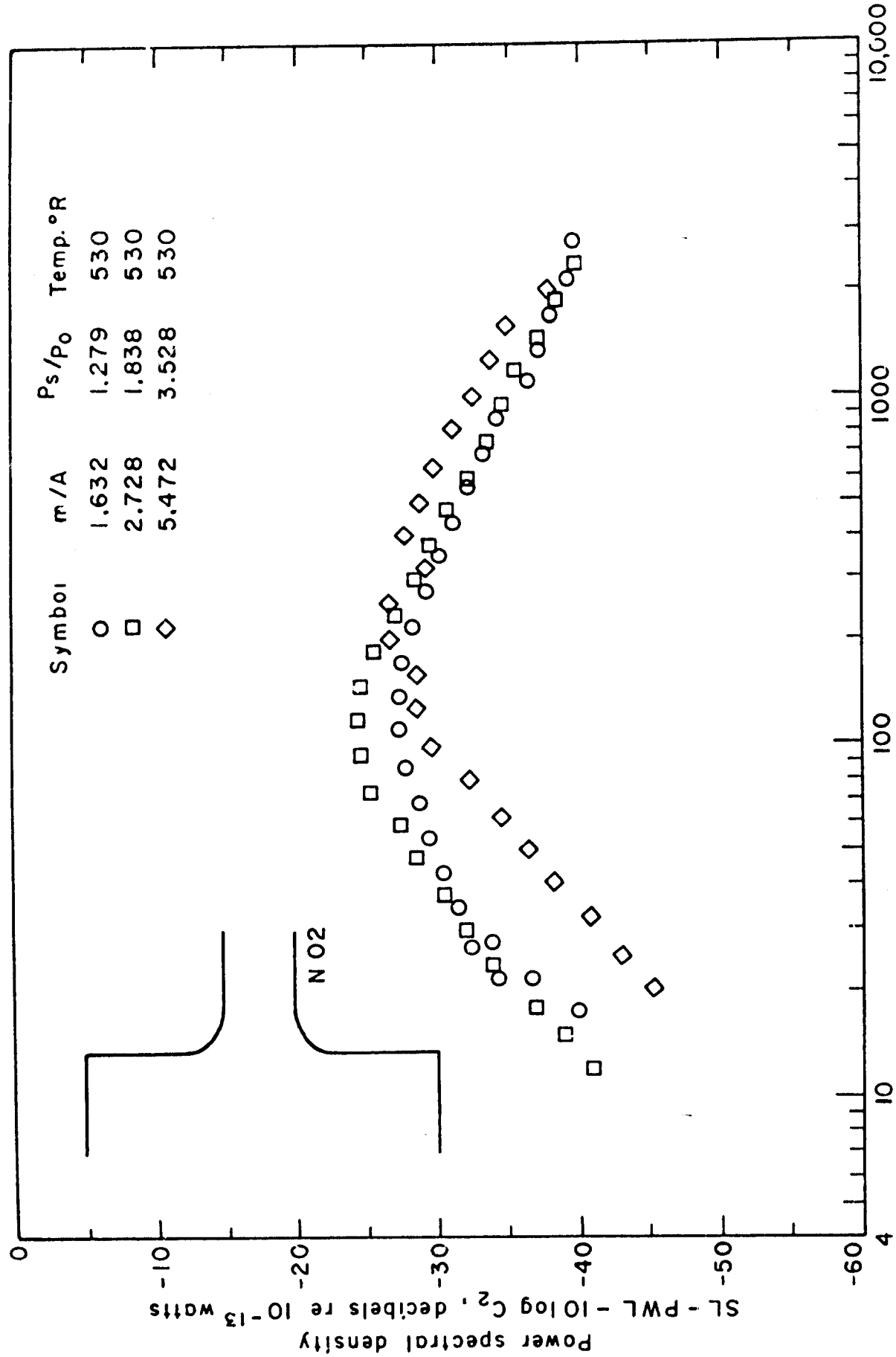

Figure 12. Frequency Analysis of Converging Nozzles
(c) Nozzle No. N02, Normalized

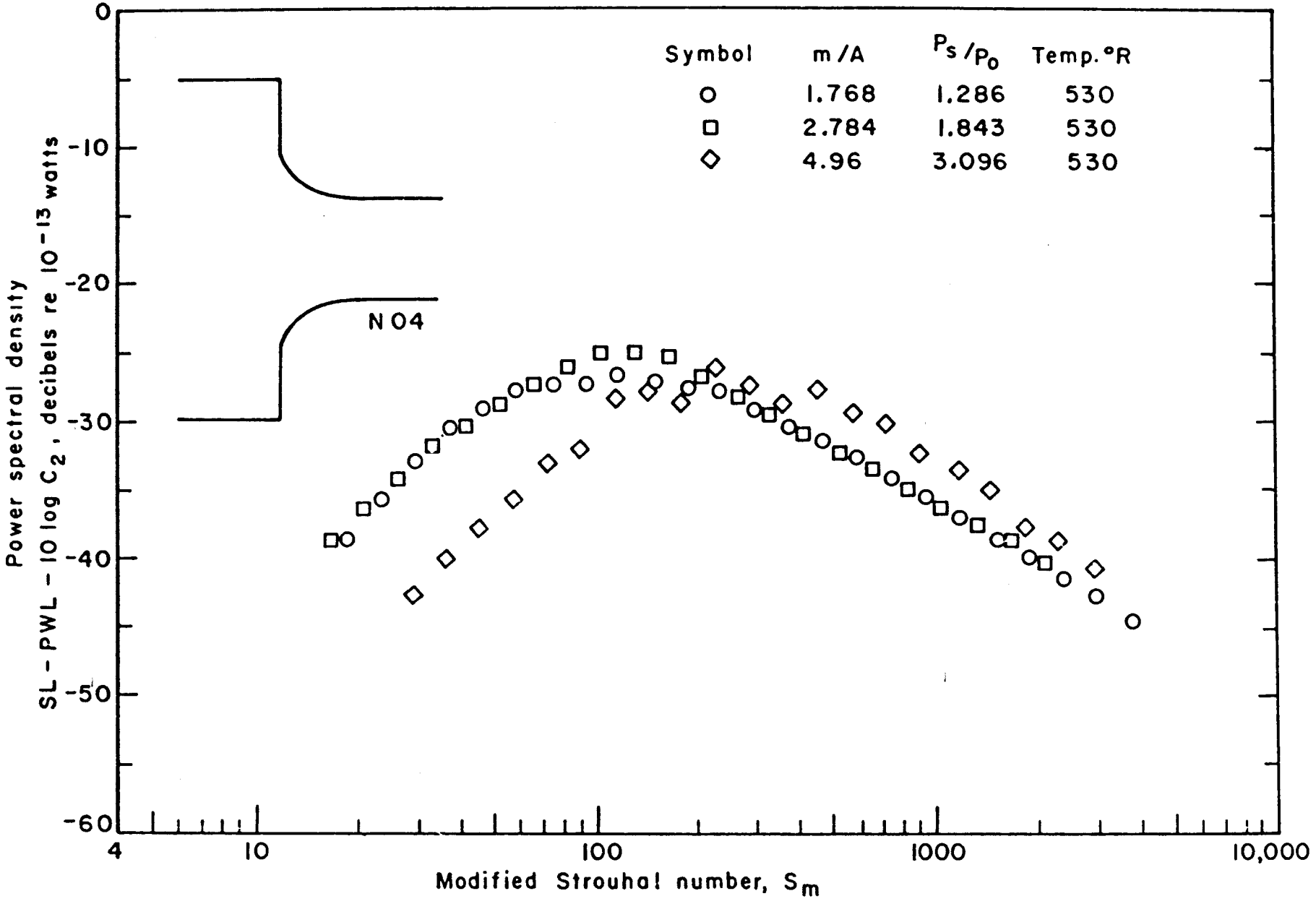

Figure 12. Frequency Analysis of Converging Nozzles
(d) Nozzle No. N04, Normalized

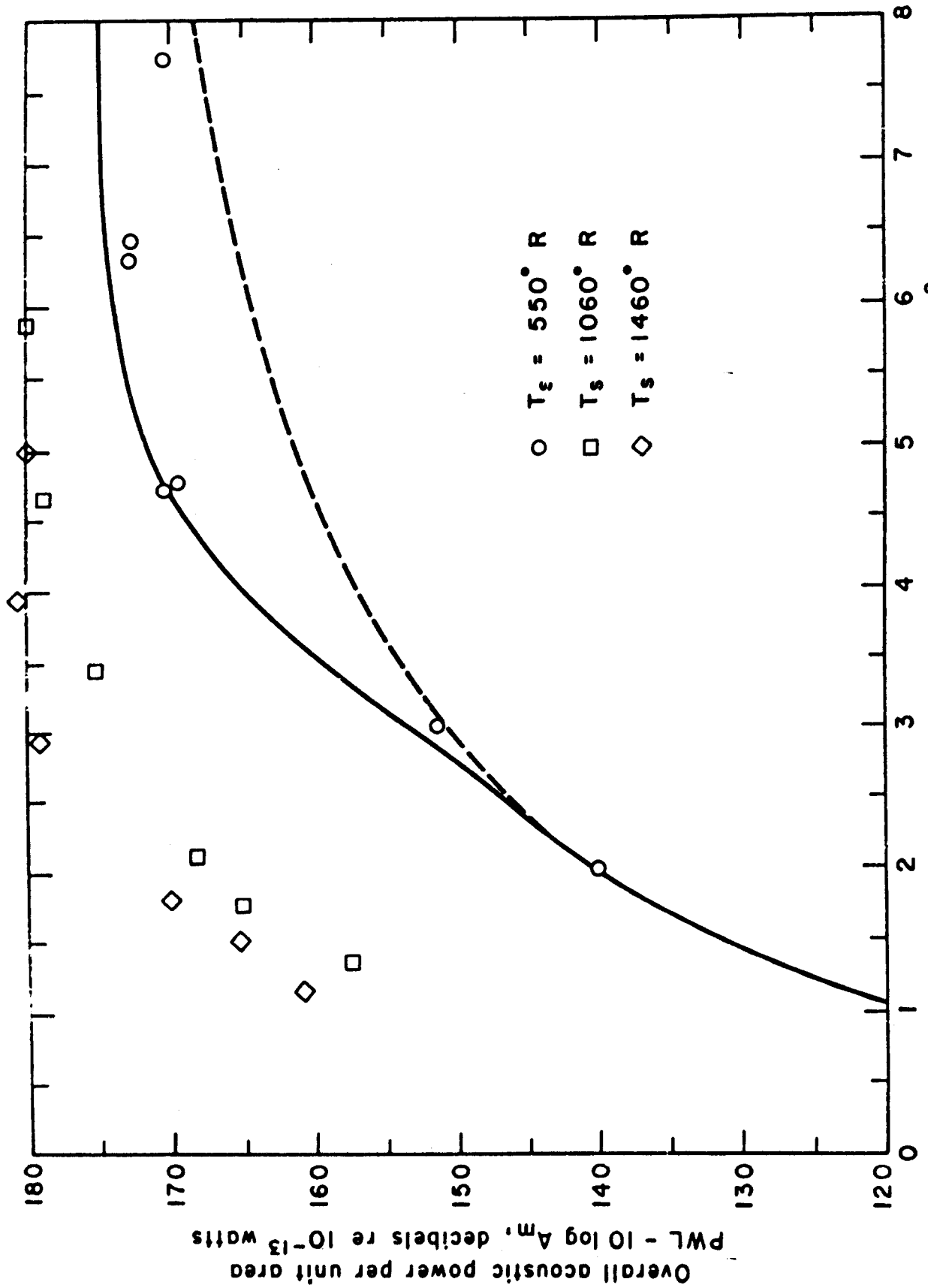

Figure 13. Acoustic Performance of Convergent Nozzle No. N02
(a) Size Normalization Only

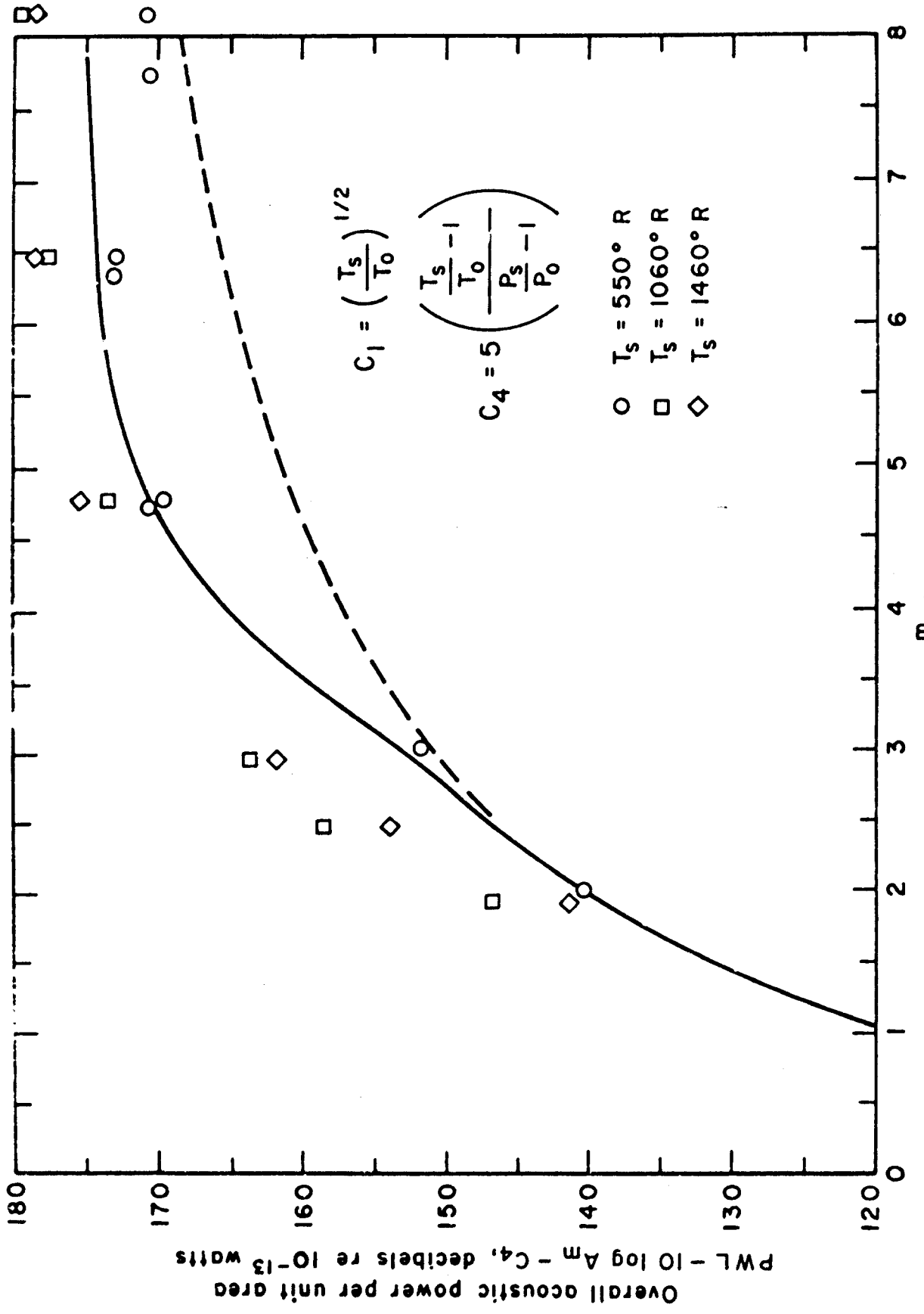

Figure 13. Acoustic Performance of Convergent Nozzle No. N02
(b) Size and Temperature Normali'ation

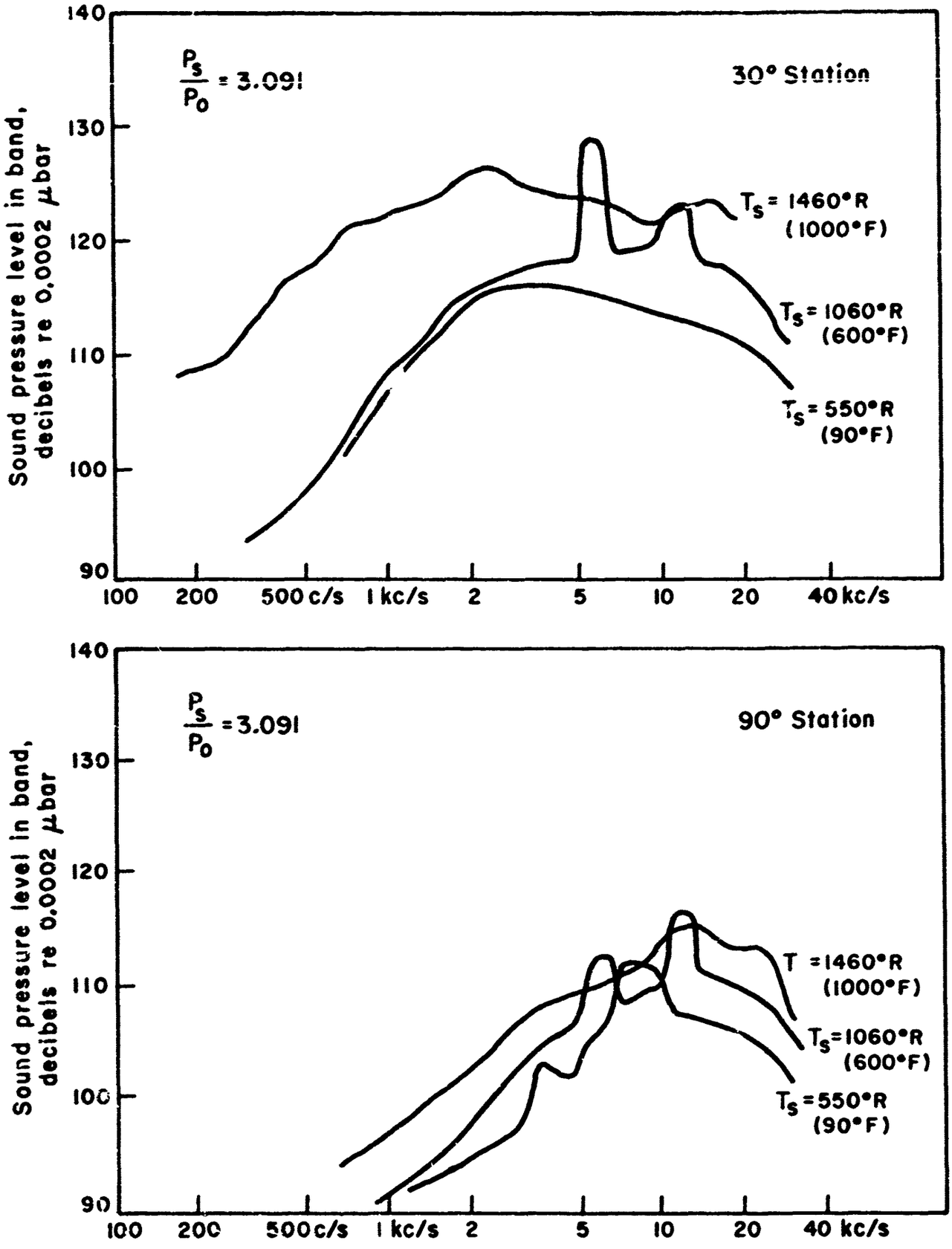

Figure 13. Acoustic Performance of Convergent Nozzle No. N02
(c) One-Third Octave Band Analysis of Converging Nozzle No. N0?

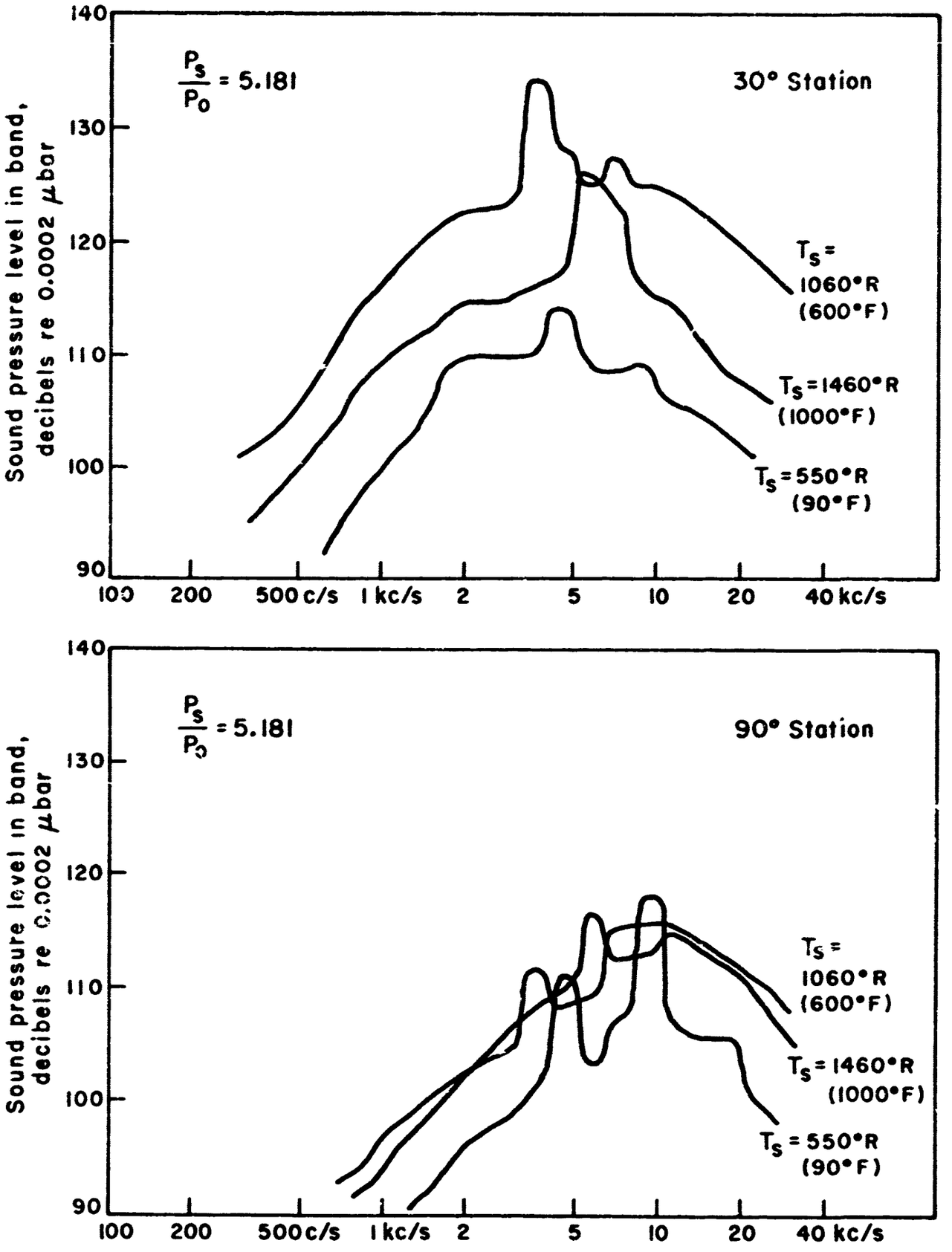

Figure 13. Acoustic Performance of Convergent Nozzle No. N02
(d) One-Third Octave Band Analysis of Converging Nozzle No. N02

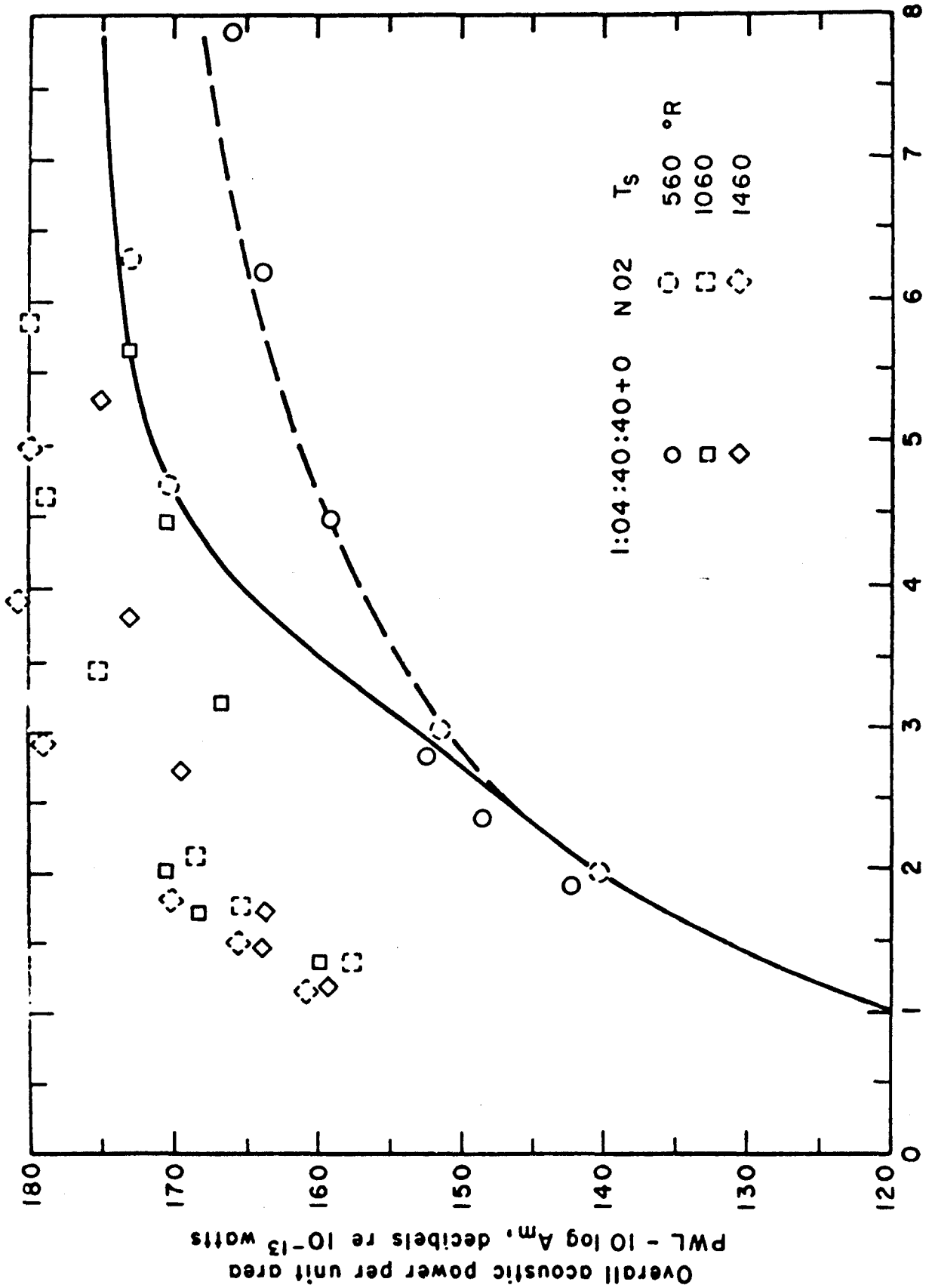

Figure 13. Acoustic Performance of Convergent Nozzle No. N02
(e) Acoustic Performance of Plug Nozzle No. 1:04:40:40 + 0

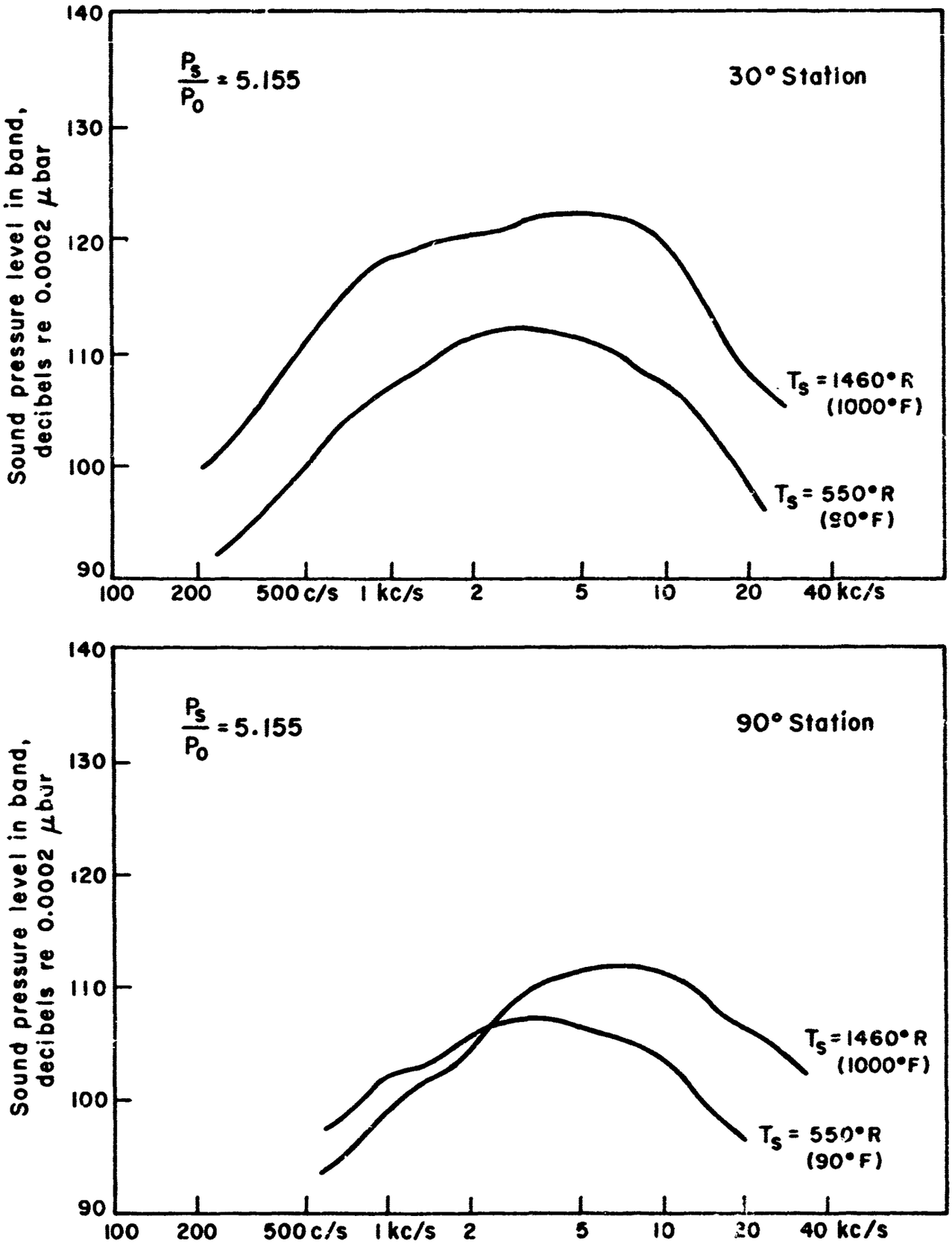

Figure 13. Acoustic Performance of Convergent Nozzle No. N02
(f) One-Third Octave Band Analysis of Plug Nozzle No. 1:04:40:40 + 0

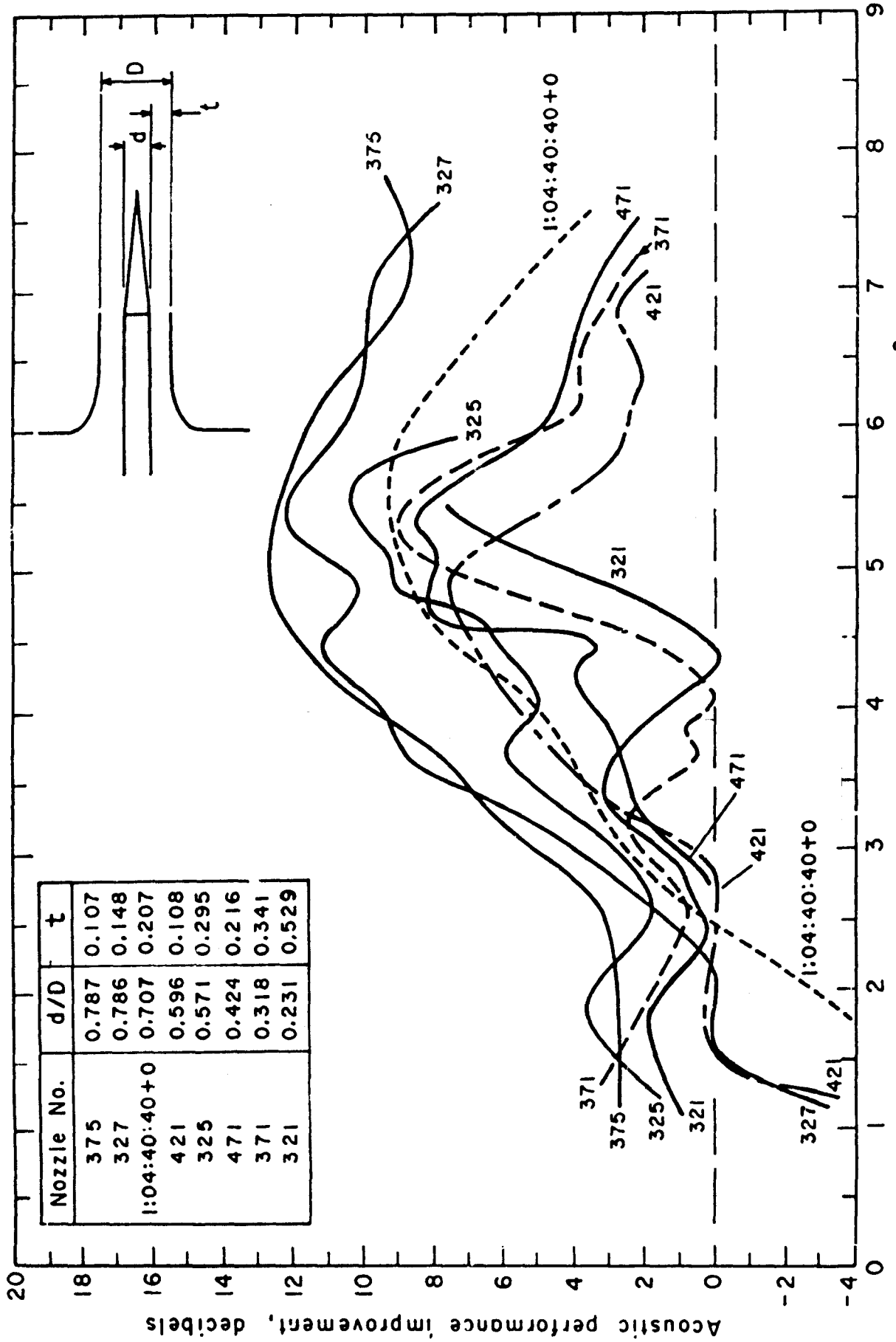

Figure 14 (a). Acoustic Performance of Plug Nozzles

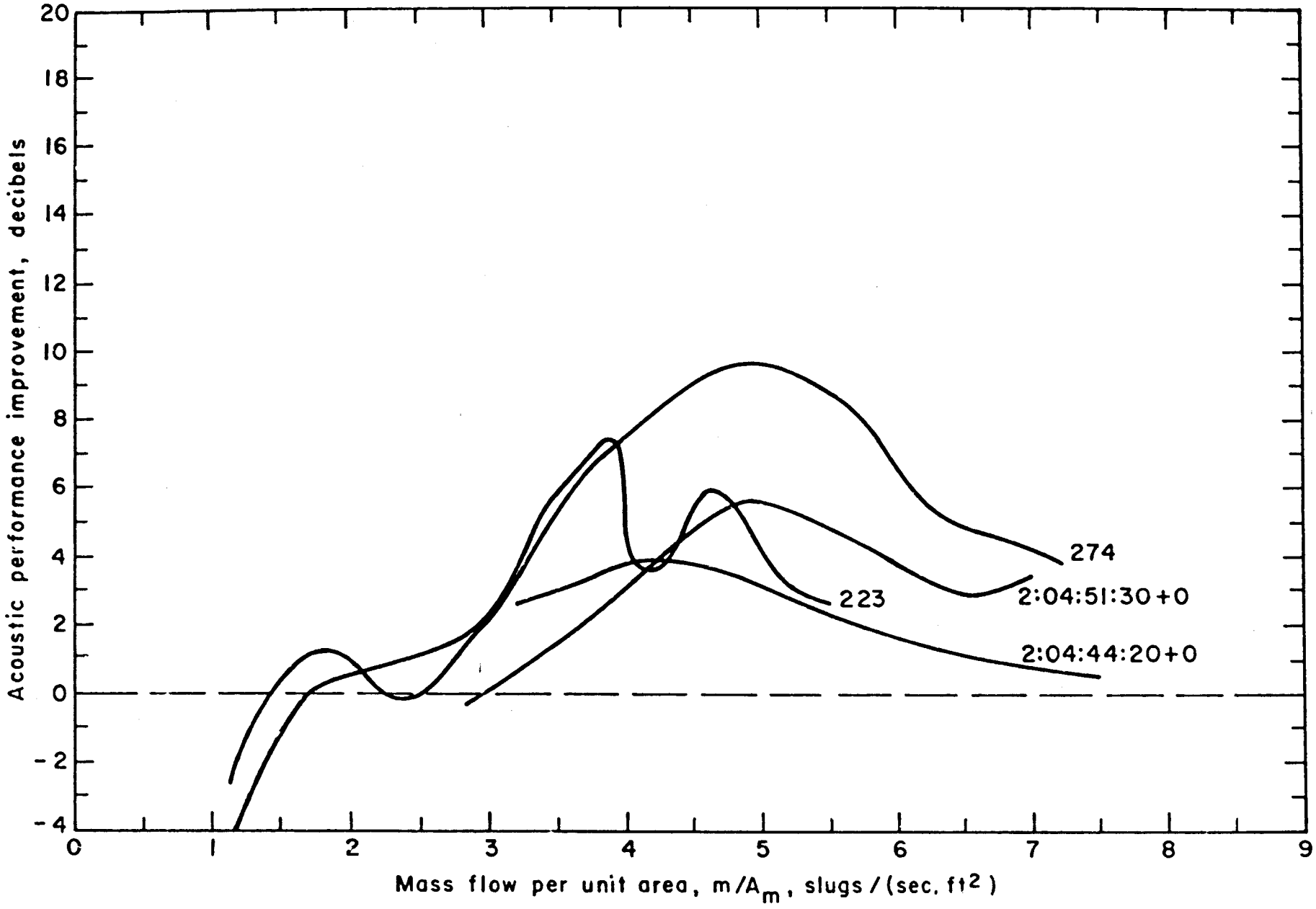

Figure 14 (b). Acoustic Performance of Center Core Flow Nozzles

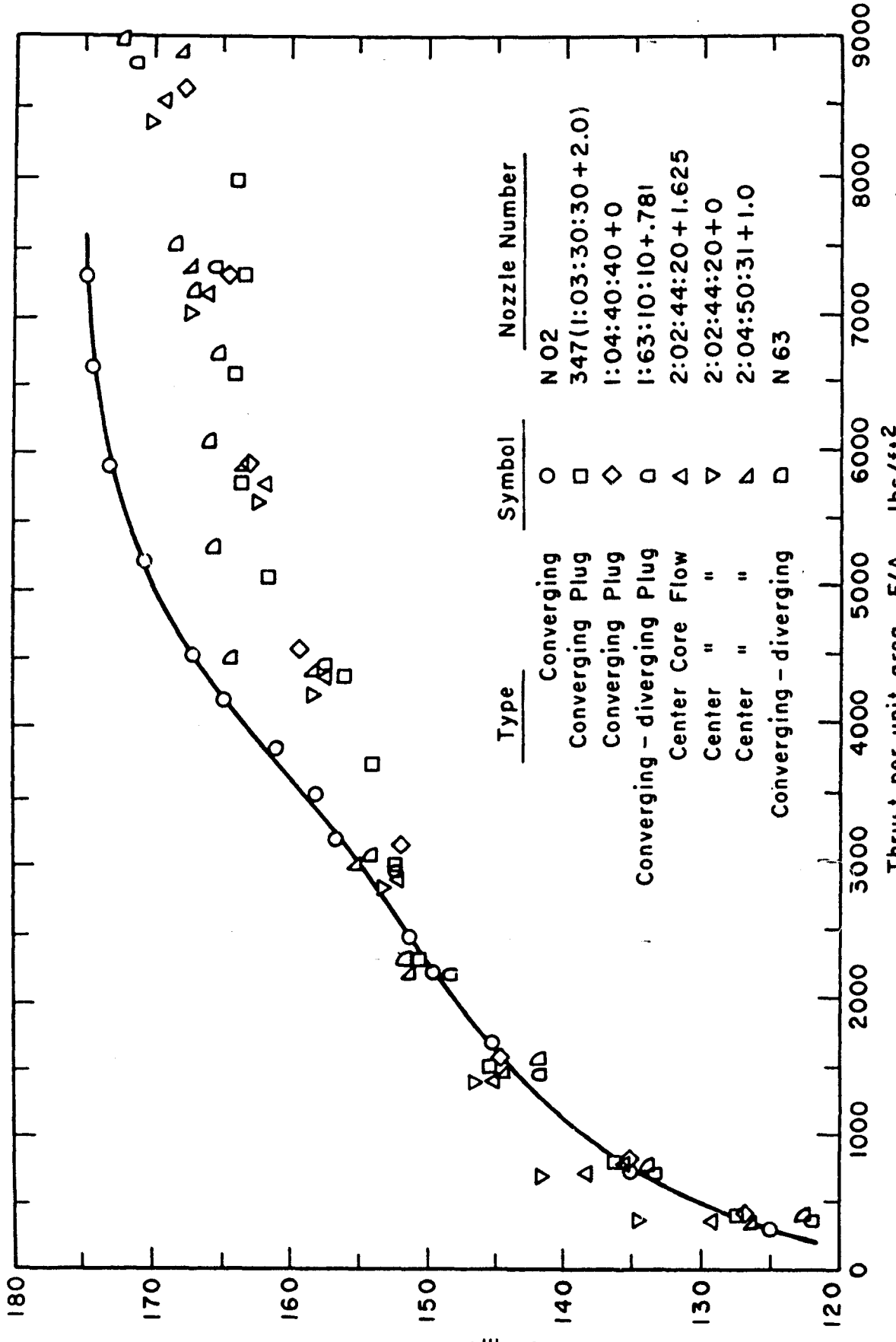

Figure 15. Acoustic Performance of Nozzles